

**UNIVERSIDADE DE SÃO PAULO
INSTITUTO DE FÍSICA DE SÃO CARLOS**

Elisa Iahn Goettems

On the physics of dissipative systems:
classical dynamics and quantum dissipative adaptation

São Carlos

2024

Elisa Iahn Goettems

On the physics of dissipative systems:
classical dynamics and quantum dissipative adaptation

Thesis presented to the Graduate Program in Physics at the Instituto de Física de São Carlos da Universidade de São Paulo, to obtain the degree of Doctor in Science.

Concentration area: Theoretical and Experimental Physics

Advisor: Prof. Dr. Diogo de Oliveira Soares-Pinto

Coadvisor: Prof. Dr. Daniel Mendonça Valente

Corrected Version
(original version available on the Program Unit)

São Carlos
2024

I AUTHORIZE THE REPRODUCTION AND DISSEMINATION OF TOTAL OR PARTIAL COPIES OF THIS DOCUMENT, BY CONVENTIONAL OR ELECTRONIC MEDIA FOR STUDY OR RESEARCH PURPOSE, SINCE IT IS REFERENCED.

Goettens, Elisa Iahn

On the physics of dissipative systems: classical dynamics and quantum dissipative adaptation / Elisa Iahn Goettens; advisor Diogo de Oliveira Soares-Pinto; co-advisor Daniel Mendonça Valente - corrected version -- São Carlos 2024.

162 p.

Thesis (Doctorate - Graduate Program in Theoretical and Experimental Physics) -- Instituto de Física de São Carlos, Universidade de São Paulo - Brasil Universidade Federal de Mato Grosso, 2024.

1. spectral function. 2. Brownian motion. 3. dissipative adaptation. 4. thermodynamics. 5. asymmetric potential. I. Soares-Pinto, Diogo de Oliveira, advisor. II. Valente, Daniel Mendonça, co-advisor. III. Title.

Este trabalho é dedicado às mulheres que lutam diariamente para fazer ciência no Brasil.

ACKNOWLEDGEMENTS

I am incredibly grateful to my family for their fundamental support, which was instrumental in helping me achieve this accomplishment. Janio and Any, I am immensely thankful for the unwavering support you both provided. I also want to extend my gratitude to my boyfriend, Rafael Brito, whose constant encouragement and support were essential for completing this Ph.D. And I must express my appreciation to Kimy, my loyal canine companion and source of unconditional love.

I am deeply grateful to my advisor, Diogo, and co-advisor, Daniel, for their expert guidance and active involvement in inspiring discussions throughout my Ph.D. Their valuable opportunity, constructive advice, patience, and dedication have been greatly appreciated. I would like to extend special thanks to Jerê, a friend and colleague, whose collaboration was instrumental in the success of this academic journey. Additionally, I want to express my gratitude to Ivan for engaging in fruitful discussions about my work and for the pleasant company during our runs.

I would like to express my gratitude to the examination board for dedicating their time and expertise to evaluate my work. I am also thankful to the other professors who made significant contributions during this crucial stage of my academic development. In particular, I want to mention Professor Sérgio for the valuable discussions we had.

I want to extend my heartfelt thanks to my dear friends and companions who shared the days with me in room 21 at IFSC. Special appreciation goes to Guilherme and Pedro, who consistently maintained a pleasant atmosphere. I also want to express my gratitude to friends outside the group, particularly Naruna, Cica, Raphael, Gabi, and Filipe, for their support during challenging times and for being part of my personal growth journey, creating cherished memories and moments of relaxation together.

I am grateful for the technical support from IFSC, the staff, and the infrastructure of USP, which created a conducive environment for academic development and various student activities. Special recognition goes to the technical team of the IFSC library, Natalina and Neusa, as well as Angela, who provided invaluable assistance in reviewing this thesis. I also want to thank all the students of the Integrated Physics Week (SIFSC) for their contributions to the final phase of my Ph.D. and for enriching my experience in organizing such a successful event.

I want to express my gratitude to everyone who has been a part of my academic and personal journey during these challenging years, especially during the pandemic, and later on, within the USP community. I hope that we can continue to maintain these connections in the years to come. Thank you.

This study was financed in part by the Coordenação de Aperfeiçoamento de Pessoal de Nível Superior - Brasil (CAPES) - Finance Code 001.

“Science demands patience.”

Artur C. Clarke

ABSTRACT

GOETTEMS, E. I. **On the physics of dissipative systems: classical dynamics and quantum dissipative adaptation.** 2024. 162p. Thesis (Doctor in Science) - Instituto de Física de São Carlos, Universidade de São Paulo, São Carlos, 2024.

The study of dissipative systems holds significant interest in physics. This thesis aims to explore these phenomena in both classical and quantum regimes. In the first part, we utilize the system-reservoir approach to investigate the dynamics of two Brownian particles immersed in the same bath. Two methods are employed to address this problem: one with bilinear coupling and the other with nonlinear coupling between the particles and the bath. The extension of the system to include two particles with bilinear coupling yields unphysical results, such as free-particle motion for the relative coordinate and a lack of interaction between closely spaced particles. To address this issue, authors have been introduced an exponential coupling. In this work, we propose a method to reconcile both linear and nonlinear couplings. We demonstrate how to derive the same nonlinear dissipation rates starting from the bilinear Lagrangian, achieved through a modified spectral function that explicitly depends on the distance between the particles. Additionally, we implement a modified spectral function to mitigate anomalous diffusion observed in the standard nonlinear model, along with a phenomenological model describing hydrodynamic interaction between a pair of Brownian particles in a viscous fluid. In the quantum regime, we adopt the same system-reservoir approach to investigate the dissipative adaptation hypothesis proposed by Jeremy England. This hypothesis proposes a general thermodynamic mechanism that explains the self-organization of systems through the dissipation of work absorbed from an external drive. In the second part of this thesis, we explore the quantum dynamics of systems subjected to an external drive, evaluating the thermodynamic quantities of a self-organization process. To do so, we utilize a time-dependent spin-boson Hamiltonian that characterizes a particle subject to a metastable double potential with time-dependent parameters controlling the asymmetry of the wells. Our objective is to demonstrate that the asymmetric potential can localize the particle in the unstable side of the well and verify that this transition results in the highest energy absorption. In conclusion, we propose further investigations into the driven spin-boson model to establish a comprehensive theory of the system's evolution and its thermodynamic implications.

Keywords: spectral function; Brownian motion; dissipative adaptation; thermodynamics; asymmetric potential.

RESUMO

GOETTEMS, E. I. **Sobre a física dos sistemas dissipativos: dinâmica clássica e adaptação dissipativa quântica**. 2024. 162p. Tese (Doutorado em Ciências) - Instituto de Física de São Carlos, Universidade de São Paulo, São Carlos, 2024.

Os estudos de sistemas dissipativos são de grande interesse na física. Nesta tese, temos como objetivo explorar esse fenômeno tanto nos regimes clássico quanto quântico. Na primeira parte, utilizamos a abordagem sistema-reservatório para investigar a dinâmica de duas partículas Brownianas imersas no mesmo reservatório. Existem duas maneiras de abordar esse problema: um com acoplamento linear e outro com acoplamento não linear entre as partículas e o banho. A extensão do sistema de interesse para incluir duas partículas com o acoplamento bilinear resulta em resultados não físicos, como movimento de partículas livres para a coordenada relativa e a ausência de efeitos entre partículas próximas umas das outras. Para abordar esses problemas, na literatura é empregado um acoplamento exponencial entre partícula e banho. Neste trabalho, propomos uma maneira de reconciliar os acoplamentos bilinear e não linear. Demonstramos como derivar as mesmas taxas de dissipação não linear a partir da Lagrangiana bilinear. Fizemos isso por meio de uma função espectral modificada que depende explicitamente da distância entre as partículas. Além disso, implementamos uma função espectral modificada para evitar a difusão anômala observada no modelo não linear usual, juntamente com modelo fenomenológica que descreve a interação hidrodinâmica entre um par de partículas Brownianas em um fluido viscoso. No regime quântico, adotamos a mesma abordagem de sistema-reservatório para investigar a hipótese de adaptação dissipativa proposta por Jeremy England. Essa hipótese propõe um mecanismo termodinâmico geral que explica a auto-organização de sistemas por meio da dissipação de trabalho absorvido de uma fonte externa. Nesta segunda parte da tese, exploramos a dinâmica quântica de sistemas sujeitos a uma força externa, avaliando as grandezas termodinâmicas de um processo de auto-organização. Para isso, utilizamos um Hamiltoniano spin-boson dependente do tempo que caracteriza uma partícula sujeita a um potencial duplo metastável com parâmetro dependente do tempo que controla a assimetria dos poços. Nosso interesse é mostrar que o potencial assimétrico é capaz de localizar a partícula no lado instável do poço e verificar que esta transição resulta na maior absorção de energia. Em conclusão, propomos investigações adicionais no modelo de spin-boson dirigido, a fim de estabelecer uma teoria mais abrangente de como os sistemas evoluem e suas implicações termodinâmicas.

Palavras-chave: função espectral; movimento Browniano; adaptação dissipativa; termodinâmica; potencial assimétrico.

LIST OF FIGURES

Figure 1 – Spatial correlation for a) forces for both particles, b) center of mass forces, and c) relative coordinate forces. Such correlation forces are distance-relative dependent due to the dissipation rate. a) For small distances, the standard single Brownian particle behavior is recovered. Starting at approximately $(\sqrt{3})^{-1}$, the correlation function becomes negative until reaching zero for particles too far apart. b) Similar behavior as in a) , now with correlation force in the intermediate distances. c) For small distances, correlation is zero, increasing for intermediate distances until reaching two times the correlation force for a single Brownian particle.	44
Figure 2 – Spatial correlation for a) forces for both particles, b) center of mass forces, and c) relative coordinate forces, with a Gaussian modified spectral function (Eq.(2.56)). The Gaussian behavior is similar in all three plots. For small distances, the correlation force is the same of a single Brownian particle whereas for long distances, it reaches a) zero correlation and b) half of the one for a single Brownian particle. In c) , for small distances, it is zero correlation, which increases until two times the correlation force for a single Brownian particle for long distances.	46
Figure 3 – Representation of a SQUID, where I is the current.	52
Figure 4 – Representation of classical and quantum paths in the phase space. For the quantum regime, a Kernel accounts for all possible trajectories of the system.	53
Figure 5 – In the classic scenario of equilibrium statistical mechanics, a system held in contact with a thermal reservoir at temperature T for a long time τ loses all memory of its starting state i and, consequently, the probabilities of microscopic states j and k are an exponential function of their respective energies. The probability distribution of each state is dictated by their energies.	62
Figure 6 – The probability of finding a system in a given state depends on both its initial condition and precisely the way it was driven. Expressing this probability distribution in terms of thermodynamic quantities poses a significant challenge, since it involves not only the internal energy of the final states, but also the work done by the drive during transitions between states.	64
Figure 7 – Driven barrier hopping (for further details, see Ref. (27)).	68

Figure 8 – Representation of quantum dissipative adaptation in Λ system with two ground states, $|a\rangle$ and $|b\rangle$, and one excited state $|e\rangle$. **a)** density operator of the system, ρ_S , at time $t = 0$. $\Gamma_{a/b}$ are the environment-induced spontaneous emission rates and $\omega_{a/b}$ are the transition frequencies. The initial state is a mixture of the two lower energy eigenstates $\rho_S(0) = p_a^{(0)} |a\rangle \langle a| + p_b^{(0)} |b\rangle \langle b|$ at zero temperature. **b)** A nonequilibrium environment composed of a single-photon pulse $|1_a\rangle$, which serves as the work source, drives the system dynamics and induces the time-dependent transition probability $p_{a\rightarrow b}(t)$ from $|a\rangle$ to $|b\rangle$. The backward transition probability (with a time-reversed pulse) $p_{b\rightarrow a}^*$ goes to zero at zero temperature. **c)** the asymptotic state is pure, $\rho_S(\infty) = |b\rangle \langle b|$, i.e., the atoms arrange themselves spontaneously into an organized state, often referred to as self-organization. The state is conditioned to maximizing the work absorbed and the heat dissipated in the transition. The driven system undergoes an irreversible self-organizing dynamics. 71

Figure 9 – Reproduction of Fig. 1 from Ref. (83), where a one-dimensional bistable spring is subjected to sinusoidal forcing at low (green), intermediate (blue), and high (light blue) amplitudes. **(a)** The plot shows the average energy levels across a forcing period for different amplitudes, where $U(d)$ represents the bistable spring potential. **(b)** The trajectory of the average spring length illustrates distinct behaviors: remaining confined in the initial potential well ($\langle d \rangle \approx 1$) during low amplitudes (green), transitioning to the nonresonant potential well ($\langle d \rangle \approx 3$) for intermediate amplitudes (blue), and consistently oscillating between the two wells ($\langle d \rangle \approx 2$) at high amplitudes (light blue). 76

Figure 10 – Representation of energy level as a function of bias ϵ 76

Figure 11 – Representation of an asymmetric double well potential related to the sign of the separation between the two minima of energy, denoted as ϵ . Each side of the potential well has a specific frequency and energy, defined as ω_+ and ω_- , for right and left sides, respectively. Whereas the eigenvalue of $+q_0/2$ represents the right side, the eigenvalue of $-q_0/2$ represents the left side. Considering the particle starts on the left side of the well, **a)** if ϵ is positive, the particle starts in the stable well and, **b)** if ϵ is negative, the particle starts in the unstable well. 77

Figure 12 – Qualitative behavior of spin dynamics in the three main regimes of the spin-boson model with an Ohmic environment. Probability $P(t)$ corresponds to expectation value $P(t) = \langle \sigma_x(t) \rangle$, in the proposed systems, when initialized to the $+1$ eigenstate of σ_x at $t = 0$ 80

Figure 13 – Descriptions of the double spin path via Feynman-Vernon formulation involve classical variables η and ξ , which represent the spin paths and elements within the spin (reduced) density matrix.	87
Figure 14 – Reproduction of a figure of Ref.(118) regarding contours of time-dependence actions S_1 and S_2 in path integral formalism.	99
Figure 15 – Schematics of the double-well potential associated with the flux threading through the qubit. When no external sources are present, the potential exhibits symmetry, resulting in equal forward and backward tunneling rates $k^{f/b}$. Introducing a positive bias asymmetry ϵ accentuates forward tunneling, which dominates over backward tunneling. In the experiment involving the superconducting flux qubit, the coordinate associated with the double-well potential is magnetic flux ϕ within the loop. Eigenstates $ L/R\rangle$ of the flux operator correspond to currents circulating clockwise and anticlockwise in the superconducting loop, respectively.	106
Figure 16 – Reproduction of the colorplot in Fig.3(c, d, g) of Ref. (121). c, d Predicted dynamics of $P(t)$ with $P(0) = 1$. For Fig. c , $(\epsilon_d/\Delta)^2 \approx 12$, and $\epsilon_0 = 0$, whereas for Fig. d , $\epsilon_0 = \omega_d$. The values of the other parameters used in the simulations are: $\Delta/2\pi = 7.23$ GHz, $\alpha = 0.21$, $\omega_p/2\pi = 5.2$ GHz, $\omega_d/2\pi = 9$ GHz, and $T = 175$ mK. The probe is on-resonance with the undriven qubit at the symmetry point. Fig. g Time evolution of $P(t)$ calculated at the symmetry point, $\epsilon_0 = 0$. The parameters are: $\Delta/2\pi = 8$ GHz, $\alpha = 0.8$, $\omega_p/2\pi = 4$ GHz, $\omega_d/2\pi = 3$ GHz, and $T = 90$ mK. The selection of ω_p and ω_d exerts a minimal impact on the qualitative characteristics of the driven spectra. $\omega_c/2\pi = 65$ GHz for the three plots.	111

LIST OF ABBREVIATIONS AND ACRONYMS

IFSC	Instituto de Física de São Carlos
NIBA	Non-interacting blip approximation
qubit	Quantum bit
SQUID	Superconducting quantum interference device
TLS	Two level system
TPM	Two-point measurement
UFMT	Universidade Federal do Mato Grosso
USP	Universidade de São Paulo

LIST OF SYMBOLS

η	Greek letter eta
k_B	Boltzmann constant
T	Temperature
Λ	Capital Greek letter lambda
H	Hamiltonian
N	Number of harmonic oscillators
L	Lagrangian
ω	Greek letter omega, frequency
Θ	Heaviside function
Ω	Capital Greek letter omega
δ	Greek letter delta, delta function
κ	Greek letter kappa
χ	Greek letter chi
\mathbb{I}	Identity matrix
γ	Greek letter gamma
I	Current
ϕ	Magnetic flux
ρ	Density matrix
Tr	Trace
$ \bullet\rangle$	Vector, as known as a ket
$\langle\bullet $	Vector dual of ket, known as a bra
$\langle\bullet \bullet\rangle$	Inner product
\otimes	Tensor product
A^\dagger	Hermitian conjugate

\hbar	$\frac{h}{2\pi}$, modified Planck's constant
τ	Greek letter tau
σ	Greek letter sigma
α	Greek letter alpha
Δ	Capital Greek letter delta meaning variation
A^*	Complex conjugate
Γ	Capital Greek letter gamma
W	Work
Q	Heat
φ	Greek letter phi
ϵ	Greek letter epsilon
$\langle \bullet \rangle$	Expected value
$ \langle \bullet \rangle $	Absolute value
λ	Greek letter lambda
ξ	Greek letter xi
ζ	Greek letter zeta
β	Greek letter beta, $\beta = \frac{1}{k_B T}$
ν	Greek letter nu
∂	Partial derivation
Φ	Greek letter phi
\in	Is member of

CONTENTS

1	INTRODUCTION	25
2	CLASSICAL DYNAMICS	31
2.1	Standard bilinear model	31
2.2	Standard nonlinear model	35
2.3	Nonlinear dissipation from a bilinear Lagrangian: modified spectral function	39
2.3.1	Recovery of dissipation rates	43
2.3.2	Avoidance of anomalous diffusion	45
2.3.3	Hydrodynamics-inspired model	47
3	QUANTUM DYNAMICS	51
3.1	Quantum Brownian motion	51
3.2	Path integral representation of Quantum Mechanics	52
4	DISSIPATIVE ADAPTATION	61
4.1	Systems in Equilibrium	62
4.2	Out-of-equilibrium systems	63
4.2.1	Crooks's Theorem	64
4.2.2	Generalization of the second law of thermodynamics	65
4.3	Hypothesis of dissipative adaptation	66
4.4	Quantum regime of dissipative adaptation	69
4.4.1	Quantum work	69
4.4.2	Quantum dissipative adaptation	71
5	TWO-LEVEL SYSTEMS IN A DOUBLE WELL POTENTIAL	75
5.1	Spin-boson model	79
5.1.1	Quantum mechanical calculations	80
5.1.2	Path integral expression without dissipation	81
5.1.3	Influence of the environment	85
5.1.4	Dynamics with NIBA	90
5.1.5	Parameter analysis	91
6	DRIVEN SPIN-BOSON MODEL AND DISSIPATIVE ADAPTATION HYPOTHESIS	93
6.1	Perturbative driven Spin-boson model	93
6.1.1	Path integral for the driven spin-boson model	95

6.2	Thermodynamic quantities	97
6.3	Relation between transition probability and work functional	100
6.3.1	Density matrix in terms of work	102
6.4	Relation of symmetric and asymmetric bias	103
6.5	Non-equilibrium organization in the driven spin-boson model	104
7	CONCLUSIONS	113
	REFERENCES	117
	APPENDIX	127
	APPENDIX A – TWO-TIME CORRELATION FUNCTIONS AND FLUCTUATION-DISSIPATION THEOREM	129
	APPENDIX B – RESPONSE THEORY	131
B.1	Linear response theory of an environment perturbed by one particle	131
B.2	Nonlinear response theory of an environment perturbed by a pair of particles within the nonlinear coupling model	132
B.3	Nonlinear response theory of an environment perturbed by a pair of particles within the bilinear coupling model (modified bilinear model)	134
	APPENDIX C – DIFFUSION COEFFICIENT	137
	APPENDIX D – PATH INTEGRAL FORMALISM	139
	APPENDIX E – DERIVATION OF ACTION BY PATH INTEGRAL FORMALISM	141
E.1	Free harmonic oscillator	141
E.2	Driven harmonic oscillator	144
	APPENDIX F – INFLUENCE FUNCTIONAL	151
	APPENDIX G – INITIAL ENVIRONMENT DENSITY OPERATOR	157
	APPENDIX H – QUANTUM WORK OF A SINGLE PHOTON	159
	APPENDIX I – DERIVATION OF FUNCTIONAL OF WORK	161

1 INTRODUCTION

The exploration of dynamics in physics has always offered a vast realm for investigations. Since the introduction of Newton's laws of motion in the XVII century, studies of the way objects move have been a central focus in physics. In our daily lives, movements that cease when energy flow stops are witnessed - a phenomenon explained by dissipation (1). Therefore, understanding the physical system's dynamics is fundamental across several areas of physics, spanning both classical and quantum regimes.

The theoretical description of dissipative systems often involves an open system interacting with its environment through collisions or other means, facilitating energy exchanges (2). Microscopic theoretical models have been proposed towards descriptions of dissipation in classical (3,4) and quantum systems (5,6).

Brownian motion is the most widely studied example of dissipative dynamics out-of-equilibrium (1,7). Such a dynamic phenomenon describes a particle in a fluid known as thermal bath, which consists of many smaller particles. The suspended particles are typically much heavier than the medium ones. It is a random dynamics that depends on the characteristics of the fluid, such as viscosity. Since the complete dynamics of the particles in the thermal bath cannot be described, its statistical properties and stochastic theory can be used for modeling Brownian motion.

The theoretical approach that describes that phenomenon is the Langevin equation

$$m\ddot{q} + \eta\dot{q} + V(q) = f(t), \quad (1.1)$$

where q is the position coordinate, m is the mass of the particle, η is the damping coefficient, and $V(q)$ is an external potential. When an ensemble of identically prepared systems initially in thermal equilibrium and for high temperatures is considered, the fluctuating force, $f(t)$, satisfies relations $\langle f(t) \rangle = 0$ and $\langle f(t)f(t') \rangle = 2\eta k_B T \delta(t - t')$, characteristic of white noise*. In the absence of an external force applied to the particle ($f(t) = 0$), the average velocity $\langle \dot{q} \rangle$ of this dynamic system is null and its variance $\langle \dot{q}^2 \rangle$ is finite.

When a single Brownian particle is dealt with in the classical regime, both linear and nonlinear couplings result in equations of motion that describe the same dynamics for the Brownian particle in appropriate limits[†]. However, when the system of interest is extended to two Brownian particles, the most intuitive method - considering a bilinear coupling between the particles and a bath of oscillators - leads to an unphysical behavior,

* Null average and a memoryless process translate these statistical properties, indicating no correlation between fluctuating forces for times distinct to the characteristic time, t' , i.e., collisions between particles are independent.

[†] Ohmic limit and $V(x) = 0$.

which includes a free-particle motion for the relative coordinate and the absence of mutual effects between particles closer to each other, as stated by Duarte and Caldeira (8). The authors proposed a nonlinear system-reservoir coupling of an imaginary exponential type to address those issues.

The original insight for the use of the system-reservoir approach was the explanation of an otherwise intractable interaction with a complex environment. Ref.(8) provides an extension of that conventional approach to multiple particles; however, its results are still under debate. Some parameters, such as dissipation rate, require a clear explanation; therefore, researchers have investigated the relevance of environment-induced effects in various contexts, including biologically-inspired problems (9, 10), non-Markovianity (11), synchronization (12), quantum entanglement (13–16), among others.

The study in Ref.(8) was expanded into two particles in the present research, addressing a gap in the literature on bilinear Hamiltonian and equations of motions, which carry physical significance. The extension introduces a modified spectral function explicitly dependent on the relative distance between the two Brownian particles. Our method offers a versatile approach to constructing a phenomenological model for nonlinear environment-induced forces. As an application, the way to avoid the anomalous diffusion resulting from the standard nonlinear model is discussed (8) and how to phenomenologically model hydrodynamic interactions between a pair of Brownian particles in a viscous fluid is demonstrated (17).

Whereas the nonlinear model for two Brownian particles yields valuable equations of motion (8), the bilinear approach remains significant in both experimental and theoretical investigations. Recent demonstrations of environment-induced entanglement in the optical domain are related to the linear model results (18). Moreover, the linearity of the Hamiltonian system enables the model to be solvable in both quantum and classical regimes.

The importance of linearity can be highlighted, as in Ref.(19), in which the authors adopted a method that relied on an ansatz and the model's linearity to characterize entropy production by a quantum Brownian particle. By expanding the ansatz to multiple quantum Brownian particles, it could contribute to the research in the field of far-from-equilibrium thermodynamics of quantum many-body dissipative systems (20–22).

Researchers have extensively studied the model involving one Brownian particle in a set of harmonic oscillators. They have adopted it from optics, where light reflects and transmits through two mirrors, but interaction with the environment leads to energy loss. The coupling between internal and external electromagnetic fields, described by normal modes, explains such a energy loss. Each mode behaves like a harmonic oscillator, influencing energy loss over time and harmonic oscillators are treated as linearly coupled in amplitudes (23). The equations of motion resulting from the approach, under appropriate

limits, resemble Eq.(1.1), which describes the instantaneous interaction between particle and reservoir.

Despite our application of the classical regime to Brownian particles in the context of irreversible processes, Eq.(1.1) has also been used to describe the dynamics of the magnetic flux in a SQUID[‡] ring (23, 24). A classical single Brownian particle equation of motion can mathematically describe the magnetic flux, ϕ , trapped in the ring. Consequently, a similar Langevin equation can be derived for this quantum system (23), given by

$$C\ddot{\phi} + \frac{\dot{\phi}}{R} + U'(\phi) = I_f(t), \quad (1.2)$$

where C represents capacitance, R is resistance, U stands for potential, and I_f is a fluctuating current with properties such that $\langle I_f(t) \rangle = 0$ and $\langle I_f(t)I_f(t') \rangle = 2k_B T R^{-1} \delta(t - t')$ (25).

The way the systems evolve during dissipative processes must be examined towards the description of a general approach to dissipation in quantum mechanics (25). Researchers have considered two methods to generalize this study to quantum Brownian particles.

An approach involves the search for new quantization schemes and the other relies on the fact no system in nature is fully isolated. Therefore, researchers can consider a system of interest coupled with a bath or reservoir responsible for energy flow and where dissipation occurs. The latter approach, known as the system-reservoir approach, has been adopted for handling Hamiltonian systems.

The system and the environment can be considered isolated and can be quantified. Additionally, the interaction between the system of interest and the reservoir can be modelled considering the environment a set of non-interacting harmonic oscillators. Consequently, Langevin equation can be reproduced for the variable that describes the dynamics of the system of interest in appropriate limits.

Vernon first proposed a simple way to describe the bath (26), conceptualized as a set of an infinite number of harmonic oscillators coupled to the system of interest. The Hamiltonian of the total system can be written as

$$H_{SR} = H_S(x, p) + H_R(R_k, p_k) + H_I(x, R_k), \quad (1.3)$$

where H_S represents the Hamiltonian of the system of interest, with x and p corresponding to coordinate and momentum, respectively, H_R describes the bath formed by many harmonic oscillators, with R_k and p_k being coordinate and momenta, and H_I denotes the

[‡] *Superconducting quantum interference device*, where quantum tunneling can be observed on a macroscopic scale.

coupling between the system of interest and the reservoir, i.e., their interaction, which involves the coordinate of the system of interest, x , and the coordinate of the bath, R_k .

The framework has proven useful across classical and quantum domains (1, 7, 25) and can be applied to cases in which particles and the environment are linearly coupled, including strongly damped systems such as Caldeira-Leggett model. Under certain conditions, the model can accurately replicate Brownian motion in the classical regime. Initially, it addressed the quantum dissipative tunneling problem using the Brownian motion paradigm (23).

The system-reservoir Hamiltonian, denoted as H_{SR} , is expressed as

$$H_{SR} = \frac{p^2}{2m} + V(x) + \sum_{k=1}^N \left[\frac{p_k^2}{2m_k} + \frac{m_k \omega_k^2}{2} \left(R_k - \frac{C_k}{m_k \omega_k^2} x \right)^2 \right], \quad (1.4)$$

where the particle has mass m and momentum p , situated in a potential V at position x . The bath comprises N harmonic oscillators with ω_k frequencies, m_k masses, and p_k momenta, located at positions R_k . C_k depend on the specifics of the coupling between the particle and the bath.

Towards extending the study of dissipation to quantum systems, this research explores the concept of dissipative adaptation. The hypothesis, first proposed for the classical regime (27), is a generalization of Boltzmann distribution for non-equilibrium systems. Valente (21) derived the quantum extension of the hypothesis for a Λ model[§]. The present thesis investigates the driven spin-boson model and its connections with thermodynamic quantities for exploring the concept of dissipative adaptation in the driven spin-boson system.

As addressed in (28), the spin-boson model has been extensively investigated and continues to be a focal point of research. It is considered a representative example of an open quantum system, designated as a system in contact with an environment capable of exchanging energy with the surrounding medium (29–34). This theoretical framework describes the interaction of a single spin (qubit) with a dissipative environment characterized by an infinite number of bosonic modes. The model holds significance across various domains of physics and chemistry, finding applications in electron tunneling (29, 30), excitation transport within biological complexes (31, 32), advancements in superconducting qubit technologies (33, 34), among others.

In addition to reconciling both nonlinear and linear coupling with a proposed modified spectral function, our primary goal is to address the following question: Is it possible to demonstrate whether an asymmetric perturbation can cause a particle to localize in one of the potential well bottoms? If so, what is the system's energy analysis (dissipated work)?

[§] A model is a three-level system with one excited state and two nondegenerate ground ones.

Thesis outline

This thesis investigates the dissipation of classical and quantum systems and, therefore, was divided into two main research parts, namely, classical and quantum dynamics. The former, focused on two Brownian particles with a nonlinear response theory, have resulted in a paper published in a peer-reviewed journal (22).

The second part is devoted to a study of quantum dissipative systems, specifically exploring the driven spin-boson model and the dynamics of bistable quantum systems through the path integral formalism towards identifying non-equilibrium localization phenomena and their relation to thermodynamic quantities, such as work.

The thesis is structured as follows: Chapter 2 addresses standard bilinear (Sec. 2.1) and nonlinear models (Sec. 2.2) for the obtaining of Langevin equations of motion for two Brownian particles as the system of interest. Moreover, the dynamics containing a nonlinear dissipative force is derived from bilinear Lagrangian (Sec. 2.3). The method proposes a spectral function that depends on the relative distance between the particles. The approach opens path for the description of diverse scenarios, such as discussions on how to avoid the anomalous diffusion that appears in the standard nonlinear model (Sec. 2.3.2). Additionally, the application of the approach is explored towards the modelling of a pair of Brownian particles sharing the same hydrodynamic environment (Sec. 2.3.3).

Chapter 3 delves into a study of the quantum dynamics of Brownian particles (Sec. 3.1) and introduces the formalism of the path integral (Sec. 3.2), which plays a crucial role in deriving the dynamics of such systems.

Chapter 4 details dissipative adaptation by firstly introducing the key concepts of equilibrium (Sec. 4.1) and out-of-equilibrium systems (Sec. 4.2). It then briefly overviews how to derive England's equation for the hypothesis of the nonequilibrium thermodynamics mechanism known as dissipative adaptation and then revises the quantum version of that notion for a three-level system (Sec. 4.4).

Chapter 5 presents the system and models addressed towards reporting the results for the driven spin-boson model, which include the two-level systems in a double-well potential with a specific focus on the spin-boson model (Sec. 5.1).

Chapter 6 introduces our model, which involves the application of a time-dependent bias to a spin-boson model using the path integral formalism (Sec. 6.1.1). Towards verifying the possibility of organizing the system in such a non-equilibrium state, not only is the thermodynamic analysis of the dissipative system explored (Sec. 6.3), but also the transition probability is derived from a ground state to an excited one (Sec. 6.5)

Finally, Chapter 7 reports the findings and some open questions. The Appendices provide some of the detailed derivations.

2 CLASSICAL DYNAMICS

Both approaches, linear and nonlinear couplings, have extensively explored the study of a Brownian particle coupled to a bath of independent harmonic oscillators (8, 23, 25, 35). However, the development of a system-reservoir approach for multiple particles in a collective environment is not straightforward and researchers have put proposed conflicting models to tackle the problem.

This chapter revisits the equations of motion for two Brownian particles with the use of linear and nonlinear coupling between the particles and bath of oscillators. The first two sections report on the Brownian particles being coupled to only the bath and not to each other and the statistical properties of the fluctuating forces that lead to distinct dynamics are briefly reviewed. The third section is devoted to the results. The dynamics of two Brownian particles are obtained with no exponential coupling, avoiding the coupling solely to the center of mass (14). Although, in the last section, a Lagrangian with a direct coupling term between the particles was chosen, it can be made null for recovering Langevin-like equations of motion. The modification does not alter the invariance of the Lagrangian presented in Ref.(14). The way a bilinear model can obtain the nonlinear dissipation term $\eta_e[u(t)]$ from a nonlinear coupling approach is highlighted in the first part of the thesis.

2.1 Standard bilinear model

Researchers have extensively explored the usual Caldeira-Leggett model, which bilinearly couples the position coordinates of a Brownian particle to the position coordinates of the bath, in both classical and quantum regimes (1, 13, 25, 36, 37). However, its extension for multiple Brownian particles is not straightforward, since some unphysical effects may emerge (8, 25).

An explicit Lagrangian must be formulated for the total system for the obtaining of Langevin equation in the appropriate limit. For the bilinear model, the Lagrangian of two classical Brownian particles immersed in a same environment reads (8),

$$\begin{aligned}
 L = & \frac{m}{2}(\dot{x}_1^2 + \dot{x}_2^2) - V(x_1) - V(x_2) + \sum_{k=1}^N \frac{m_k}{2} (\dot{R}_k^2 - w_k^2 R_k^2) \\
 & - \sum_{k=1}^N R_k (C_k^{(1)} x_1 + C_k^{(2)} x_2) - \sum_{k=1}^N \frac{(C_k^{(1)} x_1 + C_k^{(2)} x_2)^2}{2m_k w_k^2}.
 \end{aligned} \tag{2.1}$$

The system of interest, which consists of the two Brownian particles, has two independent degrees of freedom, where \dot{x}_i and x_i ($i = 1, 2$) are the velocity and the positions of the particles, respectively, and m is mass. The bath is a collection of non-interacting harmonic

oscillators, with \dot{R}_k and R_k representing the velocity and position of the k -th harmonic oscillator, respectively, with frequency ω_k and mass m_k .

A linear coupling was assumed in the particle's position between each Brownian particle and oscillators, with distinct coupling strengths $C_k^{(i)}$ so that the particles can be distinguished and the local and non-local effects can be separable. According to Ref.(8), the local effect describes the energy dissipation of each particle. In contrast, the so-called non-local effect mediates the interaction between the particles*. The last term of the Lagrangian is a counterterm inserted for generating the environment-induced adjustment of the external potential †.

Such a microscopic model, from which the Langevin-like equation was recovered, was adopted. A bath was chosen as a set of harmonic oscillators because they are precisely solvable in both classical and quantum regimes. The choice for modelling the thermal bath is justified by techniques like Raman spectroscopy, a type of vibrational spectroscopy‡. Researchers have revealed the harmonic oscillator's behavior is consistent with the molecule's quantized vibrational energy levels (38, 39) and a quantum optical application in which the bath comprises a set of harmonic oscillators representing the light field quantized can be obtained (40, 41).

Euler-Lagrange equations§ (42) can be derived for both system and bath calculating

$$m\ddot{x}_i + \frac{dV(x_i)}{dx_i} + \sum_{k=1}^N \left(C_k^{(i)} R_k + \frac{C_k^{(i)}}{m_k \omega_k^2} (C_k^{(1)} x_1 + C_k^{(2)} x_2) \right) = 0$$

$$\sum_{k=1}^N \left(m_k \ddot{R}_k + m_k \omega_k^2 R_k + C_k^{(1)} x_1 + C_k^{(2)} x_2 \right) = 0,$$

where, $i = 1, 2$. The latter can be solved by Laplace transform method (43), from which the definition of the fluctuating force and the dissipation term can be addressed according to the relation with the system's variables. Solving the bath coordinate equation leads to relation

$$R_k(s) = \sum_{k=1}^N \left(\frac{sR_k(0)}{s^2 + \omega_k^2} + \frac{\dot{R}_k(0)}{s^2 + \omega_k^2} - \frac{(C_k^{(1)} x_1(s) + C_k^{(2)} x_2(s))}{m_k (s^2 + \omega_k^2)} \right). \quad (2.2)$$

* Although called the same way as in quantum mechanics, terms local and non-local here represent the interaction between the particles mediated by the bath not in the sense of representing quantum effects, such as locality.

† The counterterm guarantees the translational invariance of the Lagrangian.

‡ Used for the analysis of molecular vibrations.

§ The variational invariance of the (Hamilton's Principle) is imposed for the obtaining of Euler-Lagrange equations of motion.

Applying the Laplace transform results in

$$R_k(t) = \sum_{k=1}^N \left(\frac{1}{2\pi i} \int_{\sigma-i\infty}^{\sigma+i\infty} \left[\frac{sR_k(0) + \dot{R}_k(0)}{s^2 + \omega_k^2} \right] e^{st} ds - \frac{1}{2\pi i m_k} \int_{\sigma-i\infty}^{\sigma+i\infty} \frac{(C_k^{(1)} x_1(s) + C_k^{(2)} x_2(s)) e^{st} ds}{s^2 + \omega_k^2} \right), \quad (2.3)$$

where identity $\frac{1}{s^2 + \omega_k^2} \equiv \frac{1}{\omega_k^2} \left(1 - \frac{s^2}{s^2 + \omega_k^2} \right)$ can be used so that

$$\begin{aligned} R_k(t) &= \sum_{k=1}^N \left(\frac{1}{2\pi i} \int_{\sigma-i\infty}^{\sigma+i\infty} \left[\frac{sR_k(0) + \dot{R}_k(0)}{s^2 + \omega_k^2} \right] e^{st} ds - \frac{(C_k^{(1)} x_1(t) + C_k^{(2)} x_2(t))}{m_k \omega_k^2} \right. \\ &\quad \left. + \frac{d}{dt} \left[\frac{1}{2\pi m_k \omega_k^2} \int_{\sigma-i\infty}^{\sigma+i\infty} \frac{s}{s^2 + \omega_k^2} (C_k^{(1)} x_1(s) + C_k^{(2)} x_2(s)) e^{st} ds \right] \right) \\ &= \sum_{k=1}^N \left(\frac{1}{2\pi i} \int_{\sigma-i\infty}^{\sigma+i\infty} \left[\frac{sR_k(0) + \dot{R}_k(0)}{s^2 + \omega_k^2} \right] e^{st} ds - \frac{(C_k^{(1)} x_1(t) + C_k^{(2)} x_2(t))}{m_k \omega_k^2} \right. \\ &\quad \left. + \frac{d}{dt} \left[\frac{1}{m_k \omega_k^2} \int_0^t \cos \omega_k(t-t') (C_k^{(1)} x_1(t') + C_k^{(2)} x_2(t')) dt' \right] \right). \end{aligned}$$

Therefore,

$$\begin{aligned} R_k(t) &= \sum_{k=1}^N \left(R_k(0) \cos \omega_k t + \frac{\dot{R}_k(0)}{\omega_k} \sin \omega_k t - \frac{(C_k^{(1)} x_1(t) + C_k^{(2)} x_2(t))}{m_k \omega_k^2} \right. \\ &\quad \left. + \frac{\cos \omega_k t}{m_k \omega_k^2} (C_k^{(1)} x_1(0) + C_k^{(2)} x_2(0)) + \frac{1}{m_k \omega_k^2} \int_0^t \cos \omega_k(t-t') (C_k^{(1)} \dot{x}_1(t') + C_k^{(2)} \dot{x}_2(t')) dt' \right). \end{aligned} \quad (2.4)$$

The above equation is derived from the convolution theorem and Laplace transform of trigonometric functions (cosine and sine) (43).

Replacing $R_k(t)$ into the equation for the i -th particle leads to the equation of motion

$$\begin{aligned} m \ddot{x}_i + \frac{dV(x_i)}{dx_i} + \sum_{k=1}^N \frac{C_k^{(i)2}}{m_k \omega_k^2} \int_0^t \cos \omega_k(t-t') \dot{x}_i(t') dt' \\ + \sum_{k=1}^N \frac{C_k^{(i)} C_k^{(j)}}{m_k \omega_k^2} \int_0^t \cos \omega_k(t-t') \dot{x}_j(t') dt' = f_i(t), \end{aligned}$$

where $f_i(t)$ can be interpreted as the fluctuating force determined by the initial conditions of the bath,

$$f_i(t) = - \sum_k C_k^{(i)} \left[\dot{R}_k(0) \frac{\sin \omega_k t}{\omega_k} + \tilde{R}_k(0) \cos \omega_k t \right], \quad (2.5)$$

where $\tilde{R}_k(0) = R_k(0) + (C_k^{(1)} x_1(0) + C_k^{(2)} x_2(0)) / (m_k \omega_k^2)$.

m_k , ω_k , and C_k must be specified for each oscillator for characterizing the bath. A single parameter that includes all those variables would be convenient; therefore, the

bath's spectral density, $J(\omega)$, related to the normal modes of the bath and its interaction with the Brownian particles is introduced. In other words, those functions assign a weight to the influence of a given frequency of the bath spectrum on the motion of the Brownian particles (25, 44).

The sum can be replaced in $J(\omega)$ with an integral for a large number of bath's harmonic oscillators, thus making the spectral density continuous in ω , called Ohmic spectral function. Considering a continuum frequency limit for the spectrum of the bath implies smooth functions, hence, linear in ω . Below is the expression for the spectral density;

$$J(\omega) = \frac{\pi}{2} \sum_{k=1}^N \frac{C_k^2}{m_k \omega_k^2} \delta(\omega - \omega_k) \equiv \eta \omega \Theta(\Omega - \omega). \quad (2.6)$$

High-frequency cutoff Ω is the bath's characteristic frequency (45, 46). It sets the timescale of the microscopic motion of the environment's components (25) and also avoids divergence in the force-force correlation function for high frequencies (47). Here, Θ represents the Heaviside step function.

Regarding the dissipation term, the distribution of oscillators is similar to that proposed by Leggett (48), according to which the bath represents a homogeneous medium[¶]; consequently, the same effect is expected on each particle. Moreover, the recovery of a linear dependence of the velocity term is expected in the Langevin-like equation (44). Assuming an Ohmic bath with the usual spectral function for each particle as

$$J_i(\omega) = \frac{\pi}{2} \sum_{k=1}^N \frac{C_k^{(i)2}}{m_k \omega_k} \delta(\omega - \omega_k) = \eta_i \omega \Theta(\Omega - \omega), \quad (2.7)$$

and a mixed spectral function,

$$J_{12}(\omega) = \frac{\pi}{2} \sum_{k=1}^N \frac{C_k^{(1)} C_k^{(2)}}{m_k \omega_k} \delta(\omega - \omega_k) = \eta_{12} \omega \Theta(\Omega - \omega). \quad (2.8)$$

The latter describes the interaction between the particles. Those expressions introduce dissipation rates η_i and η_{12} . Although the particles do not have direct coupling between them, the bath is responsible for creating this interaction, leading to an interaction between the particles induced by the bath. The function provides satisfactory equations of motion, eliminating the distance effects; however, it must be apparent so as to justify the mixed dissipation term, for example, via response theory.

Setting new variables as $q = \frac{(x_1+x_2)}{2}$ and $u = x_1 - x_2$ as the center of mass and relative coordinates and for $V(x_i) = 0$, then Langevin-like equations can be derived

$$\begin{aligned} m\ddot{q}(t) + (\eta + \eta_{12})\dot{q}(t) &= f_q(t), \\ m\ddot{u}(t) + (\eta - \eta_{12})\dot{u}(t) &= f_u(t), \end{aligned} \quad (2.9)$$

[¶] The effects of bath on both particles separately are expected to be on average the same.

where $f_q(t)$ and $f_u(t)$ are interpreted as the fluctuating forces for the center of mass and the relative coordinates, respectively, as follows

$$f_q(t) = \frac{f_1(t) + f_2(t)}{2} = - \sum_{k=1}^N \frac{(C_k^{(1)} + C_k^{(2)})}{2} \left(\dot{R}_k(0) \frac{\sin w_k t}{w_k} + \tilde{R}_k(0) \cos w_k t \right), \quad (2.10)$$

$$f_u(t) = f_1(t) - f_2(t) = \sum_{k=1}^N (C_k^{(1)} - C_k^{(2)}) \left(\dot{R}_k(0) \frac{\sin w_k t}{w_k} + \tilde{R}_k(0) \cos w_k t \right). \quad (2.11)$$

The statistical properties of those forces depend on the initial state of the total system.

Some consequences of those results were discussed in Ref. (8). However, some of the must be focused on here. If a same coupling is assumed for each particle and bath ($C_k^{(1)} = C_k^{(2)}$)^{||}, dissipation and fluctuating force for the relative coordinate vanish, once $\eta = \eta_{12}$ and $f_u(t) = 0$ leading to free-particle motion for the relative coordinate given by

$$\ddot{u}(t) = 0. \quad (2.12)$$

Even for nonidentical couplings ($C_k^{(1)} \neq C_k^{(2)}$), η_{12} is independent of the particles's relative distance, showing an instantaneous interaction between spatially separated elements, although Eq.(2.8) is not distance-dependent.

As stated in Ref.(8), such undesired characteristics result from the lack of an adequate length scale for environment-mediated phenomena, which are supposed to appear in a real physical system (49). The authors in Ref. (8) introduced a nonlinear coupling between system and bath to account for proper dynamics features.

2.2 Standard nonlinear model

Caldeira-Leggett model can be extended for two particles through a symmetric Lagrangian

$$L = \frac{m}{2} (\dot{x}_1^2 + \dot{x}_2^2) + \frac{1}{2} \sum_{k=1}^N m_k \left(\dot{R}_k \dot{R}_{-k} - \omega_k^2 R_k R_{-k} \right) - \frac{1}{2} \sum_{k=1}^N [(C_{-k}(x_1) + C_{-k}(x_2)) R_k + (C_k(x_1) + C_k(x_2)) R_{-k}]. \quad (2.13)$$

The system of interest remains the same; however, the bath is a symmetrized collection of harmonic oscillators. Such symmetrization in k can be used, as stated in Ref. (8, 44) due to the maintenance of the Lagrangian invariance.

The coupling between the bath and the particles is nonlinear in the bath coordinates,

$$C_k(x) = \kappa_k e^{ikx}. \quad (2.14)$$

^{||} It is a reasonable assumption regarding the case of two close particles in a same environment.

The choice of an exponential coupling parameter guarantees the translational invariance of the Lagrangian. When the particle is dislocated a distance d , then

$$C_{-k}(x+d)R_k = C_{-k}(x)e^{-ikd}R_k.$$

New variables can be defined for the bath coordinate as $\tilde{R}_k = e^{-ikd}R_k$, preserving the invariance of the Lagrangian. The authors in Ref. (8) considered symmetrization and exponential coupling a way to guarantee homogeneity and translational invariance.

Therefore, the nonlinear model does not require a counterterm because of the coupling chosen. Eq.(2.13) can provide dissipative equations of motion on the variable of the particles - see Ref. (1,44) for a detailed derivation for equations of motion of one and two particles.

Index k now has dimensions of $[L]^{-1}$, which explains why it introduces the required length scale. Not only does this type of coupling (Eq.(2.14)) guarantee Lagrangian translational invariance, but it also has an experimental justification. As an example, such coupling appears in the polaron problem (1) and also with interactions in a fermionic bath (45,46).

Techniques similar to those addressed in the previous subsection lead to the following particles' equations of motion (8):

$$\begin{aligned} m\ddot{x}_i(t) + \sum_{k=1}^N \frac{k^2\kappa_k\kappa_{-k}}{m_k\omega_k^2} & \left(\int_0^t \cos k(x_i(t) - x_i(t')) \cos \omega_k(t-t')\dot{x}_i(t')dt' \right. \\ & \left. + \int_0^t \cos k(x_i(t) - x_j(t')) \cos \omega_k(t-t')\dot{x}_j(t')dt' \right) \\ & + \sum_{k=1}^N \frac{k\kappa_k\kappa_{-k}}{m_k\omega_k^2} \sin k(x_i(t) - x_j(t)) = F_i(t), \end{aligned}$$

where $i \neq j = 1, 2$ and $F_i(t)$ can be interpreted as the fluctuating force. The nonlinear dissipation kernel can be identified as

$$K(r, \tau) = \sum_{k=1}^N \frac{k^2\kappa_k\kappa_{-k}}{m_k\omega_k^2} \cos kr \cos \omega_k\tau, \quad (2.15)$$

which shows the interaction between the particles and the environment (8), as well as a potential term

$$V(r(t)) = - \sum_{k=1}^N \frac{\kappa_k\kappa_{-k}}{m_k\omega_k^2} \cos kr(t). \quad (2.16)$$

Finally, the equations of motion can be written as

$$\begin{aligned} m\ddot{x}_i(t) + \int_0^t K(x_i(t) - x_i(t'), t-t')\dot{x}_i(t')dt' + \int_0^t K(x_i(t) - x_j(t'), t-t')\dot{x}_j(t')dt' \\ + \frac{\partial}{\partial x_i} V(x_i(t) - x_j(t)) = F_i(t). \end{aligned} \quad (2.17)$$

Linear response theory expresses kernel and potential as a function of the imaginary part of the dynamical response of the environment oscillators, which is given by $\text{Im}\chi_k^{(i)}(\omega) = (\pi/2m_k\omega_k)\delta(\omega - \omega_k)$. Studies such as (45,46) exemplified this concept:

$$K(r, \tau) = \sum_{k=1}^N \int_0^\infty d\omega \, 2 k^2 \kappa_k \kappa_{-k} \frac{\text{Im}\chi_k^{(i)}(\omega)}{\pi\omega} \cos \omega_k \tau \cos kr, \quad (2.18)$$

and

$$V(r(t)) = - \sum_{k=1}^N \int_0^\infty d\omega \, 2 \kappa_k \kappa_{-k} \frac{\text{Im}\chi_k^{(i)}(\omega)}{\pi\omega} \cos kr(t), \quad (2.19)$$

which assumes the transformation of a discrete set of oscillators into a continuum. Bath is here considered a collection of damped harmonic oscillators. Therefore, delta function is modified to a Lorentzian that peaks around ω_k for an analysis of the long time limit, in which a low frequency is compared to the cutoff frequency. The Ohmic limit in which $\text{Im}\chi_k^{(i)}(\omega) \propto \omega$ has been assumed (8,44–46) is

$$\text{Im}\chi_k^{(i)} \approx \tilde{f}(k) \omega \Theta(\Omega - \omega). \quad (2.20)$$

This Ohmic approximation introduces a high-frequency cutoff Ω as the characteristic frequency of the bath. The choice of the Ohmic limit enables a separation between time and length scales, which is fundamental for the analysis. A dynamical response function $\chi_k^{(i)}$ from a harmonic oscillator with wave number k as a kernel component was used. Therefore, $\chi_k^{(i)}$ is equivalent to the spectral function of the bilinear model, $J(\omega)$.

After those considerations, the nonlinear equations of motion read

$$\begin{aligned} m\ddot{q}(t) + (\eta + \eta_e[u(t)]) \dot{q}(t) &= f_q(t), \\ m\ddot{u}(t) + (\eta - \eta_e[u(t)]) \dot{u}(t) + V_e'(u(t)) &= f_u(t), \end{aligned} \quad (2.21)$$

where

$$V_e(u) = - \frac{2\Omega\eta}{\pi k_0^2 (k_0^2 u^2 + 1)}, \quad (2.22)$$

is an environment-induced potential that depends on the relative distance. Similarly,

$$\eta_e[u(t)] = \eta \frac{(1 - 3k_0^2 u^2)}{(k_0^2 u^2 + 1)^3}, \quad (2.23)$$

represents a bath-mediated dissipation rate that also depends on relative distance.

A relation between the dissipation rate and the microscopic parameters of the bath is defined as follows (44)

$$\eta = \sum_{k=1}^N k^2 \kappa_k \kappa_{-k} \tilde{f}(k). \quad (2.24)$$

When the summation over k is turned into an integral, expression $\sum_k \rightarrow (L/2\pi) \int dk$, where L represents the system's dimension, becomes valid. The change leads to the definition of function

$$\eta g(k) \equiv \frac{L}{2\pi} \kappa_k \kappa_{-k} \tilde{f}(k), \quad (2.25)$$

such that $\int_0^\infty dk g(k) k^2 = 1$. Many functions $g(k)$ can be used and the same of Ref. (8) was chosen in this study

$$g(k) = \frac{e^{-k/k_0}}{2k_0^3}, \quad (2.26)$$

where k_0^{-1} determines the length scale of system and, for fermionic bath, for example, k_0 is proportional to k_F , which is the Fermi wave number (46, 50).

The independent Brownian movement can be recovered for arbitrarily large distances whereas for particles close to each other ($k_0 u \ll 1$), the equations of motion describe a rich environment-induced behavior. The effective potential becomes a harmonic potential,

$$V(k_0 u \ll 1) = -\frac{m\omega^2}{2k_0^2} + \frac{m\omega^2 u^2}{2}, \quad (2.27)$$

where $\omega = \sqrt{\frac{4\eta\Omega}{m\pi}}$. Additionally, the equation of motion for the relative coordinate exhibits the behavior of a harmonic oscillator.

Because both dissipative and fluctuating forces are finite for every finite $u(t)$, the free-particle anomaly found in the bilinear model is no longer present. The exponential coupling for one particle for a long time and small distances limit recovers the same results of the linear model (8).

The approach shows two dissipation terms, i.e., one due to the bath influence and given by η , and another dependent on the relative distance between the two Brownian particles, $\eta_e[u(t)]$, known as the effective dissipation term. However, effective potential $V_e(u)$ between the particles, determined by the nonlinear coupling, would act as a binding potential mediated by the bath.

The statistical properties of the fluctuating forces are such that (see Appendix C),

$$\begin{aligned} \langle f_i(t) \rangle &= \langle f_q(t) \rangle = \langle f_u(t) \rangle = 0 \\ \langle f_i(t) f_i(t') \rangle &= 2\eta k_B T \delta(t - t'), \\ \langle f_1(t) f_2(t') \rangle &= 2\eta_e[u(t)] k_B T \delta(t - t'), \\ \langle f_q(t) f_q(t') \rangle &= (\eta + \eta_e[u(t)]) k_B T \delta(t - t'), \\ \langle f_u(t) f_u(t') \rangle &= 4(\eta - \eta_e[u(t)]) k_B T \delta(t - t'), \end{aligned}$$

which yield different shapes for the correlation functions, but do not invalidating the usual fluctuation-dissipation theorem.

The nonlinear coupling is responsible for the effective potential in the equations of motion. The following section explores the consequences of those effective terms emerging from the derivation when a bilinear Lagrangian with a distance-dependent spectral function is considered. A modified spectral function dependent on the relative distance between the Brownian particles is suggested for the obtaining of the same dissipation rates used in a nonlinear coupling approach, but now starting with a bilinear Lagrangian.

2.3 Nonlinear dissipation from a bilinear Lagrangian: modified spectral function

As discussed elsewhere, exponential coupling is an alternative to avoiding unphysical results such as the ones from the bilinear coupling approach. Both bilinear (Eq.(2.9)) and nonlinear coupling models (Eq.(2.21)) were reviewed for the two Brownian particles in previous sections.

The goal here is to achieve the dynamics of two Brownian particles without using exponential coupling and coupling solely to the center of mass (14), which is important for reconciling the nonlinear dissipation with the bilinear coupling model, even with a linear Lagrangian.

The motivation for using a linear Lagrangian was reported at the opening of this chapter and it must be again highlighted the calculations can be performed more efficiently with linear systems. Some situations require linearity, as cited during the analysis of the entanglement for multiple particles (19).

Let us start with a quadratic Lagrangian with harmonic potential, a counterterm, and distinct coupling parameters (14)

$$\begin{aligned}
L = & \frac{m}{2}(\dot{x}_1^2 + \dot{x}_2^2) - \frac{1}{2}m(\omega_1 x_1^2 + \omega_2 x_2^2) - mc_{12}x_1x_2 \\
& + \sum_{k=1}^N \left(\frac{m_k \dot{R}_k^2}{2} - \frac{m_k \omega_k^2 R_k^2}{2} \right) - \sum_{k=1}^N \left(C_k^{(1)} x_1 + C_k^{(2)} x_2 \right) R_k \\
& - \sum_{k=1}^N \frac{\left(C_k^{(1)} x_1 + C_k^{(2)} x_2 \right)^2}{2m_k \omega_k^2},
\end{aligned} \tag{2.28}$$

Since the choice of the potential does not matter for deriving the Langevin-like equation, the harmonic potential, usually reported in literature, is maintained. Additionally, a coupling term, given by c_{12} , between the particles can be considered, as stated in Ref.(14).

As discussed at the end of the section, c_{12} does not change the dynamics of the two particles derived from the nonlinear coupling approach when reconciliation is dealt with in the dissipation terms.

It must be emphasized that each particle is assumed to have a distinct coupling parameterin ($C_k^{(1)} \neq C_k^{(2)}$) for avoiding the anomalous free-particle motion for the relative coordinate, as in Eq.(2.12), otherwise the bath decouples from $u = x_1 - x_2$.

The following equations of motion for the particles can be obtained by a similar calculation previously conducted

$$m\ddot{x}_i + \frac{dV(x_i)}{dx_i} + mc_{12}x_j + \sum_{k=1}^N \frac{C_k^{(i)2}}{m_k\omega_k^2} \int_0^t \cos \omega_k(t-t')\dot{x}_i(t')dt' + \sum_{k=1}^N \frac{C_k^{(i)}C_k^{(j)}}{m_k\omega_k^2} \int_0^t \cos \omega_k(t-t')\dot{x}_j(t')dt' = f_i(t), \quad (2.29)$$

where $i \neq j = 1, 2$, and $f_i(t)$ can be interpreted again as the fluctuating force,

$$f_i(t) = - \sum_{k=1}^N C_k^{(i)} \left[\dot{R}_k(0) \frac{\sin \omega_k t}{\omega_k} + \tilde{R}_k(0) \cos \omega_k t \right], \quad (2.30)$$

where $\tilde{R}_k(0)$ is defined as $\tilde{R}_k(0) = R_k(0) + (C_k^{(1)}x_1(0) + C_k^{(2)}x_2(0)) / (m_k\omega_k^2)$.

The equations of motion are rewritten for denoting the center of mass and relative coordinates as

$$m\ddot{q}(t) + \frac{1}{2} \left(\frac{dV(x_1)}{dx_1} + \frac{dV(x_2)}{dx_2} \right) + mc_{12}q(t) + \frac{1}{2} \int_0^t [K_1(t-t')\dot{x}_1(t') + K_2(t-t')\dot{x}_2(t')] dt' + \int_0^t K_{ij}(t-t')\dot{q}(t')dt' = f_q(t), \quad (2.31)$$

$$m\ddot{u}(t) + \left(\frac{dV(x_1)}{dx_1} - \frac{dV(x_2)}{dx_2} \right) - mc_{12}u(t) + \int_0^t [K_1(t-t')\dot{x}_1(t') - K_2(t-t')\dot{x}_2(t')] dt' - \int_0^t K_{ij}(t-t')\dot{u}(t')dt' = f_u(t). \quad (2.32)$$

The dissipation kernels in Eqs. (2.31) and (2.32) are distinct from those in Ref. (8). Here, the potential term mediated by the bath does not appear due to the characteristics of our coupling and the translational invariance of the Lagrangian assumed, as in Ref. (8)**.

The absence of spatial dependence in the environment-induced effects can be observed in

$$K_i(t-t') = \sum_{k=1}^N 2 C_k^{(i)2} \int_0^\infty d\omega \frac{\text{Im} \chi_k^{(i)}(\omega)}{\pi\omega} \cos \omega(t-t'), \quad (2.33)$$

$$K_{ij}(t-t') = \sum_{k=1}^N 2 C_k^{(i)} C_k^{(j)} \int_0^\infty d\omega \frac{\text{Im} \chi_k^{(ij)}(\omega)}{\pi\omega} \cos \omega(t-t'), \quad (2.34)$$

** In this reference, the counterterm was used to maintain the translational invariance of the Lagrangian. Therefore, the effective potential term arises from the effect generated by the bath, as explored in Sec. (2.1).

where the kernels are expressed in terms of the imaginary part of the bath susceptibility functions, as given by Eq.(2.18). Regarding the single-particle dissipation rates,

$$\eta \equiv \sum_{k=1}^N C_k^{(i)2} \tilde{f}(k), \quad (2.35)$$

where $\tilde{f}(k)$ arises from the Ohmic approximation in Eq.(2.33), namely,

$$\text{Im } \chi_k^{(i)}(\omega) \approx \tilde{f}(k) \omega \Theta(\Omega - \omega)$$

(similarly to Eq.(2.20)). $\sum_k C_k^{(i)2} \tilde{f}(k)$ is replaced by $\eta \int dk k^2 g(k)$, where $g(k) = \exp(-k/k_0)/(2k_0^3)$ (as in Sec. 2.2), for obtaining the continuum limit.

Two-particle susceptibility χ_k is crucial in our derivation. The response theory explains how the bath of oscillators responds to the time-dependent external influences of two Brownian particles when the particles slightly affect the bath. The bath is assumed large enough to have a continuous frequency distribution, which is a typical assumption in open systems research. The mixed susceptibility must adhere to specific characteristics.

When two Brownian particles are sufficiently close, the environment acting on each of them is assumed to be composed of the free environment dynamics plus the perturbation of the other particle's dynamics on that environment. In other words, when two particles are close enough, each of them *sees* a structured environment, i.e., *dressed* by the state of the other, and when they are far apart, they are no longer influenced by each other. Therefore, our understanding translates into a response function that should be dependent on the particle distance (or, more generally, the relative coordinate, u). The most important assumption made in this first part of the thesis was the proposal of

$$\text{Im } \chi_k^{(ij)}(\omega) \equiv \text{Im } \chi_k^{(ij)}(\omega, u). \quad (2.36)$$

Appendix B shows $\text{Im } \chi_k^{(ij)}(\omega, u)$ results from a nonlinear response theory of the environment under the perturbation of the pair of particles.

The Ohmic regime is, again, assumed to be a linear function in ω , namely,

$$\text{Im } \chi_k^{(ij)}(\omega, u) \approx h(k, u) \omega \Theta(\Omega - \omega). \quad (2.37)$$

The bath-related length scale can be defined due to the specific choice for $h(k, u)$. Starting from a bilinear Lagrangian, the nonlinear dissipation rate can be recovered assuming

$$h(k, u) = \tilde{F}(k)G(k, u). \quad (2.38)$$

where $\tilde{F}(k)$ is similar to $\tilde{f}(k)$ defined in Eq.(2.35) related to Eq.(2.24) and dependent only on bath coordinates. Additionally, there is a distance-dependent term that whose specific dependence or form are unknown.

Therefore,

$$\eta_{\text{eff}}[u] \equiv \eta \int dk g_{\text{eff}}(k) G(k, u) \quad (2.39)$$

as the continuum limit of $\sum_k C_k^{(i)} C_k^{(j)} \tilde{F}(k) G(k, u)$. This summation is obtained by applying Eqs. (2.38) and (2.37) to Eq. (2.34).

$$g_{\text{eff}}(k) \equiv k^2 g(k), \quad (2.40)$$

was also defined since selecting $G(k, u) = 1$ enables the obtaining of the single-particle dissipation rate^{††}.

Using Eqs.(2.35) and (2.39) and taking $\Omega \rightarrow \infty$ limit in Eqs.(2.33) and (2.34), the dissipation kernels become

$$K_i(t - t') = 2\eta\delta(t - t'), \quad (2.41)$$

$$K_{ij}(t - t') = 2\eta_{\text{eff}}[u]\delta(t - t'). \quad (2.42)$$

The length scale is now explicit because of the kernel's dependence on relative coordinate u . The nonlinear dissipation force appearing in the equations of motion can be adjusted by tuning $G(k, u)$, whether to recover a particular theoretical model, or to explain a specific experiment.

Finally, our equations of motion in the case of free Brownian particles, $V(x_1) = V(x_2) = 0$, and $c_{12} = 0$, read

$$\begin{aligned} m\ddot{q}(t) + (\eta + \eta_{\text{eff}}[u])\dot{q}(t) &= f_q(t), \\ m\ddot{u}(t) + (\eta - \eta_{\text{eff}}[u])\dot{u}(t) &= f_u(t), \end{aligned} \quad (2.43)$$

where the center of mass and relative fluctuating forces are, respectively, given by $f_q(t) = (f_1 + f_2)/2$ and $f_u(t) = f_1 - f_2$.

Although nonlinear dissipation forces were found, our modified bilinear model was unable to recover the effective bath-induced potential $V_e(u)$ from Eq.(2.21). If a particular experiment reveals bath-mediated conservative forces, the theoretical model should likely begin with nonlinear system-bath coupling. As discussed in what follows, experiments with Brownian particles immersed in a fluid whose dynamics show no effective potential can be conducted. Therefore, our result can correctly make the connection with certain experiments such as those that take hydrodynamic interactions into account.

Depending on the physical system being studied, the type of coupling (bilinear or non-linear) between particle and thermal bath can be chosen. The choice depends on the level of detail required to adequately describe the dynamics of the physical system. On the one hand, linear coupling is used, for instance, in classical or quantum harmonic

^{††} $\eta_{\text{eff}}[u] \equiv \eta \int_0^\infty dk g_{\text{eff}}(k) = \eta \int_0^\infty dk k^2 \frac{e^{-k/k_0}}{2k_0^3} = \eta$

oscillators coupled to a thermal bath, or in optical tweezers experiments (51,52). On the other hand, nonlinear coupling is adopted for studies of complex fluids and biological systems where nonlinearity is in play (53,54).

Here, again, the limit of validity for the dissipation term is $k_0u \ll 1$, as discussed in Sec. 2.1. Indeed, for particles to be close to each other, the equations of motion written above (Eq. 2.43) do not describe the correct physics, since the distance between the particles is not taken into account.

This section provides a way to derive the equations of motion very similar to the nonlinear approach by proposing a modified spectral function. The effective potential mediated by the bath has been eliminated, thus allowing specific interactions to be recovered. The proposal of modified spectral function distance-dependent leaves the Lagrangian approach free from any nonlinearity and complex insertion of terms, notwithstanding the cost of redefining a spectral function dependent on the distance between the particles.

2.3.1 Recovery of dissipation rates

Our aim was to demonstrate a bilinear Lagrangian (14) can generate the same dissipation rates as the one with a nonlinear coupling parameter, as in Ref. (8). The previous subsection showed a partial nonlinear effect can be achieved by a constructed spectral function. Similar equations of motion can be generated; however, our approach cannot recover an effective potential mediated, mediated by the bath.

Equations of motion dependent on $G(k, u)$ can be explicitly written adjusting it in adequately for recovering nonlinear dissipation $\eta_e[u]$ from Eq.(2.23) and taking

$$G(k, u) = \cos(ku), \quad (2.44)$$

which is used in Eq.(2.39), thus leading to

$$\eta_{\text{eff}}[u] = \eta \int_0^\infty dk k^2 \frac{e^{-k/k_0}}{2k_0^3} \cos(ku) = \eta \frac{(1 - 3k_0^2u^2)}{(k_0^2u^2 + 1)^3}. \quad (2.45)$$

As expected, $\eta_{\text{eff}}[u] = \eta_e[u]$. Consequently, the equations of motion can be written as Eq.(2.21). Setting $V(x_1) = V(x_2) = c_{12} = 0$, the equations of motion can be recovered for illustrating the similarities between both sets of equations clearly.

Taking the limit of long distances, $k_0u \rightarrow \infty$, the effective dissipation vanishes and the particles execute authentic Brownian motion

$$\begin{aligned} m\ddot{q}(t) + \eta\dot{q}(t) &= f_q(t), \\ m\ddot{u}(t) + \eta\dot{u}(t) &= f_u(t). \end{aligned} \quad (2.46)$$

Our aim here was to derive a similar expression for the equations of motion for the particles. Other trigonometric functions $G(k, u)$ could generate similar dissipation coefficients with the same behavior.

Constant dissipation rate η_{12} in Eq.(2.8), can also be recovered in the domain of the standard bilinear model. By choosing $G(k, u) = G_0$, which is a constant, then

$$\eta_{\text{eff}}[u] = \eta \int_0^\infty dk k^2 \frac{e^{-k/k_0}}{2k_0^3} G_0 = \eta G_0 = \eta_{12}. \quad (2.47)$$

Eq.(2.9) is recovered again considering $V(x_1) = V(x_2) = c_{12} = 0$. Regarding dissipation, our result can show a path that may connect the usual bilinear model to the nonlinear one.

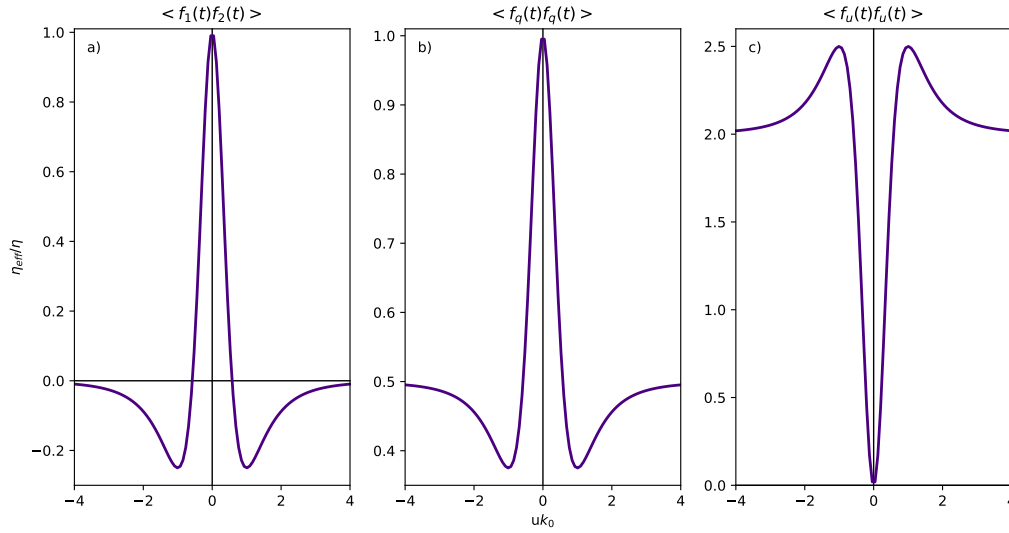


Figure 1 – Spatial correlation for **a)** forces for both particles, **b)** center of mass forces, and **c)** relative coordinate forces. Such correlation forces are distance-relative dependent due to the dissipation rate. **a)** For small distances, the standard single Brownian particle behavior is recovered. Starting at approximately $(\sqrt{3})^{-1}$, the correlation function becomes negative until reaching zero for particles too far apart. **b)** Similar behavior as in **a)**, now with correlation force in the intermediate distances. **c)** For small distances, correlation is zero, increasing for intermediate distances until reaching two times the correlation force for a single Brownian particle.

Source: By the author

A different equation of motion for the correlation force in terms of distance between the particles was found for both center of mass and relative coordinates, as in Ref. (8). White noise properties can be recovered with a relative distance-dependent term $\eta_{\text{eff}}[u(t)]$, as depicted in Figure 1, which shows a spatial anticorrelation behavior for $f_1(t)$ and $f_2(t)$.

Fig.1-a shows the correlation between the particle's forces, which represents a process of attraction and repulsion of the particles in function of the relative distance. However, if the particles do not have charge or any external force, the process cannot be

expected to occur (25,46). Although not our primary interest, the same behavior described by our model can also be derived with the nonlinear coupling model (Sec.2.2).

Despite the avoidance of non-standard diffusion not being strictly essential, as stated in the early models of Brownian motion, our approach enables the construction of the usual diffusion behavior even for a two-particle scenario. The following subsections provide examples of the applicability of the modified spectral function.

2.3.2 Avoidance of anomalous diffusion

The previous sections provided arguments to justify the definition of the distance-dependent spectral function, which partially recovered the literature results for nonlinear dynamics without using a specific coupling, thus leading to a general description for analyses of different distance-dependent functions. Anomalous diffusion appears when some nonlinearity is being dealt with. Here, the effects of a distinct choice of the distance-dependent term are investigated towards the derivation of a different behavior that might still work under the fluctuation-dissipation relation and eliminates the anomalous anti-correlation effect.

The specific form of $\eta_{\text{eff}}[u]$ in Eq.(2.45) promotes a deeper investigation of anomalous diffusion, as discussed in Appendix C. The diffusion coefficients appear in the correlation functions of Langevin forces as

$$\langle f_1(t)f_2(t') \rangle = 2D_{12}(u)\delta(t-t'), \quad (2.48)$$

$$\langle f_u(t)f_u(t') \rangle = 2D_u(u)\delta(t-t'), \text{ and} \quad (2.49)$$

$$\langle f_q(t)f_q(t') \rangle = 2D_q(u)\delta(t-t'), \quad (2.50)$$

and can be derived from the fluctuation-dissipation theorem (55,56), thus reading

$$D_{12}(u) = \eta_{\text{eff}}[u]k_B T. \quad (2.51)$$

Similarly, for the center of mass and relative coordinates,

$$D_q(u) = (\eta + \eta_{\text{eff}}[u])k_B T/2, \quad (2.52)$$

and

$$D_u(u) = 2(\eta - \eta_{\text{eff}}[u])k_B T. \quad (2.53)$$

Up to this point, the results showed the diffusion coefficients are nonlinear concerning time. According to Fig. 1-a, the anomalous diffusion arises when

$$\eta_{\text{eff}}[|u|] > k_0^{-1}/\sqrt{3} < 0, \quad (2.54)$$

which, at intermediate separations, implies a decrease in diffusion coefficient D_q , along with an anticorrelation ($D_{12} < 0$) between the Langevin forces acting on the particles.

The anomalous diffusion, i.e., the coefficient with nonlinearity in time, is explored in Appendix C. Interestingly, nonlinearity emerges due to η_{eff} . Since experiments for Brownian particles in a same bath do not support that behavior, the generation of a positive force correlation, avoiding the anticorrelation between Langevin forces for the particles, is aimed at, by tuning function $G(k, u)$.

Towards an experimental contrast, let us consider the spectral functions that model the interaction of localized excitons with a bath of acoustic phonons (57,58). Such models typically use Gaussian features, which motivate setting

$$G(k, u) = e^{-kk_0u^2}. \quad (2.55)$$

The assumption results in an effective dissipation rate given by

$$\eta_{\text{eff}}[u] = \frac{\eta}{(1 + k_0^2u^2)^3}. \quad (2.56)$$

Eq.(2.55) guarantees the positivity $\eta_{\text{eff}}[u] \geq 0$ and also recovers the independent Brownian

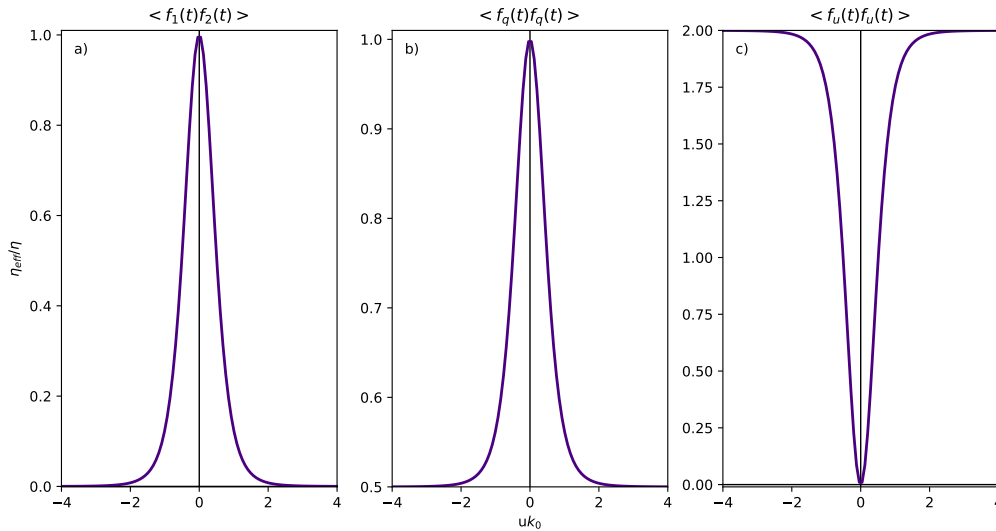


Figure 2 – Spatial correlation for **a)** forces for both particles, **b)** center of mass forces, and **c)** relative coordinate forces, with a Gaussian modified spectral function (Eq.(2.56)). The Gaussian behavior is similar in all three plots. For small distances, the correlation force is the same of a single Brownian particle whereas for long distances, it reaches **a)** zero correlation and **b)** half of the one for a single Brownian particle. In **c)**, for small distances, it is zero correlation, which increases until two times the correlation force for a single Brownian particle for long distances.

Source: By the author

motions of two arbitrarily distant particles (in the $|u| \rightarrow \infty$ limit). In fact, any positive

and convergent function ($G(k, u) \geq 0$ and $G(k, |u| \rightarrow \infty) = 0$) is sufficient to guarantee $\eta_{\text{eff}}[u] \geq 0$ and $\eta_{\text{eff}}[|u| \rightarrow \infty] = 0$.

Figure 2 shows the behavior of the dissipation term as a function of the relative coordinate. The anticorrelation behavior vanishes for the right choice of $G(k, u)$ and the noise correlation $\langle f_1(t)f_2(t) \rangle$ for short distances exhibits the standard Brownian behavior, whereas for long distances, the normal diffusion is recovered (Fig. 2-a).

The choice for the spectral function may seem arbitrary at first. However, it casts a deeper relation between other setups, from which the Brownian motion of several particles can be derived in a different medium. Our choice was motivated by similar behaviors in the hydrodynamic situation.

2.3.3 Hydrodynamics-inspired model

Despite many studies of Brownian motion and hydrodynamics effects, the literature reports no specific diffusion coefficient analysis in this context. In this sense, our study can provide such a connection, taking into account a small change in the dependence of the relative distance on the spectral function.

This section addresses a hydrodynamic application of the model towards a better understanding of the reason for the distance-dependence choice of the spectral function. This part of the research was based on Ref. (17), which studied the dynamics of N Brownian particles with hydrodynamic interactions and proposed a method that simulates the diffusive process of those particles in a fluid environment. In contrast to our description, the authors studied Brownian particles in three dimensions and introduced a distance-dependent friction tensor to support the hydrodynamics of interactions. The tensor, called Oseen tensor, described diffusion, addressed in what follows.

In the classical Brownian motion theory, the particles of the surroundings are typically much smaller than those of the system of interest. According to the literature, fluid particles are usually neglected. However, in this section, our discussion is based on a system with two Brownian particles immersed in a viscous fluid that is assumed to mediate interactions between particles. As shown in Ref. (17), dissipative forces may depend on the interparticle distance. Our analysis is restricted to the limit at which the radius of each Brownian particle is smaller than their relative distance, i.e., the regime of validity of Oseen tensor, which, for $i \neq j$, is given by

$$D_{ij} = \frac{k_B T}{8\pi\kappa r_{ij}} \left(\mathbb{I} + \frac{\vec{r}_{ij}\vec{r}_{ij}}{r_{ij}^2} \right), \quad (2.57)$$

where κ is the fluid viscosity, \mathbb{I} is the identity matrix, \vec{r}_{ij} is the center-to-center vector for the particles, and $r_{ij} = |\vec{r}_{ij}|$.

Our purpose is to indicate the correspondence between Refs. (17, 59) and our

modified model of the spectral function. Therefore, let us recall the definition of diffusion coefficient definition (Appendix C) and analyze D_{ij} in configuration space, noticing it has the dimension of the diffusion coefficient

$$[D_{ij}] = \frac{[lenght]^2}{[time]},$$

where the viscosity dimension is $[\kappa] = [mass]/([lenght][time])$. Here, $[\eta_{\text{eff}}^{\text{hydro}}] = [mass]/[time]$. Since $[\kappa][r_{ij}] = [mass]/[time] = [\eta_{\text{eff}}^{\text{hydro}}]$, then

$$D_{ij} = \frac{k_B T}{\eta_{\text{eff}}^{\text{hydro}}[r_{ij}]},$$

where

$$\eta_{\text{eff}}^{\text{hydro}}[\vec{u}] = 8\pi\kappa|\vec{u}| \left(\mathbb{I} + \frac{\vec{u}\vec{u}}{u^2} \right)^{-1}.$$

Furthermore, a one-dimensional limit of Brownian motion $\vec{u} = u\hat{x}$ can be assumed, leading to $|\vec{u}| = |u|$, and $\mathbb{I} = 1$. Then

$$\left(\mathbb{I} + \frac{\vec{u}\vec{u}}{u^2} \right) = 2.$$

In that case, an effective dissipation rate mediated by the hydrodynamic environment and derived with the help of the fluctuation-dissipation relation (55) is given by

$$\eta_{\text{eff}}^{\text{hydro}}[u] = 4\pi\kappa|u| = \gamma_h|u|, \quad (2.58)$$

where γ_h is a constant proportional to the solvent viscosity.

By contrast, no conservative forces emerge from the hydrodynamic environment, i.e., the behavior of the hydrodynamic scenario discussed in Ref. (17) is more similar to that of our modified bilinear model than to that of the standard nonlinear model (which produces $V_e(u)$, as shown in Eq.(2.22)). In other words, our modified spectral function can generate a similar behavior when dealing with Brownian motion with a hydrodynamic source.

The following linear distance-dependence function can be easily selected for the derivation of a dissipation rate^{‡‡} similar to Eq.(2.58), which is proportional to relative distance:

$$G(k, u) = k|u|, \quad (2.59)$$

since

$$\eta_{\text{eff}}[u] = \eta \int_0^\infty dk k^2 \frac{e^{-\frac{k}{k_0}}}{2k_0^3} k|u| = \gamma_m|u|, \quad (2.60)$$

^{‡‡} The effective potential term is not recovered with our modified bilinear model.

with $\gamma_m = 3\eta k_0$.

As a result, a simple technique has been explored for mapping environment-mediated hydrodynamic dissipation into a fictitious bath composed of a continuous set of harmonic oscillators. The configuration space shows a correspondence between the dimensions of Eqs. (2.58) and (2.60).

Nevertheless, the way to obtain Eqs. (2.56) and (2.60) from the standard nonlinear model must be clarified, since the right choice for system-environment couplings as a function of particle positions in the Lagrangian is not obvious. Up to this point, the results have shown our method, which is the modified spectral function, is more accurate and straightforward for handling such interactions.

The equations of motion can be recovered according to the same procedure reported in the first two sections,

$$\begin{aligned} m\ddot{q}(t) + (\eta + 3\eta k_0|u|)\dot{q}(t) &= f_q(t), \\ m\ddot{u}(t) + (\eta - 3\eta k_0|u|)\dot{u}(t) &= f_u(t). \end{aligned} \tag{2.61}$$

The fluctuating forces still retain the characteristics of white noise. The more significant expressions for time correlation functions are

$$\begin{aligned} \langle f_1(t)f_2(t') \rangle &= 6k_B T \eta k_0 |u| \delta(t - t'), \\ \langle f_q(t)f_q(t') \rangle &= k_B T [\eta + 3\eta k_0|u|] \delta(t - t'), \\ \langle f_u(t)f_u(t') \rangle &= 4k_B T [\eta - 3\eta k_0|u|] \delta(t - t'). \end{aligned} \tag{2.62}$$

According to the fluctuation-dissipation relation, the diffusion coefficient in velocity space can be related to the time correlation function of the force by

$$\langle f(t)f(t') \rangle = 2D_v \delta(t - t').$$

Therefore, the diffusion coefficient was analyzed for the particular choice of spectral function $G(k, u)$ and the hydrodynamic behavior was recovered, as in Ref. (17)

$$D = 3\eta k_0 |u| k_B T. \tag{2.63}$$

For long distances, the diffusion coefficients associated with the center of mass and relative coordinates (D_q and D_u Eq.(2.62)) tend to normal diffusion with a factor of two. When the particles are close to each other, D_q is obtained as normal diffusion and D_u vanishes.

Our method shows a straightforward way to connect linear dynamics to the diffusion coefficient due to the hydrodynamic interaction mediated by the bath. The units of the coefficients can be analyzed towards the proposal of a $G(k, u)$ with the same linear behavior in u , as in Ref. (17). An experimental result can be connected with our

modified model and complementary studies of a three-dimensional equation of motion for two particles can lead to a more evident agreement between our modified model and hydrodynamics effects.

3 QUANTUM DYNAMICS

The previous section discussed the classical dynamics of two Brownian particles immersed in a fluid. This chapter addresses the quantum dynamics of those particles using the path integral formalism. Quantum models often adopt approaches based on quantum Langevin or quantum master equations to describe dissipation. However, such approaches can treat only weakly damped systems. Low temperatures violate the conditions of weak coupling systems, where tunneling transitions are permitted. The path integral approach, therefore, is introduced, for it enables studies of quantum mechanical dynamics at arbitrarily low temperatures and for arbitrarily strong damping (6).

3.1 Quantum Brownian motion

Many problems in quantum mechanics assume the system of interest is isolated, which is not a realistic feature, since other aspects must be considered when the effect of coupling with a bath is taken into account. As an example, the universe's energy can no longer be described by the sum of the energy of the individual components because quantum systems are not extensive and Gibbs canonical ensemble cannot be applied (60).

Classically, the problem can be approached by Langevin equation (Eq.(1.1)), as addressed in the previous section. The question arises during attempts to quantize a dissipative system (61). The classical equations of motion can be usually generated by the evolution of a Hamiltonian with canonical quantization procedures. However, no Hamiltonian generates Langevin equations without time dependence. Either new quantization methods, or a system-reservoir approach can, therefore, be assumed. The latter is the most usual and considers the dissipative system a system of interest in contact with a thermal bath (or reservoir). Such a total composite system conserves energy and obeys the usual rules of quantization. The environment dissipates transferred energy, preventing its return to the system of interest within a viable time. Consequently, the reservoir model must be carefully selected towards ensuring the Langevin equation's recovery in the classical limit (1).

SQUID is a quantum example with a magnetic flux equation that behaves like a classical Brownian particle*. The superconductivity of electrons in the ring is a macroscopic variable that can be measured in laboratory, even though it has a quantum origin. Caldeira and Leggett (23) used the Langevin equation mechanism to study tunneling in a superconducting ring with a Josephson junction interruption. Figure 3 illustrates such a system, where the superconducting ring is interrupted by a Josephson junction. By

* The momentum in time of magnetic flux (in the proper limits) is identical to that of a classical Brownian particle

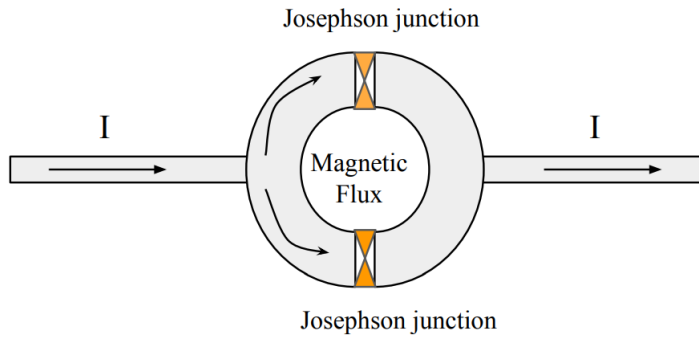


Figure 3 – Representation of a SQUID, where I is the current.

Source: By the author

applying a current I through the device, half the current flows one way and half flows another. The magnetic flux (ϕ) through the device establishes a phase difference between the opposite sides of the ring (25).

3.2 Path integral representation of Quantum Mechanics

The concept of action is the center of the formulation of quantum mechanics through Lagrange formalism of classical mechanics. The formulation avoids the use of operators, although it does not necessarily simplify the solution of quantum mechanical problems. Instead of the determination of the eigenfunctions of a Hamiltonian, a functional integral, which directly produces the propagator required for the understanding of a quantum system dynamics, must be assessed. Due to the close relationship between Feynman's formulation and classical mechanics, the path integral formalism often offers the significant advantage of a more intuitive approach. This section provides a brief overview of the path integral expression for the propagator of a quantum system, following the derivation in Ref. (62).

Classically, the dynamics of a particle depend on the principle of minimal action, and only one trajectory that the particle will follow, which is the one that extremize the action. However, Kernel $K(a, b)$ describes the quantum dynamics, which is the amplitude between initial and final points (a and b , respectively) and can interpreted as the summation of all possible contributions to the trajectories between those points[†]. Such formalism was named path integral, or Feynman approach, after the seminal work of Richard Feynman in the 1940s (63, 64). Many other studies have, therefore, explored the approach. Refs. (26, 65) must be highlighted, since they investigated the coupling of a system of interest to a linear dissipative system.

Our main goal is to characterize the dynamics of a Brownian particle in a quantum

[†] Absolute square of a probability amplitude, $P(b, a) = |K(a, b)|^2$.

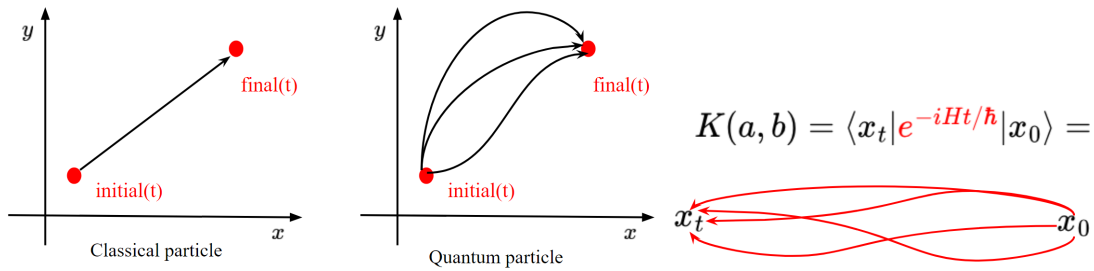


Figure 4 – Representation of classical and quantum paths in the phase space. For the quantum regime, a Kernel accounts for all possible trajectories of the system.

Source: By the author

regime. A reduced description of the system is required, i.e., the dynamics of the reduced state of the system is described so that the time evolution of the Brownian particle can be evaluated (8). Feynman’s integral approach is applied for that purpose (26, 66, 67).

Classically, a particle starts at point x_a at time t_a and ends at point x_b at time t_b , i.e., it goes from a to b following the time-dependent position with properties of $x(t_a) = x_a$ and $x(t_b) = x_b$ (67). As addressed elsewhere, in quantum mechanics, this dynamics is described by a so-called Kernel $K(a, b)$, differently from classical mechanics, in which only one particular trajectory is determined by the so-called principle of least action. Still in quantum mechanics, it is not a particular trajectory that extremizes the action that will contribute for the dynamics, but all trajectories contribute to the quantum dynamics of the particle (see Fig. 4), with equal magnitudes and different phases.

Such formalism emerged in the context of problems of infinite self-energy of the electron. Feynman developed it to deal with non-relativistic quantum mechanics. The action principle for quantum systems was studied so that classical mechanics could arise as a particular case of quantum mechanics in specific limits[‡](67). Appendix E reports some of the details of the derivation for the action’s expression using that formalism for both free harmonic oscillator (Appendix E.1) and driven harmonic oscillator (Appendix E.2). Therefore, the formalism can also be used to deal with classical systems, but mainly for calculating the action of the system. The path integral is a sum of all possible trajectories that deviate a little from the trajectory that extremizes the action. On the other hand, in quantum mechanics, the path integral formalism enables descriptions of a system’s evolution by deriving the reduced density matrix by summing up all possible paths in configuration space.

The Hamiltonian must be first specified for investigations of the reduced dynamics by the path integral formalism. Following the reference for quantum Brownian mo-

[‡] Classical limit $\hbar \rightarrow 0$ when the only paths considered are the classical paths of the system (68). The foundation of quantum effects lies in the fluctuations surrounding classical paths (69).

tion (25), the total Hamiltonian of the system-reservoir is given by

$$H_{SR} = H_S(x, p) + H_R(R_k, p_k) + H_I(x, R_k),$$

where H_S is the Hamiltonian of the system of interest and, in our case, the quantum Brownian particle, with x and p representing the position and momentum coordinates of the particle. H_R is the environment or reservoir Hamiltonian, whose components consist of momentum and position of a set of harmonic oscillators denoted as p_k and R_k , respectively. H_I represents the interaction Hamiltonian, which includes the linear coupling in the position coordinates of both environment and particle (see Eq.(1.4)). In what follows, a general analytical solution for the reduced density matrix is derived - neither the system of interest, nor bath was specified.

Since our interest is only in the temporal evolution of the particle, the degrees of freedom of the environment, which are not accessed, can be traced out

$$\rho_S(t) = \text{Tr}_R[\rho(t)],$$

where the condition of separability of the initial state is considered for simplicity

$$\rho(0) = \rho_S(0)\rho_R(0). \quad (3.1)$$

The condition encompasses the initial density operator of the particle and the bath density operator, $\rho_R(0) = Z_R^{-1}e^{-H_R/k_B T}$ [§](44, 70). The initial state is assumed to have no interaction between the bath and the particle at initial time $t = 0$. Therefore, the evolution of the system-reservoir density operator is written as

$$\rho(t) = U(t)\rho(0)U^\dagger(t),$$

where $U(t) = e^{-\frac{iHt}{\hbar}}$ is the temporal evolution operator. The Hamiltonian of Caldeira-Leggett model Eq.(1.4)[¶] was used so that the dynamics of the system could be studied from the initial time.

Path integral method can calculate the reduced density matrix of the system, which involves the calculation of the matrix elements of the operators by summing all paths in the space of configurations (66). The states of the system-reservoir are then defined as

$$|x, \mathbf{R}\rangle = |x, R_1, \dots\rangle,$$

where the general bath vector is $\mathbf{R} = (R_1, \dots, R_N)$, representing all environment's degrees of freedom, and x is the particle's position coordinate. Writing the evolution of the density operator in the coordinate representation leads to

$$\langle x, \mathbf{R}|\rho(t)|y, \mathbf{Q}\rangle = \langle x, \mathbf{R}|U(t)\rho(0)U^\dagger(t)|y, \mathbf{Q}\rangle.$$

[§] Canonical density operator of the nonperturbed bath, with Z_R representing the partition function.

[¶] $H_{SR} = \frac{p^2}{2m} + V(x) + \sum_{k=1}^N \left[\frac{p_k^2}{2m_k} + \frac{m_k\omega_k^2}{2} \left(R_k - \frac{C_k}{m_k\omega_k^2} x \right)^2 \right]$

The insertion of completeness relation $\int dx |x\rangle \langle x| = \mathbb{I}$ results in

$$\begin{aligned} \langle x, \mathbf{R} | U(t) \mathbb{I} \rho(0) \mathbb{I} U^\dagger(t) | y, \mathbf{Q} \rangle &= \int dx' dy' d\mathbf{R}' d\mathbf{Q}' \langle x, \mathbf{R} | U(t) | x', \mathbf{R}' \rangle \\ &\times \langle x', \mathbf{R}' | \rho(0) | y', \mathbf{Q}' \rangle \\ &\times \langle y', \mathbf{Q}' | U^\dagger(t) | y, \mathbf{Q} \rangle. \end{aligned}$$

The path trajectories enables identifying the quantum propagator of the total system (see Appendix D)

$$\langle x, \mathbf{R} | U(t) | x', \mathbf{R}' \rangle \equiv K(x, \mathbf{R}, t; x', \mathbf{R}', 0) = \int \int \mathcal{D}x(t) \mathcal{D}\mathbf{R}(t) e^{\frac{i}{\hbar} S[x(t), \mathbf{R}(t)]}$$

and

$$\langle y', \mathbf{Q}' | U^\dagger(t) | y, \mathbf{Q} \rangle \equiv K^*(y, \mathbf{Q}, t; y', \mathbf{Q}', 0) = \int \int \mathcal{D}y(t) \mathcal{D}\mathbf{Q}(t) e^{\frac{-i}{\hbar} S[y(t), \mathbf{Q}(t)]}$$

where the final points are $x(t) = x$, $x(0) = x'$, $\mathbf{R}(t) = \mathbf{R}$, $\mathbf{R}(0) = \mathbf{R}'$, $y(t) = y$, $y(0) = y'$, $\mathbf{Q}(t) = \mathbf{Q}$, and $\mathbf{Q}(0) = \mathbf{Q}'$. $\int \mathcal{D}x$ and $\int \mathcal{D}y$ symbolically denote summation in function space over all paths with the end-points held fixed. The Euclidean action is given by

$$S_{SR} = S_S + S_R + S_I = \int_0^t L(\dot{x}, x, t) dt'.$$

where L is the Lagrangian of the total system. The density operator is written as

$$\begin{aligned} \langle x, \mathbf{R} | \rho(t) | y, \mathbf{Q} \rangle &= \int dx' dy' d\mathbf{R}' d\mathbf{Q}' K(x, \mathbf{R}, t; x', \mathbf{R}', 0) \\ &\times K^*(y, \mathbf{Q}, t; y', \mathbf{Q}', 0) \langle x', \mathbf{R}' | \rho(0) | y', \mathbf{Q}' \rangle \end{aligned} \quad (3.2)$$

The operator describes the total system. If the focus is only the system of interest, then Eq.(3.2) can be integrated in all environment's coordinates. Therefore, the so-called reduced density operator of the total system is described by

$$\begin{aligned} \tilde{\rho}(x, y, t) &\equiv \int d\mathbf{R} \langle x, \mathbf{R} | \rho(t) | y, \mathbf{R} \rangle \\ &= \int dx' dy' d\mathbf{R}' d\mathbf{Q}' d\mathbf{R} K(x, \mathbf{R}, t; x', \mathbf{R}', 0) \\ &\times K^*(y, \mathbf{R}, t; y', \mathbf{Q}', 0) \langle x', \mathbf{R}' | \rho(0) | y', \mathbf{Q}' \rangle. \end{aligned} \quad (3.3)$$

The interaction between system of interest and environment is considered to be initially in a separable state, as in Eq.(3.1). After $t = 0$, both system of interest and reservoir change in time. Inserting Eq.(3.1) into Eq.(3.3) leads to

$$\begin{aligned} \tilde{\rho}(x, y, t) &\equiv \int d\mathbf{R} \langle x, \mathbf{R} | \rho(t) | y, \mathbf{R} \rangle \\ &= \int dx' dy' d\mathbf{R}' d\mathbf{Q}' d\mathbf{R} K(x, \mathbf{R}, t; x', \mathbf{R}', 0) \\ &\times K^*(y, \mathbf{R}, t; y', \mathbf{Q}', 0) \langle x', \mathbf{R}' | \rho_S(0) \rho_R(0) | y', \mathbf{Q}' \rangle, \end{aligned}$$

and replacing the propagators and the action,

$$\begin{aligned}
\tilde{\rho}(x, y, t) &= \int dx' dy' d\mathbf{R}' d\mathbf{Q}' d\mathbf{R} \int \int \mathcal{D}x(t) \mathcal{D}\mathbf{R}(t) e^{\frac{i}{\hbar} S[x(t), \mathbf{R}(t)]} \int \int \mathcal{D}y(t) \mathcal{D}\mathbf{Q}(t) e^{\frac{-i}{\hbar} S[y(t), \mathbf{Q}(t)]} \\
&\quad \times \langle x', \mathbf{R}' | \rho_S(0) \rho_R(0) | y', \mathbf{Q}' \rangle \\
&= \int dx' dy' d\mathbf{R}' d\mathbf{Q}' d\mathbf{R} \left[\int \int \mathcal{D}x(t) \mathcal{D}y(t) e^{\frac{i}{\hbar} S_S[x(t)]} e^{\frac{-i}{\hbar} S_S[y(t)]} \right] \\
&\quad \times \int \int \mathcal{D}\mathbf{R}(t) \mathcal{D}\mathbf{Q}(t) e^{\frac{i}{\hbar} S_I[x(t), \mathbf{R}(t)]} e^{\frac{i}{\hbar} S_R[\mathbf{R}(t)]} e^{\frac{-i}{\hbar} S_I[y(t), \mathbf{Q}(t)]} e^{\frac{-i}{\hbar} S_R[\mathbf{Q}(t)]} \\
&\quad \times \langle x', \mathbf{R}' | \rho_S(0) \rho_R(0) | y', \mathbf{Q}' \rangle,
\end{aligned}$$

the so-called *Influence functional*^{||} is highlighted,

$$\begin{aligned}
\mathcal{F}[x, y] &= \int d\mathbf{R}'(t) d\mathbf{Q}'(t) d\mathbf{R}(t) \rho_R(\mathbf{R}', \mathbf{Q}', 0) \\
&\quad \times \int \int \mathcal{D}\mathbf{R} \mathcal{D}\mathbf{Q} e^{\frac{i}{\hbar} (S_I[x(t), \mathbf{R}(t)] - S_I[y(t), \mathbf{Q}(t)] + S_R[\mathbf{R}(t)] - S_R[\mathbf{Q}(t)])}.
\end{aligned} \tag{3.4}$$

In terms of operators, the above expression has the form

$$\mathcal{F}[x, y] = Tr_R \left(\rho_R U_{RI}^\dagger [y] U_{RI} [x] \right), \tag{3.5}$$

where $U_{RI} = e^{-i(H_R + H_I)t/\hbar}$ is the temporal evolution operator for environment's and interaction's Hamiltonian. This functional is the average of the product of two evaluations in time on the initial state of the environment, which is a property of the reservoir and its influence on the system of interest. It provides a way to calculate the effect of an external force or interaction, given by the environment Lagrangian, on the probability amplitude of different paths (25). It also adds a nonlocal term** to the density operator, which is the functional of the particle trajectory containing all bath information.

The behavior of the system can be evaluated in terms of a double integral of trajectories as (67)

$$\mathcal{J}(x, y, t; x', y', 0) = \int \int \mathcal{D}x \mathcal{D}y e^{\frac{i}{\hbar} (S_S[x(t)] - S_S[y(t)])} \mathcal{F}[x, y], \tag{3.6}$$

called superpropagator, which controls the time evolution of the system's reduced operator density. There are two dynamical terms in the above expression, of which one refers to the non-dissipative dynamics of the total system, $e^{\frac{i}{\hbar} (S_S[x(t)] - S_S[y(t)])}$, and the other represents the dissipative dynamics of the total system, $\mathcal{F}[x, y]$ (70).

Therefore,

$$\tilde{\rho}(x, y, t) = \int dx' dy' \mathcal{J}(x, y, t; x', y', 0) \rho_S(x', y', 0). \tag{3.7}$$

When no interaction is established between the system of interest and the reservoir, the influence functional is equal to one.

^{||} As usually described in the literature of path integral formalism(67).

** Represents the interaction taken far apart. The expression of non-local does not refer to the meaning that appear in quantum mechanics.

The resulting expression is a general form for the reduced density operator of a system of interest interacting with a reservoir. A minimal model where the environment is considered a set of N non-interacting harmonic oscillators can now be defined and, under certain conditions, reproduces the Brownian dynamics in the classical limit. First, the expression of the reduced density matrix is evaluated through the calculation of the influence functional, Eq.(3.4) with the use of an expression for the Lagrangian of the total system (35):

$$L = L_S + L_R + L_I \quad (3.8)$$

$$= \frac{m\dot{x}^2}{2} - V(x) + \sum_k \frac{m_k \dot{R}_k^2}{2} - \sum_k \frac{m_k \omega_k^2}{2} \left(R_k - \frac{C_k x}{m_k \omega_k^2} \right)^2. \quad (3.9)$$

Details on the Gaussian integral calculations for the influence functional can be found in Appendix F. The expression for the propagator of the k -th oscillator of the environment when acting with external force $C_k x(t)$ is then used, as in (25)

$$K_{RI}^{(k)} = \sqrt{\frac{m_k \omega_k}{2\pi i \hbar \sin \omega_k t}} \exp\left\{ \frac{i}{\hbar} S_{cl}^{(k)} \right\}, \quad (3.10)$$

where the k -th classical action is

$$\begin{aligned} S_{cl}^{(k)} = & \frac{m_k \omega_k}{2 \sin \omega_k t} \left[(R_k^2 + R_k'^2) \cos \omega_k t - 2R_k R_k' - \frac{2C_k R_k}{m_k \omega_k} \int_0^t x(t') \sin \omega_k t' dt' \right. \\ & - \frac{2C_k R_k'}{m_k \omega_k} \int_0^t x(t') \sin \omega_k (t - t') dt' - \frac{2C_k^2}{m_k^2 \omega_k^2} \int_0^t dt' \int_0^{t'} dt'' x(t') x(t'') \\ & \left. \times \sin \omega_k (t - t') \sin \omega_k t'' \right]. \end{aligned} \quad (3.11)$$

The influence functional is obtained by averaging the product of two time evolutions acting on the initial state of the environment. One of such evolutions represents the environment's response to the system of interest, whereas the other is its time-reversed counterpart. Both histories (or trajectories) are essential to describe the time evolution of the system's reduced density operator. Additionally, they must be multiplied by one another for all k and averaged over the initial environment state and the environment's initial state must be specified. Following the assumptions in Refs.(19,25,44), the environment is assumed to be in thermal equilibrium at temperature T . In this case, the initial environment density operator can be expressed as (for details, see Appendix G)

$$\begin{aligned} \rho_R(R', Q', 0) &= \prod_k \rho_R^{(k)}(R_k', Q_k', 0) \\ &= \prod_k \frac{m_k \omega_k}{2\pi \hbar \sinh\left(\frac{\hbar \omega_k}{k_B T}\right)} \exp\left\{ -\frac{m_k \omega_k}{2\hbar \sinh\left(\frac{\hbar \omega_k}{k_B T}\right)} \left[(R_k'^2 + Q_k'^2) \cosh\left(\frac{\hbar \omega_k}{k_B T}\right) - 2R_k' Q_k' \right] \right\}. \end{aligned} \quad (3.12)$$

Substituting the above expressions results in influence functional expression (Eq.(3.4)). The superpropagator (Eq.(3.6)) can be written as

$$\begin{aligned} \mathcal{J}(x, y, t; x', y', 0) &= \int_{x'}^x \int_{y'}^y \mathcal{D}x(t') \mathcal{D}y(t') \exp \left\{ \frac{i}{\hbar} (S_S[x(t')] - S_S[y(t')]) \right\} \\ &\quad - \int_0^t \int_0^\tau d\tau d\sigma [x(\tau) - y(\tau)] \alpha_I(\tau - \sigma) [x(\sigma) + y(\sigma)] \\ &\quad \times \exp - \frac{1}{\hbar} \int_0^t \int_0^\tau d\tau d\sigma [x(\tau) - y(\tau)] \alpha_R(\tau - \sigma) [x(\sigma) - y(\sigma)], \end{aligned} \quad (3.13)$$

where

$$\begin{aligned} \alpha_I(\tau - \sigma) &= - \sum_k \frac{C_k^2}{2m_k \omega_k} \sin \omega_k(\tau - \sigma) \\ \alpha_R(\tau - \sigma) &= \sum_k \frac{C_k^2}{2m_k \omega_k} \coth \left(\frac{\hbar \omega_k}{2k_B T} \right) \cos \omega_k(\tau - \sigma). \end{aligned}$$

The damping function can be written as

$$\eta(\tau - \sigma) = 2m\gamma(\tau - \sigma) \equiv \sum_k \frac{C_k^2}{2m_k \omega_k^2} \cos \omega_k(\tau - \sigma),$$

and the relation with α_I is given by

$$\alpha_I(\tau - \omega) = \frac{d\eta(\tau - \omega)}{d\tau}.$$

Taking continuous limit $\sum_k \rightarrow \int d\omega$, as in Chapter 2, the above expression can be written as

$$\begin{aligned} \alpha_I(\tau - \sigma) &= - \frac{1}{\pi} \int_0^\Omega d\omega \eta \omega \sin \omega(\tau - \sigma), \\ \alpha_R(\tau - \sigma) &= \frac{1}{\pi} \int_0^\Omega d\omega \eta \omega \coth \left(\frac{\hbar \omega}{2k_B T} \right) \cos \omega(\tau - \sigma). \end{aligned}$$

Inserting those above expressions in Eq.(3.6) and taking the appropriate limits^{††}, the propagator can be written in the semi-classical limit, where $k_B T \gg \hbar \omega$ for frequencies $\omega \ll \Omega$, as

$$\begin{aligned} \mathcal{J}(x, y, t; x', y', 0) &= \int_{x'}^x \int_{y'}^y \mathcal{D}x(t') \mathcal{D}y(t') \\ &\quad \times \exp \left\{ \frac{i}{\hbar} \left(S_S[x(t')] - S_S[y(t')] + \frac{\eta}{2} \int_0^t (y(t') - x(t')) (\dot{x}(t') + \dot{y}(t')) \right) \right\} \\ &\quad \times \exp \left\{ - \frac{2\eta k_B T}{\hbar^2} \int_0^t d\tau [x(\tau) - y(\tau)]^2 \right\}. \end{aligned} \quad (3.14)$$

^{††} Ohmic limit;

Long time scale compared to cutoff frequency, i.e., $t \gg \Omega^{-1}$, where t is the time interval; The particles' movements are confined to a limited space compared to the characteristic length scale of the system, k_0^{-1} .

The initial conditions can be then set for a system of interest and the reduced density matrix is calculated. The expression for the reduced density matrix can be explicitly evaluated for a system of interest composed of a Brownian particle, for example (see Ref. (70)). Chapter 6 addresses the choice of a specific system of interest, namely, driven spin-boson, and the derivation of the expression for the reduced density matrix.

4 DISSIPATIVE ADAPTATION

This chapter introduces the hypothesis proposed by England in 2015 (Ref.(27)). Firstly, it must be stressed discussions on whether biological processes are quantum or not have still been held. Nevertheless, biology and open quantum systems have a clear connection, since biological systems can be treated as systems of interest in contact with an environment, which is responsible for the energy loss of those systems. Living organisms require a continuous influx of free energy to sustain the non-equilibrium condition inherent to life (32).

The dynamics of a collection of particles allowed to reach thermal equilibrium show the energy of a given microscopic arrangement and the probability of observing the system in that arrangement obey a simple exponential relationship known as Boltzmann distribution. However, when those particles are driven away from equilibrium by forces that perform work on the system over time, relating the likelihood of a given outcome to a familiar thermodynamic quantity, as work or heat, becomes significantly more challenging. Therefore, the development of a general understanding of the thermodynamics of such non-equilibrium scenarios might ultimately enable our controlling and imitating the remarkable successes living things achieve in driven self-assembly (27).

Since living organisms seem to not obey the equilibrium thermodynamics physics, the nonequilibrium regime must be studied for the understanding of the way life-like behaves. Boltzmann distribution is not valid for that regime, since the systems are evaluated in finite time and with external forces acting on them. With this apparent connection to biological systems, England derived an expression called dissipative adaptation hypothesis, which is a generalization of Boltzmann distribution for out-of-equilibrium systems. The hypothesis provides a general thermodynamic mechanism that explains self-organization in a broad class of driven classical systems. Specifically, the likelihood of a particular structure emerging in non-equilibrium evolution is significantly influenced by the amount of work absorption and dissipation heat during its evolution history.

The idea draws parallels with the understanding of evolutionary adaptation in biological contexts, i.e., structures formed far from equilibrium may exhibit characteristics that seem specially conducive to efficient work absorption from the driving environment. This perspective prompts a discussion on the relevance of the dissipative adaptation hypothesis in the study of the physics of self-organization (71).

This chapter provides a brief overview of the hypothesis and the derivation of the expression for it. The main concepts of equilibrium systems are reviewed and a generalization for out-of-equilibrium systems shows how the thermodynamics of such driven and

time finite systems are connected when Boltzmann distribution is not valid. The connection with England's equation is established, with a generalization of the distribution for non-equilibrium systems, providing a way to connect living mechanics to thermodynamics equations. The quantum version of the hypothesis, called quantum dissipative adaptation, is discussed in the last sections of the chapter. Moreover, some quantum definitions of work are provided towards a better understanding of the connection of transition probability and thermodynamics quantities.

4.1 Systems in Equilibrium

Let us consider an assembly of particles in a system S in contact with a large environment at temperature T . After a sufficiently long time ($\tau \rightarrow \infty$), the system eventually reaches equilibrium. The occupation probability of each state is given by an exponential relation of energy, given by $p_n = \exp\{E_n/k_B T\}$, where E_n is the energy of each state. Supposing an initial state of system i and considering two final configurations of the system, denoted as j and k , with energies E_j and E_k , respectively, their connection with thermodynamic quantities can be evaluated. Therefore, the probability of reaching each of those states is given by Boltzmann distribution (see Fig. 5)

$$\frac{p(j)}{p(k)} = \exp\left\{-\frac{E_j - E_k}{k_B T}\right\}. \quad (4.1)$$

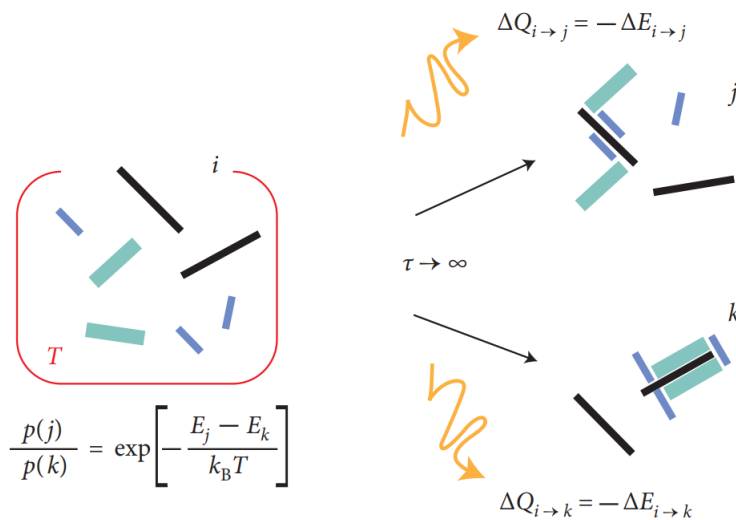


Figure 5 – In the classic scenario of equilibrium statistical mechanics, a system held in contact with a thermal reservoir at temperature T for a long time τ loses all memory of its starting state i and, consequently, the probabilities of microscopic states j and k are an exponential function of their respective energies. The probability distribution of each state is dictated by their energies.

After a very long time, an energy change occurs from a starting state (i) to an ending one (j , for example) and will be equal to the heat released into the bath during the process. Due to the first law of thermodynamics, which establishes the conservation of energy, the heat released into the reservoir (ΔQ) during a transition from one state to another is equal and opposite to the change in internal energy (ΔE) that occurs during the process.

Systems in thermal equilibrium can be described when a system of interest is very weakly connected to a heat bath at temperature T and the nature or exact duration of the coupling to the bath is uncertain. Moreover, the limit of a very long time in which all rapid events have occurred while the slower ones have not is considered (72).

The timescale of the process involved must be taken into account for the understanding of the thermalization process*. As an example, quantum systems that will equilibrate might exist, yet their equilibrating timescale is of the order of the Universe's age. Conversely, certain systems, such as glasses, may never relax to equilibrium, but, instead, maintain metastable states characterized by prolonged lifetimes (73).

4.2 Out-of-equilibrium systems

Systems in equilibrium are the exception in nature, since most systems are out-of-equilibrium and even living things are not in thermodynamic equilibrium. Two features cause a system to be out-of-equilibrium: the first concerns the time necessary for a system to equilibrate - if it is much longer than the accessible timescale, $t_{eq} \gg t$, the system never equilibrates; the other is related to driven systems on which an external force acts, providing extra energy and resulting in non-equilibration.

This section explores systems in which time is finite and external forces can perform work on them (see Fig.6). Comprehension and analyses of such systems require two fundamental physical principles, namely, time-reversal symmetry[†] and energy conservation[‡] be considered (55,71).

Crooks's theorem is presented towards the understanding of the derivation of England's expression. Thermal equilibrium systems consider the probabilities of states. On the other hand, for non-equilibrium systems, probabilities of occupation of certain states, as well as trajectories, i.e., sequences of states, are taken into account. Crooks's relation expresses the difference in sequences of states probabilities with forward and backward probabilities distribution ratio.

* Systems that evolve to equilibrium states.

[†] When time is reversed, the laws of physics behave similarly.

[‡] For closed systems, the system's internal energy is described as $\Delta E = Q + W$, where Q is total heat transferred to the system during the process and W is total work applied on the system.

The next sections address a very brief derivation of the dissipative adaptation expression with few details - the entire derivation can be seen in Refs.(27, 55, 71, 74, 75). The generalization of the second law of thermodynamics and Crooks's relation, presented in what follows, were used for deriving England's expression.

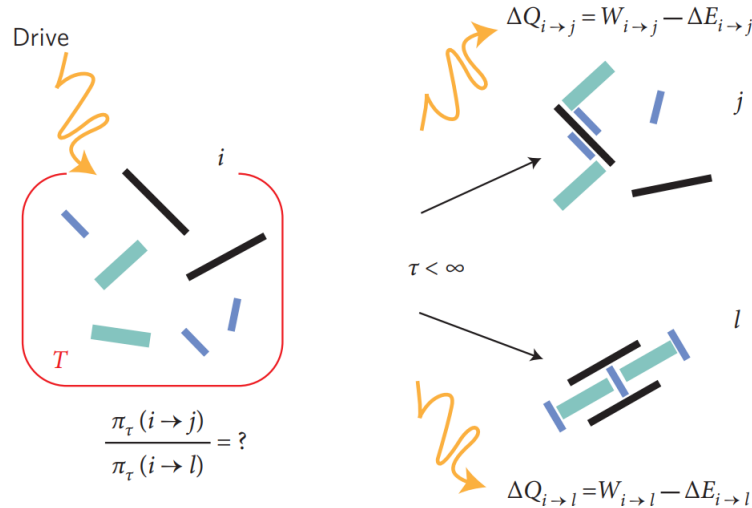


Figure 6 – The probability of finding a system in a given state depends on both its initial condition and precisely the way it was driven. Expressing this probability distribution in terms of thermodynamic quantities poses a significant challenge, since it involves not only the internal energy of the final states, but also the work done by the drive during transitions between states.

Source: ENGLAND (27).

4.2.1 Crooks's Theorem

In 1999, Crooks (55) formulated an expression that combines time-reversal symmetry and energy conservation, delineating the probabilities of different dynamic trajectories that a thermal fluctuation within a system might follow.

The expression, Eq.(4.2), establishes a connection between the probabilities of forward and backward paths, linking them to the heat released into the reservoir during the forward trajectory (for details of the derivation, see Ref. (76)). The direction that tends to evolve more heat into its surroundings is the one the system is more likely to follow

$$\frac{\pi(\gamma)}{\pi^*(\gamma^*)} = \exp\left(\frac{\Delta Q(\gamma)}{k_B T}\right) \quad (4.2)$$

where $\gamma \equiv [x(t), v(t)]$ is the dynamical trajectory and the time-reversed one is given by $\gamma^* \equiv [x(\tau - t), -v(\tau - t)]$. $\pi(\gamma)$ and $\pi^*(\gamma^*)$ are forward and backward probabilities, respectively, and ΔQ represents the heat exchanged during the forward trajectory.

The expression above suggests forward microtrajectory γ is more probable than its time-reversed counterpart γ^* (backward). The difference in probability between those trajectories is expressed exponentially, with the exponent determined by the amount of heat released into the surrounding thermal reservoir during the forward path ($\Delta Q(\gamma)$). According to the energy conservation law, the total heat ΔQ typically consists of two components, namely, internal energy change ΔE within the system from initial to final states and the work W performed by the applied field throughout the entire process (27). Eq.(4.2) derives a generalization of the second law of thermodynamics for providing England's expression.

4.2.2 Generalization of the second law of thermodynamics

A general experimental scenario starting and ending in out-of-equilibrium must be considered for the derivation of the second law of thermodynamics generalization. Setting up a framework for analyzing how a system transitions between two states, defined as X, X' [§] when subjected to an external driving force, with a particular frequency and considering the probabilities of such transition, defined as $\pi_\tau(X \rightarrow X')$, occurring within a finite time τ , backward probability is represented as $\pi_\tau^*(X' \rightarrow X)$ and the generalization of the second law of thermodynamics can be written combining the laws of thermodynamics[¶] with Crooks's relation (Eq.(4.2))^{||}

$$\langle W \rangle_{X \rightarrow X'} - \langle \Delta E \rangle_{X \rightarrow X'} + T \Delta S_{int} \geq k_B T \ln \left[\frac{\pi_\tau(X \rightarrow X')}{\pi_\tau^*(X' \rightarrow X)} \right] \quad (4.4)$$

where $\langle \dots \rangle_{X \rightarrow X'}$ denotes averaging over repeated measurements of a transition from X to X' states, ΔE represents the internal energy change, ΔS is the external entropy change, and extra term W is the external work performed on the system.

[§] Each of them with internal entropy S_{int}^X and $S_{int}^{X'}$ and average internal energy given by $\langle E \rangle_X$ and $\langle E \rangle_{X'}$. x is the starting state and X' is the ending one.

[¶] First law: for closed systems $\Delta E = W + Q$, ΔE is the system's internal energy, W is the work performed on the system, and Q is the heat absorbed by the system.

Second law: the entropy of every closed and isolated system increases monotonically $\Delta S \geq 0$. The quantity of heat exchanged by the system during a reversible process at equilibrium temperature T can be written as $\Delta S = \frac{\Delta Q_{rev}}{k_B T}$.

Third law: the entropy change in any isothermal process approaches zero as the temperature at which the process occurs approaches zero, i.e., $(\Delta S)_{T \rightarrow 0} \rightarrow 0$.

^{||} Combining the exponential properties of $e^x \geq x + 1$ and $\langle e^x \rangle \geq \langle x \rangle + 1$ and applying them to Crooks's relation, the generalization of the second law of thermodynamics can be derived as

$$\Delta S_{total} \geq \ln \frac{\pi^*(\gamma^*)}{\pi(\gamma)}. \quad (4.3)$$

Therefore, the more irreversible something, the larger the increase in the entropy of the universe.

An irreversible process, in which the transition probability from X to X' states is greater than the opposite, i.e., the forward transition probability is bigger than the backward one, can be considered towards the understanding of the aforementioned equation. As the statistical irreversibility of a spontaneous process increases, leading to a higher likelihood of transitioning from state X to state X' compared to the reverse under specific non-equilibrium driving conditions, the minimum total entropy required also increases. Increased irreversibility implies a greater amount of work done on the system being dissipated rather than stored in the system (27).

4.3 Hypothesis of dissipative adaptation

The way to treat the thermodynamics of out-of-equilibrium systems has been extensively explored in the past few years (77–79). The hypothesis of dissipative adaptation emerges towards a step forward in understanding the relation of Gibbs distribution for those systems (27, 74) and aims to find a general principle applicable even to situations far from equilibrium for providing insights or replicating the behavior of living organisms, which are essentially out-of-equilibrium open systems.

In biology, the idea of adaptation has arisen from the fact certain configurations are effective at absorbing energy from the environment and self-replicating, inheriting the configuration from their parents and evolving to never returning to their initial one (e.g., a mammal will never become an embryo again) (80, 81). In other words, a system efficient in replication must be good at absorbing work from the environment.

Using that idea as the basis of adaptation in a physical system, England suggested it might be true for any ensemble of atoms (82, 83). The dissipative adaptation hypothesis is the ability of a system to become very finely tuned to its out-of-equilibrium environment, taking into account the history of absorption of work and heat dissipation during the process (27, 74). Consequently, more organized states at the end of the process consume the greater absorbed work. England basically generalized Boltzmann distribution so that it can hold for out-of-equilibrium systems. What is essential for that hypothesis is the focus is not on the probabilities of achieving certain states, but rather, on the probabilities of the trajectories leading to those states.

Using Crooks' relation, Jarzynski equality**, and the generalization of the second law of thermodynamics, England summed different possible microtrajectories and their

** Which relate the probability distribution of out-of-equilibrium values of work with free energy difference, $\langle e^{-\beta W_{abs}} \rangle = e^{-\beta \Delta F}$, where ΔF is the free energy difference (27).

associated probabilities (27, 71)^{††}, resulting in

$$\frac{\pi_\tau(i \rightarrow j)}{\pi_\tau(i \rightarrow k)} = \exp\left\{-\frac{\Delta E_{jk}}{k_B T}\right\} \frac{\pi_\tau^*(j^* \rightarrow i^*) \langle e^{-W/(k_B T)} \rangle_{i \rightarrow k}}{\pi_\tau^*(k^* \rightarrow i^*) \langle e^{-W/(k_B T)} \rangle_{i \rightarrow j}} \quad (4.5)$$

The expression above describes the transition probabilities from initial state i to final states j and k , i.e., within a classical theoretical framework, dissipative adaptation can be understood through the demonstration of the way certain final states of the system are statistically privileged as a result of having consumed more work.

The equation can be interpreted as the summation of the distinct pressures pushing the systems towards particular outcomes (71). The probability ratio, Eq.(4.5) is expressed through three terms detailed in what follows:

1. $\exp\left\{-\frac{\Delta E_{jk}}{k_B T}\right\}$ enables the recovery of Boltzmann distribution. In the absence of an external drive ($W = 0$) and for long times ($t \rightarrow \infty$), the second and third terms of the right side equal one. As a result, the system in contact with a heat bath tends towards thermal equilibrium.
2. $\frac{\pi_\tau^*(j^* \rightarrow i^*)}{\pi_\tau^*(k^* \rightarrow i^*)}$, called kinetic accessibility, indicates not all states are equally accessible to each other on a finite timescale. The term can dominate in case of a kinetically trapped system in a high-energy arrangement.
3. $\frac{\langle e^{-W/(k_B T)} \rangle_{i \rightarrow k}}{\langle e^{-W/(k_B T)} \rangle_{i \rightarrow j}}$ is a measure of reliable work absorption during the transition history. The term dominates if transitioning from state i to state j absorbs plenty of work with little fluctuation. The term takes into account the trajectories of the system.

As claimed by England, the equation elucidates the system's ability for self-organizing. Essentially, the system tends to settle into a particular state because that state has proven stable through a history of work absorption. The equation summarizes England's dissipative adaptation hypothesis, which describes a general thermodynamic mechanism for self-organization via dissipation of absorbed work under external driving forces, applicable to out-of-equilibrium systems evaluated over finite time intervals. More

^{††} For an initial state i and two possible final states j, k , the probability ratio for each transition is

$$\frac{\pi_\tau(i \rightarrow j)}{\pi_\tau^*(j^* \rightarrow i^*)} = e^{\beta \Delta Q_{diss}^{ij}}; \quad \frac{\pi_\tau(i \rightarrow k)}{\pi_\tau^*(k^* \rightarrow i^*)} = e^{\beta \Delta Q_{diss}^{ik}}.$$

Dividing the two expressions above and rearranging the parameter result in

$$\frac{\pi_\tau(i \rightarrow j)}{\pi_\tau(i \rightarrow k)} = \frac{\pi_\tau^*(j^* \rightarrow i^*)}{\pi_\tau^*(k^* \rightarrow i^*)} e^{\beta(\Delta Q_{diss}^{ij} - \Delta Q_{diss}^{ik})}.$$

England's expression can be derived through Jarzynski equality and the first law of thermodynamics.

adapted states, i.e., the most probable and longest-lasting ones, are typically those with a history of higher work absorption followed by heat dissipation.

Whereas any changes to the system's configuration may initially seem random, the most enduring and irreversible ones occur when the system temporarily enhances its capability of absorbing work and dissipating energy. Over time, only the memory of those paths that involve energy dissipation will persist, resulting in the system appearing self-organized in a state well-adapted to its environmental conditions. In essence, dissipative adaptation can be conceptualized as a generalization of Boltzmann distribution for out-of-equilibrium systems.

The essential aspect of irreversibility in such systems is important for the characterization of a system that might exhibit the adaptation of a dissipative one. Towards guaranteeing adaptation to those systems, the energy absorbed during the transition from one state to another must be consumed after the process so that no more energy is used by the system for returning to its initial configuration.

The hypothesis discussed here involves the idea that a classical particle solely influenced by random thermal fluctuations may be unable to surpass an energy barrier. However, when an external drive is introduced into the system, the particle can jump over the barrier using the energy provided by the external source for the transition to that other side. By the principle of conservation of energy, that energy is subsequently dissipated and, consequently, the particle cannot revert to its initial state (Fig.7).

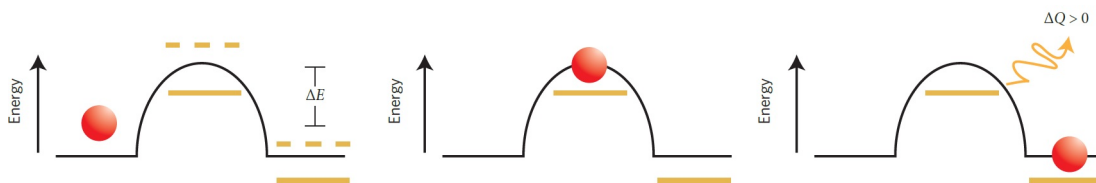


Figure 7 – Driven barrier hopping (for further details, see Ref. (27)).

Source: ENGLAND (27).

Another fundamental aspect of dissipative adaptation, which revolves around a certain type of asymmetry, must be emphasized. When a system is subjected to symmetric drive, regardless of the drive intensity, it will show equilibrium symmetrically. Therefore, asymmetry in the drive induces population accumulation on one side of the potential well, subsequently leading to adaptation. Such a characteristic is important for the driven system explored in Chapter 6.

4.4 Quantum regime of dissipative adaptation

Introducing the hypothesis of dissipative adaptation to the quantum regime is a natural progression. However, two main obstacles are encountered during the establishment of a connection between nonequilibrium organization and thermodynamic quantities. The first refers to limit $T \rightarrow 0$, where quantum fluctuations become significant and neither Crooks's, nor dissipative adaptation hypothesis is valid. Consequently, directly translating England's expression, Eq.(4.5), to the quantum realm is not straightforward. The second challenge is related to the definition of work in quantum regime. The following sections detail those issues and provide a brief overview of both.

4.4.1 Quantum work

The definition of work in quantum mechanics is challenging and one of the many questions that remain open in the field of quantum thermodynamics. Several authors have tried to propose a suitable definition of work, as addressed in what follows.

In the classical regime, work is the transfer of energy that results from a force applied over a distance, i.e., it is the product of the force applied to an object and the distance over which it is applied. However, in the quantum regime, resulting from Heisenberg uncertainty principle, momentum and position cannot be determined simultaneously, invalidating the aforementioned definition.

The definition of work in quantum thermodynamics is difficult, for it does not fall into the category of observables^{‡‡}, like position or momentum. Differently from those quantities, work does not have a corresponding operator that can be easily explored within the formalism of quantum mechanics (84). That is a problem, since quantum mechanics relies on a clear connection between observables and measurement outcomes, and in the context of thermodynamics, quantities like work and heat are associated with processes rather than with static states. The integration of thermodynamics with quantum mechanics is challenging, since the usual framework of quantum mechanics may not directly apply to those thermodynamics quantities.

Among the numerous definitions of work in quantum thermodynamics, one of the most accepted is based on the two-point measurement (TPM) method. A way to define work in a quantum regime is using the second law of thermodynamics. For a closed quantum system, work can be written with two contributions, namely, heat transferred between system-environment and internal energy change. Since heat cannot be considered in a closed system, work can be defined as the difference of final and initial internal energies

^{‡‡} The observables of a physical system are quantities that can be measured and represented by Hermitian operators.

as

$$W_{n \rightarrow m} = E_f^m - E_i^n \quad (4.6)$$

where E_f^m is the m -th eigenenergy of the final system and E_i^n is the n -th eigenenergy of the initial one.

In such a definition, two projective measures are performed at the protocol's beginning and end and quantum work is, therefore, defined as the difference in energy eigenvalues between those two measures for a single realization. Its distribution can be evaluated by repeating the TPM protocol (85–87). Such a definition is valid when there is no coupling between system-environment and when the dynamics are unital^{§§}.

Other definitions of quantum work can be used considering a quantum system described by density matrix ρ . The mean value of an observable A can be

$$\langle A \rangle = \text{Tr}\{\rho A\}. \quad (4.7)$$

Therefore, the system's internal energy is considered $E = \text{Tr}\{\rho H\}$. The change in this expression is

$$\Delta E = \text{Tr}\{\rho(t_f)H(t_f)\} - \text{Tr}\{\rho(t_0)H(t_0)\}. \quad (4.8)$$

An infinitesimal change (∂)^{¶¶} in the internal energy associated with the temporal evolution of the system leads to

$$\partial E = \partial \text{Tr}\{\rho(t)H(t)\} = \text{Tr}\{\partial \rho(t)H(t)\} + \text{Tr}\{\rho(t)\partial H(t)\}. \quad (4.9)$$

The change in the energy of state ρ is due to a change in the Hamiltonian by the application of an external parameter, i.e., the change can be identified as a quantity of work done during the system's evolution. Alternatively, due to the dynamical change in state ρ , i.e., a reconfiguration for the system that can be associated with heat, the work done by the system and the heat absorbed are written as

$$\partial Q \equiv \text{Tr}\{\dot{\rho}(t)H(t)\}dt, \quad (4.10)$$

$$\partial W \equiv \text{Tr}\{\rho(t)\dot{H}(t)\}dt. \quad (4.11)$$

where dots represent derivation in time.

Furthermore, some authors may have used a definition based on classical work, which is related to Heisenberg's definition. The next section explores a reference for the quantum dissipative adaptation, when this classical similar definition is adopted.

^{§§} The dynamics do not alter the populations of the density matrix.

^{¶¶} It is not an exact differential that guarantees those quantities of work and heat are not observables.

4.4.2 Quantum dissipative adaptation

As addressed in previous sections, the classical equation for the dissipative adaptation and Crooks's relation are not well defined in the $T = 0$ limit. Valente et.al. (21) employed a simpler system related to England's barrier to derive the relation between transition probability and thermodynamics quantities such as absorbed work from a single photon pulse. The barrier was represented by a three-level system in Λ configuration. The authors derived a relationship for the so-called quantum dissipative adaptation using the system-environment approach, where the system is influenced by an external drive characterized by a single photon pulse.

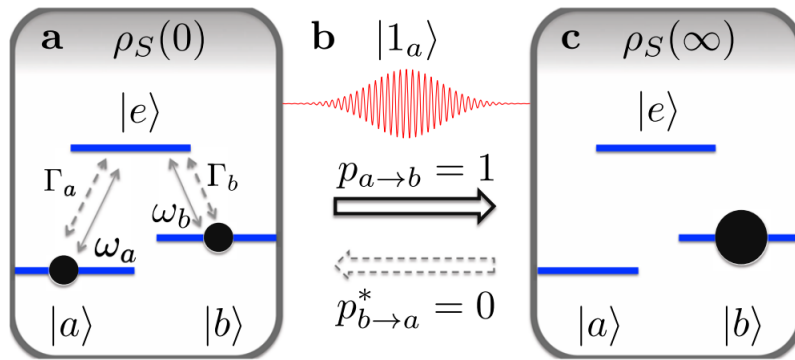


Figure 8 – Representation of quantum dissipative adaptation in Λ system with two ground states, $|a\rangle$ and $|b\rangle$, and one excited state $|e\rangle$. **a)** density operator of the system, ρ_S , at time $t = 0$. $\Gamma_{a/b}$ are the environment-induced spontaneous emission rates and $\omega_{a/b}$ are the transition frequencies. The initial state is a mixture of the two lower energy eigenstates $\rho_S(0) = p_a^{(0)} |a\rangle \langle a| + p_b^{(0)} |b\rangle \langle b|$ at zero temperature. **b)** A nonequilibrium environment composed of a single-photon pulse $|1_a\rangle$, which serves as the work source, drives the system dynamics and induces the time-dependent transition probability $p_{a \rightarrow b}(t)$ from $|a\rangle$ to $|b\rangle$. The backward transition probability (with a time-reversed pulse) $p_{b \rightarrow a}^*$ goes to zero at zero temperature. **c)** the asymptotic state is pure, $\rho_S(\infty) = |b\rangle \langle b|$, i.e., the atoms arrange themselves spontaneously into an organized state, often referred to as self-organization. The state is conditioned to maximizing the work absorbed and the heat dissipated in the transition. The driven system undergoes an irreversible self-organizing dynamics.

Source: VALENTE *et al.* (21).

Fig. 8 shows the driven system's evolution. The excited state can spontaneously decay to two possible lower states, mimicking an energy barrier. However, Λ system has no tunneling parameter. Equation (4.12) describes a similar relation to England's for classical systems, associating the transition probability to the work done on the system

by the driving source.

$$p_{a \rightarrow b}(\infty) = \frac{\Gamma_b}{\Gamma_a + \Gamma_b} \frac{\langle W_{abs} \rangle_a}{\hbar \omega_a}, \quad (4.12)$$

$$p_{b \rightarrow a}^*(t) = 0. \quad (4.13)$$

The expressions were analyzed for the limit of zero temperature. On the one hand, the more the work on average absorbed and released by an atom for transitioning from one configuration to another, the higher the probability transition for those states. On the other hand, if the driving force is reversed in time, the system does not return to the initial configuration, i.e., the backward transition probability is zero. The quotient between the transitions probabilities undergoes a singularity, explaining why the $T = 0$ limit cannot be taken in England's expression.

A more adapted quantum state (self-organized) is the one with the highest historical of absorption of work followed by maximum heat dissipation. The relationship between absorbed work and system behavior is established by calculating Schrodinger's equation for the entire system and deriving expressions for work and heat as consequences of solving the equation. The work defined in this study is an analogue to the classical one (some details on the definition and derivation of quantum work for this system can be found in Appendix H). Therefore,

$$\langle W_{abs} \rangle_a = \langle Q_{diss} \rangle_a + \langle H_S(\infty) \rangle - \langle H_S(0) \rangle, \quad (4.14)$$

where $\langle Q_{diss} \rangle$ represents the dissipated heat and $\langle H_S(\infty) \rangle$ and $\langle H_S(0) \rangle$ denote the internal energy of the system at final and initial states, respectively. Eq. (4.14) obeys the conservation of energy principle, according to which the work done on the system is partially dissipated as heat, while the remainder contributes to the change in the internal energy of the system.

Such a three-level system with the drive as a single photon pulse does not thermalize and is always kept out-of-equilibrium. Another important aspect of dissipative adaptation hypothesis in both classical and quantum regimes is the irreversibility of the processes, as discussed in this chapter. The system must follow irreversible paths so that its adaptation is in the highest work-absorbed state. In quantum regime, such irreversibility became clear from the asymmetry in the probabilities transition in forward and backward processes.

The main points in Ref.(21) refer to the absorption of work, which is not directly associated with transitions from the lowest energy states to the highest ones. Although the highest work absorbed by the photon in Λ system leads to a significant transition from state $|a\rangle$ to state $|b\rangle$, it does not result in the most significant transition from state $|a\rangle$ to state $|e\rangle$. In other words, if the system is too excited, it does not necessarily maximize

the absorbed work. Another important point is the work performed on the atom does not depend on the energy gap between $|a\rangle$ and $|b\rangle$ states, suggesting the system's ability to absorb work is not solely determined by the energy difference between its initial and final states. Those findings underscore one of the initial insights into the behavior of dissipatively adapted systems in the quantum regime.

The next chapters explore other quantum systems towards deriving a concept similar to quantum dissipative adaptation for a simpler system, specifically a two-level system.

5 TWO-LEVEL SYSTEMS IN A DOUBLE WELL POTENTIAL

So far, discussions on both classical and quantum dynamics of dissipative systems have been explored and the hypothesis of dissipative adaptation was introduced in the previous chapter for classical systems composed of a barrier and similarly for quantum systems with a three-level system in Λ configuration.

Inspired by the bistable potential considered in England's research (83), this chapter analyzes the two-level system (TLS) in a double well potential coupled to a dissipative environment. The model is a very successful open quantum system that has been investigated over the past few years and whose dynamics has been adopted for studies of several physical systems (e.g., superconducting devices with Josephson junctions (88), two-level atoms in optical cavities (89), and semiconductor quantum dots (90), to name a few).

England numerically investigated driven disordered mechanical networks composed of bistable springs and characterized by a multiple stable configuration resulting from the dual stable rest lengths of each spring. The two wells have distinct frequencies (ω_0, ω_1) and their results indicate presence of a specific range of forcing amplitudes, wherein the attractor states of those driven disordered multistable mechanical networks are finely tuned to exhibit low energy absorption from the external forcing pattern (see Fig. 9) (83).

A TLS in a double well potential with a driven force, called driven spin-boson model, investigated a quantum system that might exhibit the dissipative adaptation mechanism in a more simpler configuration than the tree-level system in Ref.(21). The symmetry of such potential is considered through an analysis of the separation between the two well-parameter, ϵ . If a symmetric bistable potential is considered ($\epsilon = 0$), then the energy spectrum of the system is degenerate. On the other hand, if an asymmetric double potential ($\epsilon \neq 0$) is taken into account, the energies are not degenerate and some interesting features must appear, as discussed in chapter 6.

The temperature regime must be analyzed for the TLS validity. The model can be seen as an approximation in Hilbert space associated with the bistable system, which can be taken when the temperature is sufficiently low. Therefore, the system's dynamics can be confined to the subspace defined by the lowest doublet, composed of the eigenstates $\{|g\rangle, |e\rangle\}$ of the bare Hamiltonian (Fig. 10)*.

On the other hand, when temperatures approach the energy gap between lowest and subsequent energy levels, the approximation of TLS becomes invalid and the complex multilevel characteristics of the bistable potential become significant and cannot be

* $|g\rangle$ denotes ground state and $|e\rangle$ denotes excited state.

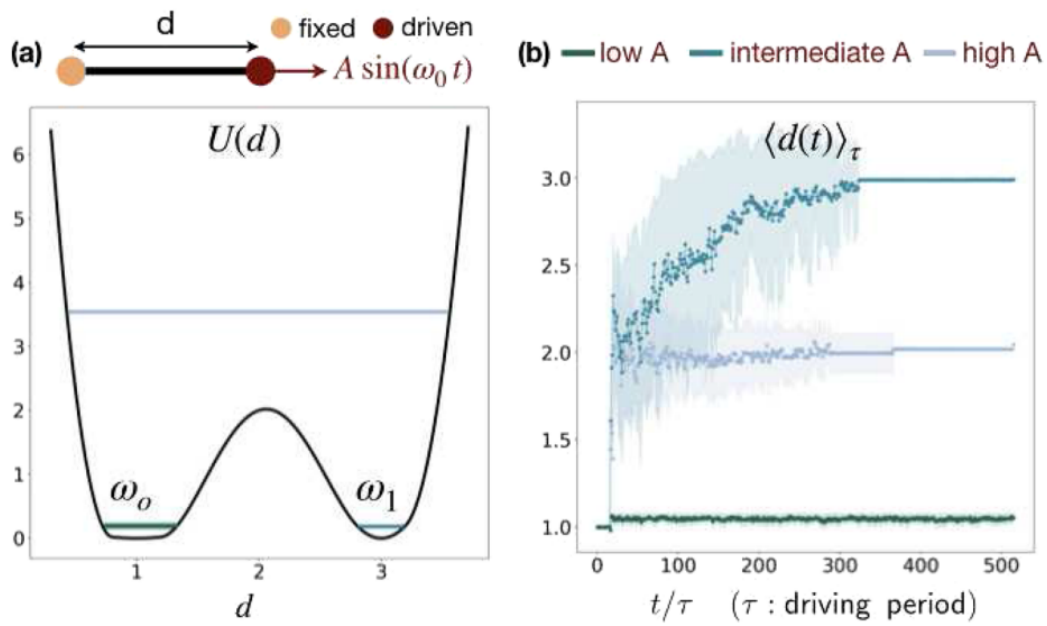


Figure 9 – Reproduction of Fig. 1 from Ref. (83), where a one-dimensional bistable spring is subjected to sinusoidal forcing at low (green), intermediate (blue), and high (light blue) amplitudes. **(a)** The plot shows the average energy levels across a forcing period for different amplitudes, where $U(d)$ represents the bistable spring potential. **(b)** The trajectory of the average spring length illustrates distinct behaviors: remaining confined in the initial potential well ($\langle d \rangle \approx 1$) during low amplitudes (green), transitioning to the nonresonant potential well ($\langle d \rangle \approx 3$) for intermediate amplitudes (blue), and consistently oscillating between the two wells ($\langle d \rangle \approx 2$) at high amplitudes (light blue).

Source: KEDIA *et al.* (83).

disregarded (91–94). Such a situation arises, for instance, in chemical processes, in which the existence of a higher tunneling doublet under an effective potential barrier contributes to activated rates at specific temperatures. TLS in a double well potential is of profound

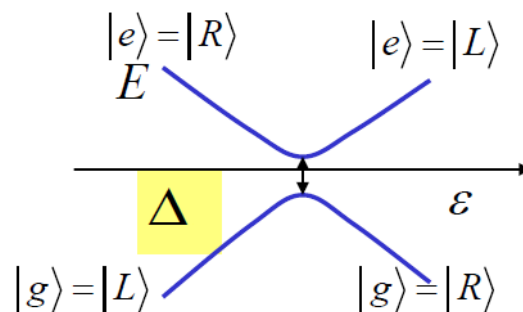


Figure 10 – Representation of energy level as a function of bias ϵ .

Source: GRIGONI; HÄNGGI (95).

importance as the simplest fundamental model for the study of thermal relaxation and

quantum tunneling phenomena in a number of physical and chemical systems, e.g., electron transfer reactions (96), proton tunneling (97,98), tunneling of Bose-Einstein condensates (99,100), superconducting quantum interference devices (SQUID's) (28,101,102), nuclear fusion (103), among others.

Fig. 11 (28,47,104) illustrates the model, where the quantum tunneling, represented by Δ , enables transition between the states in two dimensions. Moreover, if the separation between the two minima of the double well, given by ϵ , is small enough and the barrier is not too high, quantum mechanical tunneling can occur between the wells.

In classical regime, when barrier crossing is not driven by thermal effects, a particle remains in a potential minimum indefinitely, differently from the quantum regime, in which even at absolute zero temperature, the particle remains confined in one potential well until tunneling allows escape.

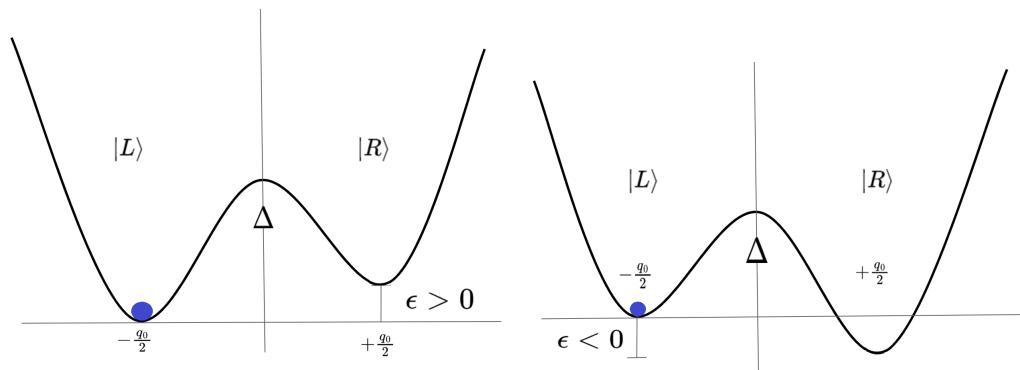


Figure 11 – Representation of an asymmetric double well potential related to the sign of the separation between the two minima of energy, denoted as ϵ . Each side of the potential well has a specific frequency and energy, defined as ω_+ and ω_- , for right and left sides, respectively. Whereas the eigenvalue of $+q_0/2$ represents the right side, the eigenvalue of $-q_0/2$ represents the left side. Considering the particle starts on the left side of the well, **a)** if ϵ is positive, the particle starts in the stable well and, **b)** if ϵ is negative, the particle starts in the unstable well.

Source: By the author

A way to illustrate TLS in a double well potential dynamics is describing tunneling in terms of localized basis, where left/right well states $|L/R\rangle$ are combinations of $|g\rangle$ (ground) and $|e\rangle$ (excited) states[†] and spin operators can be written as $\sigma_x = |R\rangle\langle L| + |L\rangle\langle R|$ and $\sigma_z = |R\rangle\langle R| - |L\rangle\langle L|$. The position operator is given by $q = q_0\sigma_z/2$ and $\pm q_0/2$ eigenvalues of q correspond to the positions of the localized states. Such states are related to eigenstates ($|g\rangle, |e\rangle$) of the Hamiltonian, respectively, through an orthogonal

[†] Refers to either a clockwise current, or a counterclockwise one within the superconducting loop of a three-junction Josephson qubit, or more broadly, the qubit's two logical states (105).

transformation

$$|R\rangle = \cos \frac{\varphi}{2} |g\rangle + \sin \frac{\varphi}{2} |e\rangle \quad (5.1)$$

$$|L\rangle = \sin \frac{\varphi}{2} |g\rangle - \cos \frac{\varphi}{2} |e\rangle \quad (5.2)$$

where $\tan \varphi = -\frac{\Delta}{\epsilon}$.

The double well is usually characterized by barrier height V_0 , separation $\hbar\omega_0$ between the ground state and the first excited state within each well, and an intrinsic “detuning” energy ϵ between the ground states in the two wells. In $V \gg \hbar\omega_0$ regime, which is much greater than both ϵ and $k_B T$, the system effectively resides within a two-dimensional Hilbert space spanned by the two ground states (106).

For convention, if the particle starts the dynamics on the left side of the well ($\epsilon > 0$), i.e., the left well is lower and the particle is initially in the stable well[‡]. The difference in the population of the two wells, given by $\langle \sigma_z \rangle = P_R - P_L$, is positive, because the population of the right well must be thermodynamically higher. Conversely, if the sign of ϵ is negative, the particle starts the dynamics in the unstable well, i.e., the highest state of the potential. (see Fig.11 for more details).

The dissipation process is included in TLS in a double well potential by linearly coupling the system with a thermal reservoir. As aforementioned, the reservoir, or environment, is modeled as a large set of harmonic oscillators initially in equilibrium. Using this description for the environment, a dissipative TLS in a double well potential can be equivalently represented as a versatile and well-studied spin-boson model (106, 107). Since our aim is to study dissipative adaptation hypothesis in a simpler quantum system, the dissipation included in TLS means an establishment of a clear connection with the hypothesis. The lack of a crucial component in the study of TLS in a double well potential motivated the design of a model called driven spin-boson, described in the following chapter.

The goal here is to show a system simpler than the one with three-level states and analyze the possibility of finding the dissipative adaptation mechanics in it. Differently from England’s and Valente’s studies, tunneling is taken into account in our proposed quantum model[§]. Instead of a single path or trajectory to be followed by the particles to reach the other side of the barrier, the system can tunnel through the wells; therefore, several trajectories that are not classically accessible must be taken into account. Since our interest is in investigating a quantum dissipative adaptation in such driven TLS, the path integral formalism must be used, for it finds all possible trajectories the system may follow for transitioning from one side to another of the well.

[‡] It is the minimum of energy when the two sides of the wells are compared.

[§] Driven spin-boson model, explored in chapter 6.

This chapter introduces the dissipative TLS spin-boson model, covering the dynamics with path integral formalism for the case of asymmetric spin-boson (1,28).

5.1 Spin-boson model

Spin-boson model, which is a variant of Caldeira-Leggett model, involves a spin or a TLS in a double well potential interacting with a bosonic bath. In such systems, the hopping dynamics between two trapped positions is well studied effects and is connected by hopping amplitude Δ , under perturbation caused by coupling to the environment (34). The environment can be considered with an Ohmic spectral function, as discussed previously in chapter 2. The theoretical analysis of spin-boson dynamics and path integral approach was provided by Leggett *et al.* (28).

This section addresses the spin-boson dynamics, which is formally solved by a path integral method. However, approximations must be invoked towards the derivation of closed-form analytical results - the usual non-interacting blip approximation (NIBA) is adopted in this study for an unbiased case ($\epsilon = 0$), as reported at the end of the chapter.

Depending on various coupling regimes and system parameters, distinct spin dynamics can be found (see Fig.12). As an example, the localization of a particle[¶] is performed under specific conditions and, particularly, when the coupling strength, such as dissipation to the bath, becomes strong, which is experimentally achievable (108,109). Figure 12 illustrates the difference in population over time in different regimes (110). Each parameter regime exhibits characteristic dynamical behaviors, including localization, exponential or incoherent relaxation, exponential decay, and strongly or weakly damped coherent oscillations (2,28).

In a general scenario, if the particle is initially in the left-hand side well, the probability of finding it again on the same side later depends on the hopping amplitude and interaction with the environment. In the absence of bath and for very low dissipation strengths and temperatures, TLS in a double well potential exhibits coherent oscillations between the two wells, known as Rabi oscillations. Conversely, under sufficiently high damping and/or temperatures, the dynamics become incoherent. Numerous studies have explored the crossover between coherent-to-incoherent dynamics (1,28).

Coherence is another characteristic dependent on the system's parameters, particularly when the two states have equal energy (zero-energy bias or unbiased case $\epsilon = 0$) and there is either zero, or weak dissipation. Theoretical predictions suggest the system will exhibit macroscopic quantum coherence at sufficiently low temperatures in such a

[¶] A particle or a quantum state is predominantly confined to one of the two possible states ($|L\rangle$ or $|R\rangle$), despite the potential for quantum superposition or tunneling between those states. The particle loses its ability to oscillate between the wells.

scenario. However, coherence within the system diminishes as the temperature increases and/or the level of dissipation strengthens (33).

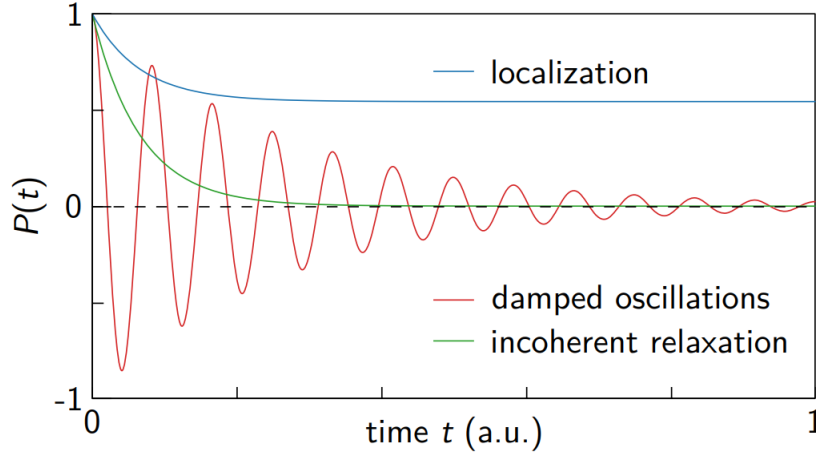


Figure 12 – Qualitative behavior of spin dynamics in the three main regimes of the spin-boson model with an Ohmic environment. Probability $P(t)$ corresponds to expectation value $P(t) = \langle \sigma_x(t) \rangle$, in the proposed systems, when initialized to the +1 eigenstate of σ_x at $t = 0$.

Source: LEPPÄKANGAS *et al.* (34).

5.1.1 Quantum mechanical calculations

The following Hamiltonian describes TLS in a double well potential when totally isolated from its environment (28), in localized basis $|R/L\rangle$

$$H_{TLS} = \frac{\hbar}{2} \left(\Delta(|R\rangle\langle L| + |L\rangle\langle R|) + \epsilon(|R\rangle\langle R| - |L\rangle\langle L|) \right), \quad (5.3)$$

and the Hamiltonian eigenvalues are given by

$$H_{TLS} |n\rangle = E_n |n\rangle, \quad (5.4)$$

$$E_n = \pm \frac{\hbar}{2} \sqrt{\Delta^2 + \epsilon^2}. \quad (5.5)$$

The energy splitting between ground and excited states is $E = E_{|e\rangle} - E_{|g\rangle} = \hbar\sqrt{\Delta^2 + \epsilon^2}$.

The transition probability expression is crucial for our analyses of the connection of a driven system and dissipative adaptation hypothesis. Using the usual quantum mechanical calculations, with energy basis, the occupation probability is given by

$$P_R(0) = 1 \quad P_R(t) = |\langle R|\Psi(t)\rangle|^2, \quad (5.6)$$

where the first expression means the system is initially on the right side of the well, and the other expression is the probability of finding the system again on the same side at time t later. In the localized basis, the probability of finding the system is written as

$$P_R(t) = |\langle R | \exp\{-it(\Delta\sigma_x + \epsilon\sigma_z)/2\} | R \rangle|^2. \quad (5.7)$$

Using the following equality for the evolution operator in TLS in a double well potential

$$e^{-i(tE/2\hbar)(\frac{\hbar\epsilon}{E}\sigma_z + \frac{\hbar\Delta}{E}\sigma_x)} = \cos(tE/2\hbar) - i \sin(tE/2\hbar) \left(\frac{\hbar\epsilon}{E}\sigma_z + \frac{\hbar\Delta}{E}\sigma_x \right). \quad (5.8)$$

Therefore, the probability is

$$P_R(t) = \cos^2(Et/2\hbar) + \left(\frac{\hbar\epsilon}{E} \right)^2 \sin^2(Et/2\hbar). \quad (5.9)$$

The same result can be recovered if the probability occupation is given by $P_L(0) = 1$. Therefore, the expression for the transition probability, following the same procedure, is

$$P_{L \rightarrow R} = P_{R \rightarrow L} = \left(\frac{\hbar\Delta}{E} \right)^2 \sin^2(Et/2\hbar), \quad (5.10)$$

which describes periodic sinusoidal motion between left and right states.

5.1.2 Path integral expression without dissipation

As aforementioned, the dynamics of a quantum system can be explained via path integral formalism. Regarding spin-boson dynamics, since many trajectories not classically accessible and quantum tunneling can occur, the formalism must again be implemented. However, since the spin-boson model has no classical analogue, i.e., classical action is not well-defined^{||}, the obtaining of dynamics is more difficult. The path integral expression for the propagator can be constructed as follows: the occupation probability is

$$P_R(t) = \left| \langle R | e^{-iH_{TLS}t/\hbar} | R \rangle \right|^2 = |K(R, t; R, 0)|^2, \quad (5.11)$$

which is expressed in terms of the propagator in the path integral formalism

$$K(R, t; R, 0) = \langle R | e^{iH_{TLS}t/\hbar} | R \rangle = \int \mathcal{D}\sigma A[\sigma]. \quad (5.12)$$

For a particle in a double-well potential, Feynman's formula can be applied

$$K(q_b, t_b; q_a, t_a) = \int_{t_a}^{t_b} \mathcal{D}q e^{iS[q]/\hbar} \equiv \int \mathcal{D}q A[q]. \quad (5.13)$$

For TLS in a double well potential Hamiltonian in its pseudo-spin form,

$$H_{TLS} = -\frac{\hbar}{2} (\Delta\sigma_x + \epsilon\sigma_z), \quad (5.14)$$

^{||} Since spin-boson Lagrangian cannot be expressed in Lagrangian form, the action of the system cannot be written in the usual form.

therefore,

$$K(\alpha, t_b, R, t_0) = \langle R | e^{-iH_{TLS}(t_b-t_0)/\hbar} | R \rangle = \sum_{l_1, \dots, l_N} \prod_{n=1}^{N+1} K(l_n, t_n; l_{n-1}, t_{n-1}), \quad (5.15)$$

where $\alpha = L, R$. The initial conditions are the system is in $|R\rangle$ at time $t_a = 0$ and $\sum_{l_\alpha=L,R} |l_\alpha\rangle \langle l_\alpha| = 1$ is used together with $\alpha = l_{N+1}$, $R = l_0$, and $t_b = t = t_{N+1}$.

Starting from the infinitesimal propagator

$$K(l_n, t_n; l_{n-1}, t_{n-1}) = \langle l_n | e^{-iH_{TLS}\tau_n/\hbar} | l_{n-1} \rangle = \langle l_n | 1 - iH_{TLS}\tau_n/\hbar | l_{n-1} \rangle. \quad (5.16)$$

leads to

$$\langle l_n | 1 - iH_{TLS}\tau_n/\hbar | l_{n-1} \rangle = \begin{cases} 1 + i\epsilon\tau_n/2, & l_n = l_{n-1} = R, \\ 1 - i\epsilon\tau_n/2, & l_n = l_{n-1} = L, \\ i\Delta\tau_n/2, & l_n \neq l_{n-1}. \end{cases} \quad (5.17)$$

Next, continuum limit $N \rightarrow \infty$, i.e., $\tau \rightarrow 0$ is taken and K is rewritten as a series expression in terms of number of tunneling transitions

$$K(R, t; R, 0) = \int \mathcal{D}\sigma A[\sigma] = \sum_{m=0}^{\infty} K^{(m)}(R, t; R, 0), \quad (5.18)$$

for zero order

$$K^{(0)}(R, t; R, 0) = \lim_{N \rightarrow \infty} \prod_{n=1}^{N+1} K(R, t_n; R, t_{n-1}) = \lim_{N \rightarrow \infty} \prod_{n=1}^{N+1} \left(1 + i\frac{\epsilon\tau_n}{2} \right) = e^{i\frac{\epsilon t}{2}}, \quad (5.19)$$

and for odd orders

$$K^{(2m+1)}(R, t; R, 0) = 0. \quad (5.20)$$

The second order has the form

$$\prod_{n=1}^{j-1} K(R, t_n; R, t_{n-1}) K(L, t_j; R, t_{j-1}) \prod_{n=j+1}^{k-1} K(L, t_n; L, t_{n-1}) K(R, t_k; L, t_{k-1}) \prod_{n=k+1}^{N+1} K(R, t_n; R, t_{n-1}). \quad (5.21)$$

Taking $\lim_{N \rightarrow \infty}$ results in

$$e^{i\frac{\epsilon}{2}t_{j-1}} \left(i\frac{\Delta\tau_j}{2} \right) e^{-i\frac{\epsilon}{2}(t_{k-1}-t_j)} \left(i\frac{\Delta\tau_k}{2} \right) e^{i\frac{\epsilon}{2}(t-t_k)} \quad (5.22)$$

and, finally, summing up all possible $l_j = l_k = L$

$$K^{(2)}(R, t; R, 0) = \lim_{N \rightarrow \infty} \sum_{k=2}^N \sum_{j=1}^{k-1} e^{i\frac{\epsilon}{2}t_{j-1}} e^{-i\frac{\epsilon}{2}(t_{k-1}-t_j)} e^{i\frac{\epsilon}{2}(t-t_k)} \left(i\frac{\Delta}{2} \right)^2 \tau_j \tau_k, \quad (5.23)$$

or** (111)

$$K^{(2)}(R, t; R, 0) = \left(i\frac{\Delta}{2}\right)^2 \int_0^t dt_2 \int_0^{t_2} dt_1 e^{i\frac{\epsilon}{2}(t_1-t_0)} e^{-i\frac{\epsilon}{2}(t_2-t_1)} e^{i\frac{\epsilon}{2}(t-t_2)}. \quad (5.24)$$

Summing all orders ($t_{2m+1} = t$) leads to

$$K(R, t; R, 0) = \sum_{m=0}^{\infty} \left(i\frac{\Delta}{2}\right)^{2m} \int_0^t dt_{2m} \cdots \int_0^{t_2} dt_1 \prod_{j=0}^m e^{i\frac{\epsilon}{2}(t_{2j+1}-t_{2j})} \prod_{j=1}^m e^{-i\frac{\epsilon}{2}(t_{2j}-t_{2j-1})}. \quad (5.25)$$

Because the integrals are in convolutive form, Laplace transform (43) must be introduced, thus obtaining

$$K_{RR}(\lambda) = \sum_{m=0}^{\infty} \left(i\frac{\Delta}{2}\right)^{2m} \prod_{j=1}^m \int_0^{\infty} d\tau_j e^{-(\lambda+i\epsilon)\tau_j} \prod_{j=0}^m \int_0^{\infty} ds_j e^{-(\lambda-i\epsilon)s_j}, \quad (5.26)$$

or

$$K_{RR}(\lambda) = \sum_{m=0}^{\infty} \left(i\frac{\Delta}{2}\right)^{2m} \left(\frac{1}{\lambda+i\epsilon/2}\right)^m \left(\frac{1}{\lambda-i\epsilon/2}\right)^{m+1} = \frac{1}{2} \frac{2\lambda+i\epsilon}{4\lambda^2+(E/\hbar)^2}. \quad (5.27)$$

Finally, the inverse Laplace transform can be performed:

$$K(R, t; R, 0) = \frac{1}{2\pi i} \int_C dt e^{\lambda t} K_{RR}(\lambda), \quad (5.28)$$

where C denotes Bromwich contour. Since the poles are in $\lambda = \pm iE/2\hbar$, the final result can be written as

$$K(R, t; R, 0) = \cos\left(\frac{Et}{2\hbar}\right) + i\frac{\hbar\epsilon}{E} \sin\left(\frac{Et}{2\hbar}\right), \quad (5.29)$$

which is in agreement with quantum mechanical calculations in localized basis Eq.(5.9)^{††}.

** Given a function $f(x)$, which is continuous in the $[a, b]$ time interval, a definite integral can be defined as

$$\int_a^b f(x) dx,$$

which can be approximated by a Riemann sum as

$$\sum_{i=1}^n f(x_i) \Delta x,$$

where $\Delta x = (b-a)/n$ is the width of each interval, n is the number of intervals into which range $[a, b]$ is divided, and x_i is a sample point in the interval. When $n \rightarrow \infty$, then $\Delta x \rightarrow 0$ and Riemann sum approaches the exact value of the integral

$$\lim_{n \rightarrow \infty} \sum_{i=1}^n f(x_i) \Delta x = \int_a^b f(x) dx.$$

^{††} $P_R(t) = |K(R, t; R, 0)|^2$.

The next step is to return to the expression for $P_R(t)$. $P_R(t) = |K(R, t; R, 0)|^2$, where $K(R, t; R, 0)$ involves a double path integral over the two-state paths σ, σ' , which is reintroduced:

$$P_R(t) = \int \mathcal{D}\sigma \int \mathcal{D}\sigma' A[\sigma] A^*[\sigma']. \quad (5.30)$$

Evaluating the matrix elements of the infinitesimal density matrix

$$\begin{aligned} \rho(l_n, l'_n, t_n; l_{n-1}, l'_{n-1}, t_{n-1}) &= \langle l_n | \rho(t_n; l_{n-1}, l'_{n-1}, t_{n-1}) | l'_n \rangle \\ &= \langle l_n | (1 - iH_{TLS}\tau_n/\hbar) | l_{n-1} \rangle \langle l'_{n-1} | (1 + iH_{TLS}\tau_n/\hbar) | l'_n \rangle, \end{aligned} \quad (5.31)$$

and using Eq.(5.17) lead to

$$\rho(l_n, l'_n, t_n; l_{n-1}, l'_{n-1}, t_{n-1}) = \begin{cases} 1, & l_n = l_{n-1} = l'_n = l'_{n-1} = L, \\ 1 - i\epsilon\tau_n, & l_n = l_{n-1} = L, l'_n = l'_{n-1} = R, \\ 1 + i\epsilon\tau_n, & l_n = l_{n-1} = R, l'_n = l'_{n-1} = L + O(\tau^2), \\ i\Delta\tau_n/2, & l_n \neq l_{n-1}, l'_n = l'_{n-1}, \\ -i\Delta\tau_n/2, & l_n = l_{n-1}, l'_n \neq l'_{n-1}, \\ 0, & l_n \neq l_{n-1}, l'_n \neq l'_{n-1}. \end{cases} \quad (5.32)$$

Introducing sojourns $\eta(\tau) = \frac{1}{2}[\sigma(\tau) + \sigma'(\tau)]^{\ddagger\ddagger}$ and blip paths $\xi(\tau) = \frac{1}{2}[\sigma(\tau) - \sigma'(\tau)]^{\S\S}$ and identifying the four matrix elements of TLS in a double well potential density matrix η diagonal states (LL , $\eta = 1$, RR , $\eta = -1$) and ξ off-diagonal states (LR , $\xi = 1$, RL , $\xi = -1$) (107), then,

$$\rho(l_n, l'_n, t_n; l_{n-1}, l'_{n-1}, t_{n-1}) = \begin{cases} 1, & l_n = l_{n-1} = l'_n = l'_{n-1}, \\ 1 - i\epsilon\tau_n, & \xi_n = \xi_{n-1} = -1, \\ 1 + i\epsilon\tau_n, & \xi_n = \xi_{n-1} = 1, \\ i\Delta\tau_n/2, & \xi_n = \mp 1, \eta_{n-1} = \pm 1 \text{ or } \eta_n = \pm 1, \xi_{n-1} = \mp 1, \\ -i\Delta\tau_n/2, & \xi_n = \pm 1, \eta_{n-1} = \mp 1 \text{ or } \eta_n = \pm 1, \xi_{n-1} = \pm 1, \\ 0, & \eta_n = \pm 1, \eta_{n-1} = \mp 1, \text{ or } \xi_n = \pm 1, \xi_{n-1} = \mp 1. \end{cases} \quad (5.33)$$

A generic double path over two-state paths σ and σ' is transformed into a four-state path over the four states of the reduced density matrix. The path consists of an alternating sequence of sojourns and blips

$$P_R(t) = \int \mathcal{D}\eta \int \mathcal{D}\xi A[\eta, \xi]. \quad (5.34)$$

^{\ddagger\ddagger} Time intervals spent in a diagonal $\xi(\tau) = 0$ state (112).

^{\S\S} Time intervals spent in an off-diagonal $\eta(\tau) = 0$ state (112).

Taking continuum limit $N \rightarrow \infty$, i.e., $\tau \rightarrow 0$ and rewriting $P_R(t)$ as a series expression in the number of tunneling transitions result in

$$P_R(t) = \int \mathcal{D}\sigma A[\sigma] \int \mathcal{D}\sigma' A[\sigma'] = \sum_{m=0}^{\infty} P_R^{(m)}(t) \quad (5.35)$$

which, for zero order, is

$$P_R^{(0)}(t) = \lim_{N \rightarrow \infty} \prod_{n=1}^{N+1} 1 = 1, \quad (5.36)$$

and, for odd orders, is

$$P_R^{(2m+1)}(t) = 0. \quad (5.37)$$

Now, the second order becomes

$$P_R^{(2)}(t) = \lim_{N \rightarrow \infty} \sum_{k=2}^N \sum_{j=1}^{k-1} \left(\frac{i\Delta}{2} \right) e^{-i\xi \frac{\epsilon}{2}(t_{k-1}-t_j)} \left(\frac{-i\Delta}{2} \right) \tau_j \tau_k. \quad (5.38)$$

After summation over $\eta = +1, -1$, the series then reads

$$P(t) = 1 + \sum_{n=1}^{\infty} \frac{(-\Delta^2)^n}{2^n} \int_0^t dt_{2n} \int_0^{t_{2n}} dt_{2n-1} \cdots \int_0^{t_2} dt_1 \sum_{\{\xi_j = \pm 1\}} \cos \left(\sum_{j=1}^n \epsilon \xi_j \tau_j \right) \quad (5.39)$$

$$= 2P_R(t) - 1. \quad (5.40)$$

Evaluating $P_R(t)$ upon the inverse Laplace transformation

$$P_R(t) = \frac{1}{2\pi i} \int_C dt e^{\lambda t} P_R(\lambda) \quad (5.41)$$

leads to the same result of the quantum mechanical approach (Eq.(5.9))

$$P_R(t) = \cos^2 \left(\frac{Et}{2\hbar} \right) + \left(\frac{\hbar\epsilon}{E} \right)^2 \sin^2 \left(\frac{Et}{2\hbar} \right). \quad (5.42)$$

5.1.3 Influence of the environment

Since our focus is on studying dissipation in the spin-boson model, expressions should be derived for the transition and occupation probabilities considering the influence of the environment. As reported in the preceding sections, the influence of bath on the spin system was neglected. Towards a realistic situation, such influence must be taken into account, since it leads to decoherence and dissipation processes in the dynamics of the total system (105).

The coupling of the particle with the environment being exclusively to σ_z , the so-called ‘‘position coordinate’’, means the interaction primarily affects the component of the particle’s spin aligned with z -axis. This interaction opposes the tunneling effect, represented by σ_x , suggesting the environment tends to influence the system, thus preventing

its ability to tunnel between the two states. Instead, the environment's influence tends to localize the system into one of the two wells, favoring one particular state over the other (112).

The Hamiltonian of the spin-boson model is given by

$$H_{SR} = H_S + H_R + H_I \quad (5.43)$$

$$= \frac{\hbar}{2} (\Delta\sigma_x + \epsilon\sigma_z) + \sum_k \left(\frac{m_k\omega_k x_k^2}{2} + \frac{p_k^2}{2m_k} \right) + \frac{q_0\sigma_z}{2} \sum_k C_k x_k \quad (5.44)$$

where x_k, p_k, m_k, ω_k are, respectively, coordinate, momentum, mass, and frequency of the k -th harmonic oscillator representing the environment and q_0 is a parameter that, in a system with an extended coordinate, represents the distance between the two potential minima. Constant C_k denotes the strength of the coupling of the system to the k -th oscillator.

Studies on the dynamics of the spin-boson system involve various approximations. Typically, when the system is weakly coupled to its environment, Born-Markov master equation is commonly applied for describing the reduced density matrix. However, the perturbative nature of the approach, which focuses on weak coupling, renders it unsuitable for situations with strong coupling. In such cases, the real-time path integral method becomes valuable, since it eliminates bath degrees of freedom, providing an exact formal expression for the reduced density matrix. Although the expressions can be numerically solved in specific instances, the task is challenging, particularly at long times, as claimed by Ref. (47).

Dynamics can be analyzed through verifications of the reduced density matrix of the total density matrix. System preparation involves activating the coupling between the system and the bath, typically assumed to occur at time $t_0 \leq 0$. Subsequently, a scenario where system has been maintained in a particular state for a long time, for instance, $\sigma_z = +1$, is selected, allowing bath to equilibrate with the system. The selection effectively implies $t_0 \rightarrow \infty$. Consequently, at time $t = 0$, the constraint is released and the system evolves according to the spin-boson Hamiltonian^{¶¶} (112).

A system with a coordinate $x(\tau)$ begins with a value x_i and the environment begins in a state of thermal equilibrium - the probability $p(x_f, t)$ denotes the likelihood of the systems reaching a coordinate x_f at a later time t , regardless of the environment's state at that time. This probability is represented by element $\rho(x_f, x_f, t)$ of the reduced density matrix:

$$p(x_f, t) = \int \mathcal{D}x(\tau) \int \mathcal{D}y(\tau') A[x(\tau)] A^*[y(\tau')] \mathcal{F}[x(\tau), y(\tau')], \quad (5.45)$$

where the double path integral runs over all paths $x(\tau), y(\tau')$ such that $x(t_0) = y(t_0) = x_i, x(t) = y(t) = x_f$. $A[x(\tau)]$ is the amplitude for the system to follow path $x(\tau)$ in the

^{¶¶} The assumption ensures the system begins evolving in a state of equilibrium.

absence of the environment and quantity $\mathcal{F}[x(\tau), y(\tau)]$ is the influence functional that expresses the effect of the environment.

For Gaussian statistics^{***},

$$\mathcal{F}[q, q'] = \exp \left\{ - \int_0^t dt' \int_0^{t'} dt'' [q(t') - q'(t')] [K(t' - t'')q(t'') - K^*(t' - t'')q'(t'')] \right\} \quad (5.46)$$

where $K(t) \equiv \langle \zeta(t)\zeta(0) \rangle_\beta$ represents the force autocorrelation function^{††}.

Regarding the two-state problem, variables $x(\tau)$ and $y(\tau)$ are limited to the discrete values of $\pm \frac{q_0}{2}$. Eq.(5.45) is, therefore, an integral that considers all possible pairs of paths and each integral represents a transition between these two states ($\pm \frac{q_0}{2}$). For our purposes, it is more convenient to conceive it as an integral over a single path that jumps between four states. Those paths can be fully described by specifying, for each time τ , pair $[x(\tau), y(\tau)]$. Let us denote the states as $A = +, +$, $B = +, -$, $C = -, +$, and $D = -, -$, where $+$ = $\frac{q_0}{2}$ and $-$ = $-\frac{q_0}{2}$. States A and D correspond to the diagonal elements of the reduced density matrix, whereas B and C correspond to the off-diagonal ones (as in Fig.13). The integration over spin paths $\sigma(t)$ can be denoted due to the adoption of the

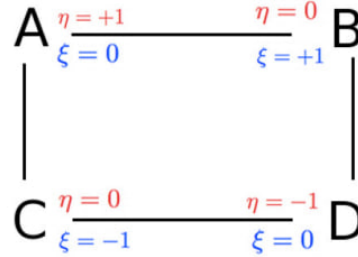


Figure 13 – Descriptions of the double spin path via Feynman-Vernon formulation involve classical variables η and ξ , which represent the spin paths and elements within the spin (reduced) density matrix.

Source: HENRIET *et al.* (113).

spin-boson model, and, therefore, the components of the reduced density matrix are given by

$$\langle \sigma_f | \rho_S(t) | \sigma'_f \rangle = \int \mathcal{D}\sigma(\cdot) \int \mathcal{D}\sigma'(\cdot) A[\sigma] A^*[\sigma'] \mathcal{F}[\sigma, \sigma']. \quad (5.47)$$

^{***} The path integrals for the bath oscillators in Eq.(3.4), which are exponentials of action functional, $S_R + S_I$ of the bath oscillators subjected to the influence of the particle, can be analytically solved, since they are Gaussian integrals (1).

^{†††} Where $\zeta(t) = \sum_k C_k x_k(t)$ is the fluctuating force. Then,

$$\langle \zeta(t) \rangle \zeta(0)_\beta = \frac{\hbar}{\pi} \int_0^\infty J(\omega) \frac{\cosh[\omega(\hbar\beta/2 - it)]}{\sinh(\hbar\beta/2)} d\omega.$$

The initial condition describes the preparation of the spin and defines $\sigma(t) = \sigma_f$ and $\sigma'(t) = \sigma_i$.

Amplitude $A[\sigma]$ can be broken into small segments, each of length dt , towards its understanding. The probability of finding the system still in the initial state, either $+\frac{q_0}{2}$ (represented as $|L\rangle$) or $-\frac{q_0}{2}$ (represented as $|R\rangle$), corresponds to $e^{-i(\epsilon/2\hbar)dt}$ and $e^{i(\epsilon/2\hbar)dt}$, respectively. However, the amplitude for switching between the two states (in either direction) is $i(\Delta/2)dt$. Applying those instructions to the four-state path and neglecting terms of order $(dt)^2$, the amplitude of finding the system in the same state is represented by $\exp\{-i\epsilon\xi(t)dt\}$ (see Eq.(5.22)), whereas the probability of transitioning states is $i\lambda(\Delta/2)dt$, where

$$\lambda = \begin{cases} 0, & \text{for } A \longleftrightarrow D \text{ and } B \longleftrightarrow C, \\ -1, & \text{for } A \longleftrightarrow B \text{ and } D \longleftrightarrow C, \\ +1, & \text{for } A \longleftrightarrow C \text{ and } B \longleftrightarrow D. \end{cases}$$

Therefore, the probability of jumping from a diagonal state to a diagonal one or jumping from an off-diagonal state to an off-diagonal one is null. On the other hand, the probability of jumping from blip to sojourn in subsequent states is $+i\frac{\Delta}{2}dt$, and for the opposite, it is $+i\frac{\Delta}{2}dt$ (95).

η and ξ introduced as symmetric and antisymmetric coordinates, measure quasiclassical propagation and deviation from the diagonal, respectively. Not only can the influence functional be written as

$$\mathcal{F}[\xi(s), \eta(s')] = \exp\left\{-\frac{1}{\pi} \int_{t_0}^t ds \int_{t_0}^s ds' [-iL_1(s-s')\xi(s)\eta(s') + L_2(s-s')\xi(s)\xi(s')]\right\} \quad (5.48)$$

where $L_{1/2}$ is real and imaginary parts of the force autocorrelation function of the environment, denoted as $L_2(t) - iL_1(t)$,

$$L_1(t) = \int_0^\infty d\omega J(\omega) \sin(\omega t) \quad (5.49)$$

$$L_2(t) = \int_0^\infty d\omega J(\omega) \coth(\beta\hbar\omega/2) \cos(\omega t), \quad (5.50)$$

but also the reduced density matrix is given by

$$\langle \sigma_f | \rho_S(t) | \sigma_f' \rangle = \int \mathcal{D}\xi \mathcal{D}\eta \int \mathcal{D}\xi' \mathcal{D}\eta' A[\xi, \eta] A^*[\xi', \eta'] \mathcal{F}[\xi, \eta]. \quad (5.51)$$

Let us consider a two-state system initially in a diagonal state of the density matrix. It becomes evident that after an even number of transitions, it will revert to a diagonal state, while after an odd number of transitions, it will assume an off-diagonal state. Due to the sudden nature of the system's transitions, a path involving $2n$ flips at

times t_j ($j = 1, 2, \dots, 2n$) can be parameterized in a general manner by

$$\xi_n(t') = \sum_{j=1}^n \xi_j [\theta(t' - t_{2j-1}) - \theta(t' - t_{2j})] \quad (5.52)$$

$$\eta_n(t') = \sum_{j=0}^n \eta_j [\theta(t' - t_{2j}) - \theta(t' - t_{2j+1})] \quad (5.53)$$

with $t_0 \equiv 0, t_{2n+1} \equiv t$ and where $\theta(t)$ represents the unit step function. Labels $\xi_j = \pm 1$ and $\eta_j \pm 1$ distinguish the two off-diagonal and diagonal states of the density matrix, respectively. Intervals $t_{2j} < t' < t_{2j+1}$ are the sojourns and $t_{2j-1} < t' < t_{2j}$ are the blips (107). The sum over the system's path histories is represented by

- the sum over all numbers n of flip pairs,
- the time-ordered integrations over $2n$ flip times $\{t_j\}$ within the given interval, and
- the sum over all arrangements $\{\xi_j\}$ and $\{\eta_j\}$ of the possible values ± 1 of the individual ξ_j and η_j .

The time integrations can be performed in the influence functional (see Appendix F) leading to

$$\mathcal{F}_n[\xi_j, \eta_j, t_j] = \exp \left\{ \frac{i}{\pi} \sum_{j>k \geq 0}^{2n} \xi_j \eta_k Q_1(t_j - t_k) \right\} \exp \left\{ \frac{1}{\pi} \sum_{j>k \geq 1}^{2n} \xi_j \xi_k Q_2(t_j - t_k) \right\} \quad (5.54)$$

where $Q_{1/2}(t)$ are the second integrals of $L_{1/2}(t)$, which, for an Ohmic spectral density, are

$$Q_1(t) = 2\pi\alpha \tan^{-1}(\omega_c t) \quad (5.55)$$

$$Q_2(t) = \pi\alpha \ln(1 + \omega_c^2 t^2) + 2\pi\alpha \ln \left(\frac{\beta}{\pi t} \sinh \left(\frac{\pi t}{\beta} \right) \right) \quad (5.56)$$

Whereas Q_1 describes a coupling among the blip and all previous sojourn parts of the path, term Q_2 contains the interaction among all blips (including a self- interaction) (114). All such elements together lead to the expression for the diagonal elements of the reduced density matrix, which describe the probability of finding the system in state $|L\rangle$ at time t , in the form of a series in Δ^2

$$\langle L | \rho_S(t) | L \rangle = 1 + \sum_{n=1}^{\infty} \left(\frac{i\Delta}{2} \right)^{2n} \int_0^t \mathcal{D}_n \{t_j\} \sum_{\{\xi_j, \eta_j\}} \mathcal{F}_n e^{i \sum_{j=1}^{2n} \xi_j \epsilon(t_j - t_{j-1})}, \quad (5.57)$$

and, for the off-diagonal elements,

$$\langle L | \rho_S(t) | R \rangle = i\xi_{2n} \sum_{n=1}^{\infty} \left(\frac{i\Delta}{2} \right)^{2n-1} \int_0^t \mathcal{D}_n \{t_j\} \sum_{\{\xi_j, \eta_j\}} \mathcal{F}_n e^{i \sum_{j=1}^{2n} \xi_j \epsilon(t_j - t_{j-1})} \quad (5.58)$$

where the above abbreviated symbol was employed

$$\int_0^t \mathcal{D}_n\{t_j\} \cdots = \int_0^t dt_{2n} \int_0^{t_{2n}} dt_{2n-1} \cdots \int_0^{t_2} dt_1 \cdots \quad (5.59)$$

The establishment of the terminology for the upcoming chapter requires the bias considered be static, i.e., remain constant over time. Therefore, the symbol can be changed to ϵ_0 , which still represents the same bias and the phase factor can be combined in the representation of parameter $\phi_n^{(0)}$ as

$$\phi_n^{(0)} = \sum_{j=1}^{2n} \xi_j \epsilon_0 (t_j - t_{j-1}). \quad (5.60)$$

Obtaining an analytical expression for the path integral becomes challenging when dealing with specific potentials due to the influence functional introducing time nonlocal correlations. Consequently, some approximations must be made for proceeding.

5.1.4 Dynamics with NIBA

Approximations are used for the obtaining of a closed analytical form for the dynamics result for the spin-boson model. This subsection briefly explores the non-interacting blip approximation (NIBA), one of such approximations. In the case of an unbiased spin-boson system ($\epsilon = 0$), NIBA yields accurate dynamics. However, for biased spin-boson systems ($\epsilon > 0$) at low temperatures, NIBA is known to be inadequate. This failure occurs because interblip interactions contribute significantly to the dissipative effects in the coupling strength (47,112,115). Our objective is to demonstrate achieving the complete dynamics requires the use of approximations. Towards briefly illustrating this point, one of such approximations will be demonstrated.

For unbiased spin-boson dynamics, the simplest approximation neglects nonlocal correlations, particularly at high temperatures and/or strong coupling. This approximation, known as NIBA, is nonperturbative in the coupling, but perturbative in tunneling element Δ (28).

More specifically, NIBA relies on the premise the system's average time spent in a diagonal state of the reduced density matrix (a sojourn) is significantly longer than the average time spent in an off-diagonal state (a blip). The assumption enables the neglect of bath-induced correlations between different blip time intervals and specific blip-sojourn correlations in the exact series expression. Formally, this approximation is derived by neglecting the interblip correlations and all blip-sojourn correlations (1,28).

The approximation is valid for large enough friction and/or high temperatures. However, the specific form chosen for the spectral density of the environment influences the range of validity. NIBA can be justified for any spectral density provided the system shows overdamped exponential relaxation (116).

The influence functional reduces to a factorized form of intrablip bath correlations in which only the signs of the blip phase terms depend on the labels of the respective preceding sojourns,

$$\mathcal{F}_n^{NIBA} = 2^{n-1} [\cos(\pi\alpha)]^n \prod_{j=1}^n \exp\left\{-\frac{Q_2(t_{2j} - t_{2j-1})}{\pi}\right\} \quad (5.61)$$

For further details on the derivation, see Appendix of Ref. (114).

5.1.5 Parameter analysis

Since the expression for spin-boson dynamics has been introduced in the context of a time-independent Hamiltonian, where ϵ remains constant over time, its impact on occupation probabilities due to parameters such as temperature of the environment, form of the spectral density (subohmic, ohmic, or supraohmic), system's coupling strength, and tunneling rate Δ can be briefly examined. Different dynamical behaviors emerge for each parameter regime, as discussed in Sec. 5.1 (28).

The formalism of path integral enables the recovery of behaviors for the unbiased case (25). In the absence of external driving (the scenario addressed up to this point in the chapter), the analysis is conducted under the thermodynamic limit ($N \rightarrow \infty$), enabling the representation of spectral density function $J(\omega)$ as ω^s with a high-frequency cut-off. When $s = 1$, Ohmic dissipation is achieved and the quantum Langevin equation governing the particle's position operator dynamics features a memoryless damping kernel, corresponding to frequency-independent damping. Under such conditions, since $\hbar \rightarrow 0$ in the classical limit, the thermal bath transforms to a white noise source (117).

The way the expression for the transition probability depends on the different range of parameters can be evaluated. As an example, when a very small static bias $\epsilon \approx 0$ is set, the two wells have almost the same energy and the system can be considered symmetric (unbiased case). The behavior is expected to be a coherent transition between the two wells if the environment is not taken into consideration ($J(\omega) = 0$). Therefore, the path integral formulation is in accordance with perturbation theory,

$$P_{L \rightarrow R} = \langle R | \rho_S(t) | R \rangle = \sum_{n=1}^{\infty} (-1)^{n+1} (\Delta)^{2n} \int_0^t \mathcal{D}_n\{t_j\} \sum_{\{\xi_j\}} 1 \sum_{\{\eta_j\}} 1 \quad (5.62)$$

where $\sum_{\{\xi_j\}} 1 = 2^n$, and $\sum_{\{\eta_j\}} 1 = 2^{n-1}$. Moreover, $\int_0^t \mathcal{D}_n\{t_j\} = \frac{t^{2n}}{(2n)!}$ and $\rho(0) = |L\rangle \langle L|$. Combining all elements,

$$P_{L \rightarrow R} = \langle R | \rho_S(t) | R \rangle = \sum_{n=1}^{\infty} (-1)^{n+1} (\Delta t)^{2n} \frac{2^{2n-1}}{(2n)!} = \sin^2(\Delta t) \quad (5.63)$$

In the intermediate analysis, when the static bias is of the same order of tunneling parameter $\epsilon = \Delta$, the behavior is

$$P_{L \rightarrow R} = \langle R | \rho_S(t) | R \rangle = \sum_{n=1}^{\infty} (-1)^{n+1} (\Delta)^{2n} \int_0^t \mathcal{D}_n \{t_j\} \sum_{\{\xi_j\}} e^{i\Delta \sum_{j=1}^{2n} \xi_j (t_j - t_{j-1})} \sum_{\{\eta_j\}} 1 \quad (5.64)$$

$$= \sum_{n=1}^{\infty} (-1)^{n+1} (\Delta)^{2n} 2^{n-1} \int_0^t \mathcal{D}_n \{t_j\} \prod_{j=1}^n \cos(\Delta(t_{2j} - t_{2j-1})) \quad (5.65)$$

Approximation $\prod_{j=1}^n \cos(\Delta(t_{2j} - t_{2j-1})) \approx 1 - \frac{1}{2} \Delta^2 \sum_{j=1}^n (t_{2j} - t_{2j-1})^2 + O(t^4)$ can be assumed. If only terms up to second order in the perturbation (as in the time-dependent perturbation theory) should be retained, then

$$P_{L \rightarrow R} = \langle R | \rho_S(t) | R \rangle = \sin^2 \Delta t - \frac{1}{2} \sum_{n=1}^{\infty} (-1)^{n+1} (\Delta)^{2n} 2^{2n-1} \int_0^t \mathcal{D}_n \{t_j\} \sum_{j=1}^n \Delta^2 (t_j - t_{j-1})^2 \quad (5.66)$$

In the lowest order, $n = 1$, $P_{L \rightarrow R}(t)$ is reduced, rather than accelerated.

Nevertheless, in case of a very large static bias, i.e., the asymmetry of the system is immense, a transition occurs for the lowest energy level of the system, and the particle is localized on this side of the well.

Regarding the driving case $\epsilon(t)$, discussed in the next Chapter, the expressions for the transition probability become challenging. Analyzing the parameters is not as straightforward as it is for the unbiased case with NIBA approximation, as will be observed.

6 DRIVEN SPIN-BOSON MODEL AND DISSIPATIVE ADAPTATION HYPOTHESIS

As discussed in the previous chapter, the hypothesis of dissipative adaptation was studied in Λ atoms with a single photon pulse (21) in the quantum regime of the spin-boson model. This chapter addresses the use of a simple system - a dissipative TLS with a drive, i.e., a driven spin-boson system - for connecting the transition probability and absorption of work throughout this process. A valid treatment can be applied for different coupling regimes and temperatures for a TLS in a double well potential, following approximations from the literature. The path integral formalism is discussed for a derivation of the dynamics of such systems and the connection between the dissipative adaptation hypothesis and the driven spin-boson system is established through a formalism outlined in Ref.(118). Focusing on quantum regime and employing path integral formalism, this study offers a framework that illustrates the intricate association of transition probabilities in such driven systems with quantum work.

6.1 Perturbative driven Spin-boson model

Following Refs. (21,114), the quantum dynamics of systems under external driving forces are analyzed towards assessments of the thermodynamic properties of the self-organization process, as postulated by England's hypothesis (27). A driven spin-boson Hamiltonian, which describes a particle subjected to a double metastable potential whose symmetry can vary with time, encoded by bias parameter $\epsilon(t)$ was adopted for that purpose and is expressed as

$$H_{SR} = H_S + H_I + H_R \quad (6.1)$$

$$= \frac{\hbar\Delta}{2}\sigma_x + \frac{\hbar\epsilon(t)}{2}\sigma_z + \frac{q_0\sigma_z}{2}\sum_k C_k x_k + \sum_k \left(\frac{m_k\omega_k x_k^2}{2} + \frac{p_k^2}{2m_k} \right). \quad (6.2)$$

The same parameters employed in the previous chapter, namely, x_k , p_k , m_k , and ω_k , which denote coordinate, momentum, mass, and frequency of the k -th harmonic oscillator representing the environment, respectively, were used in the expression. Additionally, q_0 is the distance between the two potential minima and C_k is the strength of the coupling of the system to the k -th oscillator. The time-dependent bias parameter controls the symmetry of the double well system represented by that model.

The Hamiltonian represents a symmetry double well in equilibrium, i.e., when the system is undriven (unbiased case, i.e., $\epsilon(t) = 0$). Consequently, the population difference is zero ($P(t) = \langle\sigma_z\rangle = 0$), resulting in an equal concentration of population on both sides of the wells. On the other hand, our goal is to achieve accumulation of population on one side of the wells, explicitly violating the equilibrium tendency. If ϵ positive is found,

indicating the particle begins the dynamics on the unstable side of the well, the difference in population is expected to be positive, for the population on the right side is higher than that on the left side (see Fig.11). Conversely, a negative difference in population indicates a violation in the equilibrium tendency of the system. In such a scenario, more energy is concentrated in the left well than in the right one, contradicting the expectations from the equilibrium thermodynamics process. Our objective is to study some driving mechanisms in which that phenomenon can occur and their connection with quantum work quantity.

Such dynamics with a time-dependent Hamiltonian can be calculated by Schrödinger-like equation

$$-\frac{i}{\hbar}H(t)U(t, t') = \frac{d}{dt}U(t, t'), \quad (6.3)$$

where the initial condition is given by $U(t = t') = \mathbb{I}$, where evolution operator U associated with the Hamiltonian can be written as

$$U(t, t') = \mathbb{I} - \frac{i}{\hbar} \int_{t'}^t dt_1 H(t_1)U(t_1, t'). \quad (6.4)$$

Iterating the above expression for $U(t_1, t')$ results in

$$U(t, t') = \mathbb{I} - \frac{i}{\hbar} \int_{t'}^t dt_1 H(t_1) + \left(-\frac{i}{\hbar}\right)^2 \int_{t'}^t dt_1 \int_{t'}^{t_1} dt_2 H(t_1) H(t_2) U(t_2, t'). \quad (6.5)$$

After n repetitions, the evolution operator can be represented by Dyson series

$$U(t, t') = 1 + \sum_{n=1}^{\infty} \frac{(-i/\hbar)^n}{n!} \int_{t'}^t dt_1 \cdots \int_{t'}^{t_{n-1}} dt_n H(t_1) \cdots H(t_n). \quad (6.6)$$

In situations that require the chronological sequence of operators H , the introduction of \mathcal{T} , a time-ordering operator, becomes necessary to guarantee a proper arrangement of H 's. As an example, when $n = 2$, it functions as

$$\mathcal{T}[H(t_1)H(t_2)] = \begin{cases} H(t_1)H(t_2), & t_1 > t_2 \\ H(t_2)H(t_1), & t_1 < t_2, \end{cases} \quad (6.7)$$

where operators at earlier times are placed on the left side of those at later times.

Combining all the above elements, the expression for $U(t, t')$ results in

$$U(t, t') = 1 + \sum_{n=1}^{\infty} \frac{(-i/\hbar)^n}{n!} \int_{t'}^t dt_1 \cdots \int_{t'}^{t_{n-1}} dt_n \mathcal{T}[H(t_1) \cdots H(t_n)] \quad (6.8)$$

or, symbolically,

$$U(t, t') = \mathcal{T} \left\{ \sum_{n=0}^{\infty} \frac{(-i/\hbar)^n}{n!} \left(\int_{t'}^t dt_1 H(t_1) \right)^n \right\} \quad (6.9)$$

which can be clarified by expressing U as a time-ordering exponential

$$U(t, t') = \mathcal{T} \left[\exp \left\{ \frac{-i}{\hbar} \int_{t'}^t H(t_1) dt_1 \right\} \right]. \quad (6.10)$$

When the Hamiltonians for distinct times commute $[H(t), H(t')] = 0$, Dyson series simplifies to

$$U(t, t') = e^{\frac{-i}{\hbar} \int_{t'}^t H(t_1) dt_1}. \quad (6.11)$$

The analysis of the dynamics of the driven spin-boson model can now be addressed through the path integral formalism.

6.1.1 Path integral for the driven spin-boson model

The initial state was chosen to be in the left well, $\rho_S(t_0) = |0\rangle\langle 0|$ or, similarly, $\rho_S(t_0) = |L\rangle\langle L|$, and the bath was in Gibbs state $\rho_R(t_0) = e^{-H_R/T} / \text{Tr}(e^{-H_R/T})$. Then, the initial system-reservoir state is given by

$$\rho(t_0) = \rho_S(t_0)\rho_R(t_0). \quad (6.12)$$

As in many references from the literature, the system-reservoir is assumed to start the dynamics in equilibrium and evolves with the bias, i.e., its symmetry depends on time. Additionally, Ohmic spectral function is assumed,

$$J(\omega) = \pi \sum_k \lambda_k^2 \delta(\omega - \omega_k) = 2\pi\alpha\omega e^{-\omega/\omega_c}, \quad (6.13)$$

with $\alpha \geq 0$ being the dimensionless parameter that describes the dissipation strength, defined as

$$\alpha \equiv \eta q_0^2 / 2\pi\hbar. \quad (6.14)$$

The study of the system's dynamics requires the expression for the reduced density matrix, $\rho_S(t) = \text{Tr}_R \rho(t)$, be found by the formalism of path integrals proposed by Feymann-Vernon, addressed in the previous chapters. The components of the reduced density matrix, which was derived by the path integral formalism and was introduced in the proceedings chapters, are given by

$$\langle \sigma_f | \rho_S(t) | \sigma'_f \rangle = \int \mathcal{D}\sigma(\cdot) \int \mathcal{D}\sigma'(\cdot) A[\sigma] A^*[\sigma'] \mathcal{F}[\sigma, \sigma']. \quad (6.15)$$

When the time dependence becomes relevant, an important difference in amplitude $A[\sigma]$, which is an extra term, i.e., time-dependent bias $\epsilon(t)$, must be considered. The derivation addressed in chapter 5 remains the same; however, the amplitude term can now be split into two terms, of which one is the same was discussed in Section 5.1.3 and the other is time-dependent. All contributions of the bias can be separated in amplitude $B[\sigma]$ and the contribution solely due to only the tunneling rate can be replaced in amplitude $A[\sigma]$.

Therefore, $B[\sigma]$ can be written as

$$B[\sigma] = \exp \left\{ i \int_0^{t'} dt' (\epsilon_0 + \epsilon(t')) \sigma(t') \right\} \quad (6.16)$$

which considers the historical influence of systematic bias force. The phase in the exponential receives contributions from both static bias ϵ_0 and the time-dependent one. After all components are assembled in the expression for the reduced density matrix and summing n flips pairs, the phase can be written as

$$\phi_n = \sum_{j=1}^n \xi_j [\epsilon_0(t_{2j} - t_{2j-1}) + g(t_{2j}) - g(t_{2j-1})] = \phi_n^{(0)} + \phi_n^{(1)} \quad (6.17)$$

where the external driving is described by function $g(t) = \int_0^t dt' \epsilon(t')$ and the static part of the phase is equal to the one in Eq.(5.60)*. The influence functional retains its form, as depicted in Eq.(5.54), since no significant change occurs in the term. Once again, the sole alteration lies in the time-dependent additional term of the encountered bias, denoted as $\phi_n^{(1)}$.

By combining all factors and considering all possible arrangements of blips and sojourns, as in Chapter 5, the joint probability emerges as the series in Δ as

$$P(\sigma, t; \sigma', 0) = \delta_{\sigma, \sigma'} + \sigma \sigma' \sum_{n=1}^{\infty} \left(-\frac{\Delta}{2} \right)^{2n} \int_0^t \mathcal{D}_n \{t_j\} \sum_{\{\xi_j, \eta'_j\}} F_n e^{i\Phi_n}, \quad (6.18)$$

where the prime in $\{\eta_j\}'$ indicates the outer sojourns are chosen according to the boundary conditions, i.e., $\eta_0 = \sigma'$ and $\eta_n = \sigma$.

Eq. (6.18) represents an expansion in even numbers of transitions among the four states of the density matrix. Such transitions occur at times $\{t_j\}$ and the sum over $\{\xi_j\}$ and $\{\eta_j\}'$ takes into account all possible intermediate states for $2n$ transitions. As anticipated in Ref. (95), the expressions for the diagonal elements of $\rho_S(t)$, which describe the probability of finding the system in state $|0\rangle$ at time t , are

$$\langle 0 | \rho_S(t) | 0 \rangle = 1 + \sum_{n=1}^{\infty} \left(\frac{i\Delta}{2} \right)^{2n} \int_0^t \mathcal{D}_n \{t_j\} \sum_{\{\xi_j, \eta_j\}} F_n e^{i\phi_n} \quad (6.19)$$

and the off-diagonal elements of $\rho_S(t)$

$$\langle 0 | \rho_S(t) | 1 \rangle = i \xi_{2n} \sum_{n=1}^{\infty} \left(\frac{i\Delta}{2} \right)^{2n-1} \int_0^t \mathcal{D}_n \{t_j\} \sum_{\{\xi_j, \eta_j\}} F_n e^{i\phi_n}. \quad (6.20)$$

Our interest is in investigating the transition from the lowest energy side of the well to the highest energy side, which is not achievable in an equilibrium system, i.e., with

* $\phi_n^{(0)} = \sum_{j=1}^{2n} \xi_j \epsilon_0(t_j - t_{j-1})$.

no drive. Therefore, the final transition probability from a state starting on the left side can be written as

$$P_{L \rightarrow R}(t) = - \sum_{n=1}^{\infty} \left(-\frac{\Delta}{2} \right)^{2n} \int_0^t \mathcal{D}_n\{t_j\} \sum_{\{\xi_j, \eta'_j\}} F_n e^{i\phi_n}. \quad (6.21)$$

In the usual spin-boson model, the exponential depends only on the static bias, here defined as ϵ_0 (see Eq.(5.58)), which is not governed by time. Consequently, the relation between the asymmetries in that model was not taken into account, since the static bias sets the symmetry of the two wells. Here, the difference can be evaluated when such symmetry depends on time and varied for observations of the different behaviors of the particle's dynamics.

Although those expressions are exact, the analytical evaluation is specific to a particular set of dissipation parameters and can be numerically computed for various dissipation parameters and temperatures by a stochastic Schrödinger equation. Since our interest is in the connection with the work done in the environment by the external drive, that resolution will not be detailed.

The focus is in determining whether the drive can promote the population occupation, which is not achievable in an equilibrium system. Therefore, since the concept of dissipative adaptation in that specific model (driven spin-boson) will be explored, the transition probabilities in terms of thermodynamic quantities, such as work, must be considered. Before diving into the analysis, let us revisit the discussion on how work is defined in quantum thermodynamics and examine a path integral formalism for such a definition.

6.2 Thermodynamic quantities

As addressed in Sec. 4.4, the definition of thermodynamic quantities such as work and heat in equilibrium systems is relatively straightforward and even more complex in arbitrary non-equilibrium systems (7). The authors in Ref. (119) delved into the statistics of work using Feynman's path integral formalism and discussed the way usual thermodynamics has been extended in recent years to incorporating stochastic thermodynamics (56), wherein work and heat are characterized as trajectory functionals. However, since heat and work are not directly observable, the extension does not provide a clear advantage for the definition of those quantities in the quantum domain, where the concept of trajectories is not well-defined. Consequently, the definition of work in quantum systems typically involves averages and statistical moments and aligns with classical notions in classical limit ($\hbar \approx 0$).

The authors demonstrated the definition of quantum work via path integral formalism within the framework of quantum thermodynamics, drawing inspiration from

stochastic thermodynamics literature, but incorporating dissipative systems into their analysis.

Classical stochastic thermodynamics, which is a relatively recent framework, expands the principles of thermodynamics beyond the traditional ensemble level to focusing on individual trajectories. As an example, work can be formulated as a trajectory functional; therefore, the first law of thermodynamics is reformulated via trajectories and the second law is redefined as equalities, known as fluctuation theorems. The use of path integral formalism for formulating fluctuation theorems in classical stochastic thermodynamics resembles the path integral formalism in quantum mechanics. Therefore, during the transition of classical stochastic thermodynamics to the quantum regime, the adoption of path integral methods seems natural (118–120).

The quantum redefinition of work through path integral formalism aligns with our objectives particularly for deriving the transition probability from the ground state to an excited state associated with work absorption in the driven spin-boson system. It seems pertinent to investigate the role of path integral formalism in defining work within quantum thermodynamics.

Therefore, employing the work functional, the authors in Ref. (118) developed a path integral formulation for work statistics involving a Hamiltonian of the system with an arbitrary time-dependent potential denoted as $V(\lambda_t, x)$, which drives the system out of equilibrium and injects work into it,

$$H_S(t) = \frac{p^2}{2m} + V(\lambda_t, x), \quad (6.22)$$

where time-dependence is specified by λ_t .

The TPM scheme defines quantum fluctuating work as the difference in the energies measured at times $t = 0$ and $t = \tau$,

$$W_{m,n} = E_m(\lambda_\tau) - E_n(\lambda_0). \quad (6.23)$$

Therefore, the joint probability of observing such measured energies can be written as

$$\begin{aligned} p(n, m) &= \langle n(0) | \rho_S(0) | n(0) \rangle | \langle m(\tau) | U_S | n(0) \rangle |^2 \\ &= p_n | \langle m(\tau) | U_S | n(0) \rangle |^2, \end{aligned}$$

where $|n(t)\rangle$ represents the n -th instantaneous energy eigenstate of the system at time t , $\rho_S(0)$ is the initial canonical density matrix of the system, and $U_S = \mathcal{T}\{\exp\{(-i/\hbar) \int_0^\tau dt H_S(\lambda_t)\}\}$ is the unitary operator evolution of the system. The work probability distribution is then defined as

$$P(W) = \sum_{m,n} \delta(W - W_{m,n}) p(m, n). \quad (6.24)$$

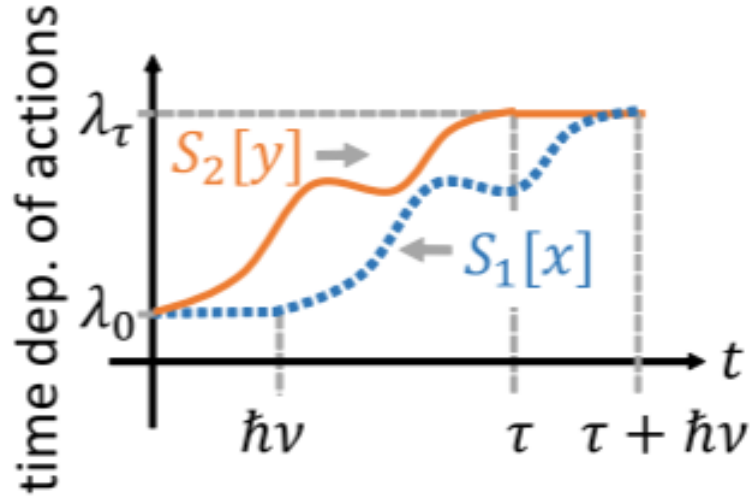


Figure 14 – Reproduction of a figure of Ref.(118) regarding contours of time-dependence actions S_1 and S_2 in path integral formalism.

Source: FUNO; QUAN. (118).

Performing a Fourier transform, the characteristic function of work is

$$\chi_W(\nu) = \int dW P(W) e^{i\nu W} = \text{Tr}[e^{i\nu H_S(\lambda_\tau)} U_S e^{-i\nu H_S(\lambda_0)} \rho_S(0) U_S^\dagger]. \quad (6.25)$$

Towards the path integral expression of the above equation, the following relations are recalled:

$$\langle x_f | U_S e^{-i\nu H_S(\lambda_0)} | x_i \rangle = \int \mathcal{D}x e^{(i/\hbar) S_1^\nu[x]}, \quad (6.26)$$

$$\langle y_i | U_S^\dagger e^{i\nu H_S(\lambda_\tau)} | y_f \rangle = \int \mathcal{D}y e^{(-i/\hbar) S_2^\nu[y]}, \quad (6.27)$$

where the contours employed in the path integral treatment of the time-dependence of actions are illustrated in Fig.14. Then,

$$\chi_W(\nu) = \int dx_i dy_i dx_f dy_f \delta(x_f - y_f) \int \mathcal{D}x \int \mathcal{D}y e^{(i/\hbar)(S_1^\nu[x] - S_2^\nu[y])} \langle x_i | \rho_S(0) | y_i \rangle. \quad (6.28)$$

Using identity $(i/\hbar)S_1^\nu[x] = (i/\hbar)S_2^\nu[x] + i\nu W_\nu[x]$ leads to

$$\chi_W(\nu) = \int dx_i dy_i dx_f dy_f \delta(x_f - y_f) \int \mathcal{D}x \int \mathcal{D}y e^{(i/\hbar)(S_2^\nu[x] - S_2^\nu[y])} \langle x_i | \rho_S(0) | y_i \rangle e^{i\nu W_\nu[x]}, \quad (6.29)$$

where the quantum work functional (see details of the derivation in Appendix I) is given by

$$W_\nu[x] = \int_0^\tau dt \frac{1}{\hbar\nu} \int_0^{\hbar\nu} ds \dot{\lambda}_t \frac{\partial V[\lambda_t, x(t+s)]}{\partial \lambda_t}, \quad (6.30)$$

Eqs.(6.29) and (6.30) are equivalent to those derived by the TPM scheme. However, some additional information on the intermediate quantum trajectories compared to TPM protocol can be found in such a formulation of the quantum work functional.

\hbar expansion can be performed in Eq.(6.30) and the quantum corrections to the classical expression of the work functional are derived,

$$W_\nu[x] = W_{cl}[x] + \frac{i\nu}{2}W_q^{(1)}[x] + \mathcal{O}(\hbar^2\nu^2), \quad (6.31)$$

where the classical work functional is written as

$$W_{cl}[x] = \int_0^\tau dt \dot{\lambda}_t \frac{\partial V[\lambda_t, x(t)]}{\partial \lambda_t}, \quad (6.32)$$

and the first-order quantum correction is

$$W_q^{(1)}[x] = -i\hbar \int_0^\tau dt \dot{x}(t) \dot{\lambda}_t \frac{\partial^2 V[\lambda_t, x(t)]}{\partial \lambda_t \partial x(t)} \quad (6.33)$$

In classical limit ($\hbar \rightarrow 0$), the quantum work functional reduces to the classical fluctuating work.

6.3 Relation between transition probability and work functional

This section investigates the feasibility of establishing a relationship between the transition probability of moving from one side of the well to another and the work extracted during this process. Similarly to other studies on both classical and quantum regime (21,27). Some simpler cases are analyzed and generalized for the entire dynamics.

The expression for the transition probabilities in the driven spin-boson model, derived in the first section of this chapter, specifically the transition from ground state to an excited one, was provided (Eq.(6.21)). Here, it is analyzed for the scenario when $n = 1$; therefore,

$$P_{L \rightarrow R}(t) = \frac{\Delta^2}{4} \int_0^t dt_2 \int_0^{t_2} dt_1 \sum_{\{\xi_1, \eta_1^{\xi_1}\}} F_1 e^{i\phi_1^{\xi_1}}, \quad (6.34)$$

where

$$\phi_1^{\xi_1} = \xi_1 [\epsilon_0(t_2 - t_1) + g(t_2) - g(t_1)] \quad (6.35)$$

$$= \xi_1 \left[\epsilon_0(t_2 - t_1) + \int_{t_1}^{t_2} dt \epsilon(t) \right]. \quad (6.36)$$

$\epsilon(t)$ represents the time-dependent drive of the system's Hamiltonian,

$$H_S(t) = H_0 - \hbar \epsilon(t) \sigma_z / 2. \quad (6.37)$$

Setting $\xi_1 \epsilon(t) \equiv -W(t)$ and differentiating both sides result in

$$- \xi_1 \dot{\epsilon}(t) = dW(t)/dt, \quad (6.38)$$

$$- \int_0^t \xi_1 \dot{\epsilon}(t') dt' = W(t). \quad (6.39)$$

The latter expression is the integration over time.

Then, the crucial concept is to recognize that

$$\phi_1^{\xi_1} = \xi_1 \epsilon_0 (t_2 - t_1) - \int_{t_1}^{t_2} W(t) dt \quad (6.40)$$

where work-like function

$$W(t) \equiv - \int_0^t \xi_1 \dot{\epsilon}(t') dt', \quad (6.41)$$

is defined, demonstrating the way work “ $W(t)$ ” selects transition $|L\rangle \rightarrow |R\rangle$, as implied by the dissipative adaptation hypothesis.

As reported in Refs. (118,120), the work functional has a semiclassical component given by

$$W_{cl} = \int_0^t \dot{f}(t) \partial_f H[f, x(t')] dt'. \quad (6.42)$$

In the driven TLS in a double well potential, where $f(t) = \epsilon(t)$ is the time-dependent component, for $\hbar = 1$,

$$W_{cl}^{TLS} = \int_0^t (-q_0/a) \dot{\epsilon} dt'. \quad (6.43)$$

Decomposing

$$q_0/a = \eta + \xi$$

leads to two contributions to the work performed in the system, namely,

$$W_{cl}^{TLS} = -\frac{1}{2} \int_0^t \eta \dot{\epsilon}(t) - \frac{1}{2} \int_0^t \xi \dot{\epsilon}(t) dt' = W_{qs}^{TLS} + W_{nonst}^{TLS} \quad (6.44)$$

where W_{qs}^{TLS} describes a “quasi-static” contribution for energy variations due to diagonal η states and W_{nonst}^{TLS} describes a “nonstationary” contribution due to coherences ξ .

Only the nonstationary contribution of the work drives transitions in the driven spin-boson model, since

$$W_{nonst}^{TLS} = - \int_0^t \xi(t') \dot{\epsilon}(t') dt' = W(t). \quad (6.45)$$

A similar notion of quantum dissipative adaptation can be better evidenced by recalling the sum over exponentials is a type of average over paths in Hilbert space

$$P_{L \rightarrow R}(t) = \sum_n (-1)^{n+1} \left(\frac{-\Delta}{2} \right)^2 \int_0^t \mathcal{D}_n \prod_{j=1}^n \left\langle e^{-i \int_{t_{2j-1}}^{t_{2j}} W_{nonst}^{(j)} dt'} \right\rangle_j, \quad (6.46)$$

where $W_{nonst}^{(j)} = -\xi_j \dot{\epsilon}(t)$, and

$$\langle \bullet \rangle_j \equiv \sum_{\xi_j = -1}^{+1} e^{i \xi_j \epsilon_0 (t_{2j} - t_{2j-1})} Q_j H_j \bullet. \quad (6.47)$$

Nevertheless, the relation between transition probability and average work is not sufficient to prove the driven spin-boson system exhibits dissipative adaptation, but suggests the existence of a phenomenon resembling it. Consequently, an expression that establishes a connection between the transition probability of moving from one side of the well to the other and the work performed by the external drive can be formulated. Our aim is to demonstrate the obtaining of that relation by the path integral formalism, which also enabled the definition of a work functional.

The next section extends the idea to the expression of the reduced density matrix, showing how to connect it with our definition of work function.

6.3.1 Density matrix in terms of work

Since the relation between transition probability and work functional was derived in the previous section, here, the matrix elements are reformulated according to the definition of work provided in the preceding section.

As demonstrated in Eq.(6.46), both exponential of the Hamiltonian and that of work are found within the framework of the path integral formalism. In contrast to Schrödinger equation formalism, which exclusively incorporates the exponential of the Hamiltonian, the establishment of a clear connection between work and path integral formalism becomes less straightforward. Schrödinger equation does not explicitly mention work within its exponential representation, focusing solely on the system's Hamiltonian. It encapsulates the dynamics of the entire system and by racing out the environment's degrees of freedom, the density matrix of the system of interest is derived. Nevertheless, the explicit manifestation of the expression for work remains absent, posing challenges for the understanding of its relationship with that formalism.

As discussed in previous sections, a more direct link between work and the density matrix arises when the path integral formalism is further employed, offering a clearer understanding of their relationship. This is primarily due to the fact the path integral is constructed using the exponential of the action, which encapsulates the trajectory integral. Consequently, both energy and coordinates explicitly appear in those equations.

First, let us recall the joint probability is (95, 107, 114)

$$P(\sigma, t; \sigma', 0) = \delta_{\sigma, \sigma'} + \sigma \sigma' \sum_{n=1}^{\infty} \left(-\frac{\Delta^2}{4} \right)^n \int_0^t \mathcal{D}_n \{t_j\} \sum_{\{\xi_j\}} Q_n e^{i\phi_n} \sum_{\{\eta_j\}'} H_n. \quad (6.48)$$

Using $F_n = Q_n H_n$, the expression of the influence functional is decomposed into two terms, each expressed in terms of diagonal η states and coherence ξ . Phase ϕ_n receives contributions from static $\phi_n^{(0)}$ and time-dependent strain field $\phi_n^{(1)}$. Then,

$$\phi_n = \phi_n^{(0)} + \phi_n^{(1)}, \quad (6.49)$$

$$\Phi_1^{(0)} = \epsilon_0 \sum_{j=1}^n \xi_j (t_{2j} - t_{2j-1}), \quad (6.50)$$

$$\Phi_1^{(1)} = \sum_{j=1}^n \xi_j [g(t_{2j}) - g(t_{2j-1})], \quad (6.51)$$

where

$$g(t_{2j}) - g(t_{2j-1}) = \int_0^{t_{2j}} dt' \epsilon(t') - \int_0^{t_{2j-1}} dt' \epsilon(t') \quad (6.52)$$

$$= \int_{t_{2j-1}}^{t_{2j}} dt' \epsilon(t'). \quad (6.53)$$

Therefore,

$$\Phi_n^{(1)} = \sum_{j=1}^n \xi_j \int_{t_{2j-1}}^{t_{2j}} dt' \epsilon(t'). \quad (6.54)$$

Writing $\phi_n^{(1)}$ in terms of work leads to

$$\Phi_n^{(1)} = - \int_{t_{2j-1}}^{t_{2j}} W_j(t) dt. \quad (6.55)$$

The matrix elements can be given as

$$P(\sigma, t; \sigma', 0) = \delta_{\sigma, \sigma'} + \sigma \sigma' \sum_{n=1}^{\infty} \left(-\frac{\Delta^2}{4} \right)^n \int_0^t \mathcal{D}_n \{t_j\} \sum_{\{\xi_j\}} Q_n e^{i\phi_n^{(0)}} e^{i\phi_n^{(1)}} \sum_{\{\eta_j\}'} H_n \quad (6.56)$$

$$= \delta_{\sigma, \sigma'} + \sigma \sigma' \sum_{n=1}^{\infty} \left(-\frac{\Delta^2}{4} \right)^n \int_0^t \mathcal{D}_n \{t_j\} \sum_{\{\xi_j\}} Q_n e^{i\phi_n^{(0)}} e^{-i \int_{t_{2j-1}}^{t_{2j}} W_j(t) dt} \sum_{\{\eta_j\}'} H_n. \quad (6.57)$$

Note the only contribution from work arises from the coherent elements. Furthermore, if the bias lacks time-dependence, work vanishes and the results for the elements of the reduced density matrix remain unchanged from the section solely featuring the static bias.

6.4 Relation of symmetric and asymmetric bias

Up to this point, the precise form of the time-dependent bias $\epsilon(t)$ has remained unspecified. Previous derivations linking the reduced density matrix to work have relied on a general bias of energy.

This section addresses a specific configuration of time dependence on the Hamiltonian and a comparative analysis between symmetric and asymmetric cases.

As discussed in chapter 4, in classical regime, the manifestation of dissipative adaptation requires an inherent asymmetry between the wells within the system, which underpins the system's capacity to adjust itself in response to varying conditions. The crucial question emerges: what distinguishes this asymmetry within the quantum domain?

Towards addressing the issues, let us delve into the scenario below for investigating the dynamic interaction between symmetric and asymmetric bias within a driven system.

The time-dependence of the bias parameter can be selected as an asymmetric perturbation

$$\epsilon(t) = \epsilon_0 + C \sin^2(\omega t), \quad (6.58)$$

where C is a constant. Setting $\epsilon_0 = 0$ (static case) yields a sinusoidal time-dependent bias and introduces a slight difference between the energy levels of the wells, ensuring the energy level of the excited state ($|R\rangle$) is always higher than or equal to that of the ground state ($|L\rangle$) in the absence of tunneling. Consequently, this perturbation consistently favors one side of the well, with lower energy, making it asymmetric.

On the other hand, a straightforward trigonometric relationship reveals such a bias can be expressed as a combination of a static bias and a symmetric one added together

$$\sin^2(\omega t) = \frac{1 - \cos(2\omega t)}{2}.$$

Therefore, if a dynamically asymmetrical drive is chosen with no static bias ($\epsilon_0 = 0$), i.e.

$$\epsilon(t) = C \sin^2(\omega t), \quad (6.59)$$

it is equivalent to a static bias alongside a drive with a frequency twice as high

$$\epsilon(t) = C \frac{(1 - \cos(2\omega t))}{2}. \quad (6.60)$$

Ultimately, the specific nature (symmetric or not) of the drive does not hold significant relevance in the context discussed here - what is important is the overall asymmetry, which can arise from a combination of a static bias and a drive. As a result, such a bias is expected to lead to non-equilibrium organization.

In fact, Ref.(121) indicates those outcomes have already been observed, although typically within a limited range of parameters. This aspect is investigated and discussed in the next section.

6.5 Non-equilibrium organization in the driven spin-boson model

In a TLS in a double well potential under usual circumstances, e.g., symmetric case, the population is equally distributed in the two spin states due to the degeneracy in their energy levels:

$$\langle \sigma_z(t \rightarrow \infty) \rangle = 0. \quad (6.61)$$

However, large quantum fluctuations of the bath induce a symmetry breaking at zero temperature, leading to more population being localized at the initial spin state, i.e.,

$$\langle \sigma_z(t \rightarrow \infty) \rangle \neq 0. \quad (6.62)$$

Such a delocalization-localization transition is a purely quantum phenomenon, since no thermal fluctuations exist at zero temperature, i.e., it can be ignored.

In the preceding chapters, the derivation of the expression for the transition probability associated with work during the process was accomplished through the path integral formalism. This section explores a similar behavior displayed when the population is concentrated on the unconventional side of the wells, i.e., on the side that is not the system's lower energy state, consequently suppressing the tunneling rate.

Ref.(121) shows a narrow range of parameters in which the population is negative in a stationary manner even with a positive ϵ . The authors experimentally implemented a driven spin-boson model. The central question revolves around the extension to which intense coherent driving influences a strongly dissipative system. They demonstrated the drive strengthens the suppression of quantum coherence by the environment and that adjusting the drive amplitude enables a transition from a coherent state to an incoherent one.

The model adopted for that purpose was a superconducting qubit, specifically a two-state system known as a flux qubit in a superconducting circuit consisting of a loop interrupted by four Josephson junctions. The qubit is coupled to an electromagnetic environment, which forms a bosonic one comprised of electromagnetic modes in the superconducting transmission line. It is subjected to a strong continuous-wave drive (coherent drive) applied through the transmission line. For further details on the experimental setup, refer to Fig.(1) of Ref.(121). The drive's frequency and amplitude can be adjusted over a broad range and a weak probe additionally introduced demonstrated an out-of-equilibrium detailed balance relation.

As in this doctoral thesis, spectral density corresponds to Ohmic damping. The bias between the potential wells is given by

$$\epsilon(t) = \epsilon_0 + \epsilon_p \cos \omega_p t + \epsilon_d \cos \omega_d t, \quad (6.63)$$

where ϵ_0 represents the static component related to externally applied flux ϕ_ϵ . Ref. (121) reported an extra term due to the contribution of the probe, with ϵ_p representing the amplitude and ω_p denoting frequency. The third term accounts for the contribution of the drive, with ϵ_d , ω_d representing amplitude and frequency, respectively. The authors aimed at the derivation of linear susceptibility ($\chi(\omega)$), which characterizes the qubit's response at the probe frequency.

Our aim is not to delve deeply into the technical details of that aspect, since our focus is on the transient dynamics of the population difference, denoted as $P(t)$, in presence of drive only ($\epsilon_p = 0$), which is pertinent to our objectives, i.e., connection between transition probability from a ground state to a non-equilibrium state with work.

The dynamics of the susceptibility parameter can be analyzed by a generalized

master equation that incorporates two non-equilibrium kernels, $K^{+/-}(t)$, which, in the absence of a probe field, exhibit symmetry/antisymmetry concerning static bias ϵ_0 . The Laplace space representation of kernel $K^+(\lambda)$ can be formulated as a $K^f(\lambda) + K^b(\lambda)$ combination of the non-equilibrium forward and backward kernels.

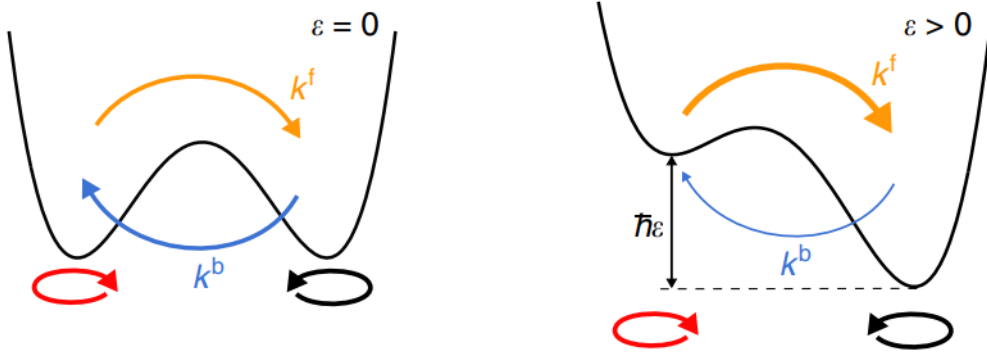


Figure 15 – Schematics of the double-well potential associated with the flux threading through the qubit. When no external sources are present, the potential exhibits symmetry, resulting in equal forward and backward tunneling rates $k^{f/b}$. Introducing a positive bias asymmetry ϵ accentuates forward tunneling, which dominates over backward tunneling. In the experiment involving the superconducting flux qubit, the coordinate associated with the double-well potential is magnetic flux ϕ within the loop. Eigenstates $|L/R\rangle$ of the flux operator correspond to currents circulating clockwise and anticlockwise in the superconducting loop, respectively.

Source: MAGAZZÙ *et al.* (121).

$$K^{f/b}(\lambda) = \frac{\Delta}{2} \int_0^\infty dt e^{-Q'(t-\lambda t)} J_0[d(t)] \cos [Q''(t) \mp \epsilon_0 t], \quad (6.64)$$

with $d(t) = 2\epsilon_d \omega_d^{-1} \sin(\omega_d t/2)$. Correlation function $Q(t) = Q'(t) + iQ''(t)$ describes the environmental influence and is related to the noise and dissipation kernels (see section 5.1.3), which, under appropriate regimes, are given by

$$Q'(t) = 2\alpha \ln \left[\sqrt{1 + \omega_c^2 t^2} \frac{\sinh(\pi t/\hbar\beta)}{\pi t/\hbar\beta} \right], \quad (6.65)$$

$$Q''(t) = 2\alpha \arctan(\omega_c t) \quad (6.66)$$

The influence of the drive is captured by the time-dependent argument of Bessel function of the first kind J_0 .

What particularly drew our focus in that article were the figures (3-c, d, g), which were replicated in Fig.16. The plots illustrate the difficulty in identifying the parameter region where population inversion occurs. Fig.16-c displays transient dynamics, where $P(t)$ shows a negative value when the static bias is zero and a small driven bias is applied.

Conversely, according to Fig.16-d, a population inversion between the double wells can occur with a specific drive and appropriate parameters. Here, the static bias is of the same order as the driven frequency. Additionally, Fig.16-g shows even with the drive, the population difference vanishes for a large α .

The steady state population reaches the value of $P_0 = (K^f - K^b)/(K^f + K^b)$, regardless of the initial preparation. Here, $K^{f/b} = K^{f/b}(\lambda = 0)$ represent nonequilibrium backward and forward rates. In the symmetric scenario illustrated in Fig. 16-c, where backward and forward rates are identical, $P_0 = 0$.

However, Fig. 16-d displays a distinct non-equilibrium phenomenon within the region bounded by the initial zeros of J_0 and J_1 , where steady-state qubit population P_0 assumes a negative value, implying a higher population in the left state despite $\epsilon_0 > 0$. The phenomenon is observable only within a narrow range of Fig.16-d for a positive and stationary static bias of the order of the driven frequency, i.e., $\epsilon_0 = \omega_d$. Such a narrow region was the target when the relation between transition probabilities and work was derived. Despite the existence of a form of dissipative adaptation phenomenon for the driven spin-boson model, addressing this specific portion of the possible spectrum proved exceptionally challenging and a numerical analysis alone was insufficient to link dissipative adaption phenomenon and driven spin-boson model. The origin of that behavior lies in the effective detailed balance relation, expressed as

$$K^f = K^b e^{\hbar\epsilon_{\text{eff}}/k_B T} \quad (6.67)$$

where ϵ_{eff} is the effective asymmetry which, in the absence of the drive, coincides with the static one.

The authors demonstrated the population's inversion is achievable for a very specific set of parameters and proposed the use of an external drive (coherent) for tuning the direction of long-range electron chemical reactions, employing a drive-induced effective bias originally proposed for Chemistry (122,123), as summarized in the next paragraphs.

Ref. (122) discussed the nonadiabatic regime of electron transfer reactions and how they can be influenced by the implementation of a strong static electric field. The authors derived a kinetic equation for a spin-boson model that relates the probability of finding the system in the initial states to the rate constants for forward and back reactions. In that mode, TLS is associated with electronic basis states corresponding to an electron localized on the donor or acceptor site of an electron transfer complex. Solvent effects are described as an ensemble of harmonic oscillators interacting with TLS.

A similar Hamiltonian adopted in this work was employed. In presence of a time-dependent electric field ($E(t) = E_0 \cos(\omega_0 t)$), perturbations appear in the asymptotic populations of the base states of the spin-boson model. Therefore, the dynamics of the spin-boson system depend intimately on both spectral density of the phonon bath and

intensity and frequency of the applied laser field. An analysis of the equations revealed forward and backward rate constants are strongly dependent on the applied field.

Ref. (123) studied the control of transfer rates through the implementation of a periodic external drive. Once again, a driven TLS described by the spin-boson model was adopted. The authors derived a master equation for expectation value σ_z using the path integral technique, with energy bias

$$\epsilon(t) = \epsilon_0 + \hbar A \cos(\Omega t). \quad (6.68)$$

As an example, they considered the long-range electron transfer in a donor-acceptor complex embedded in a condensed medium and subjected to the influence of a strong external field.

The results for the master equation can be interpreted as a superposition of the transfer rates known from the conventional theory of electron transfer. An intriguing behavior is exhibited regarding apparent energy bias ϵ_{eff} , which can become negative under specific choices of the external field's amplitude and frequency. Consequently, the final steady-state distribution of donor and acceptor levels may undergo inversion. Such a remarkable non-equilibrium phenomenon stems from the destruction of the detailed balance condition, a consequence of the presence of a strong periodic field. Ref. (122) partially corroborates the findings concerning the equation of the effective rate constant and the potential manipulation of the final level population by the external field, particularly in the case of polar media.

The authors of Ref.(121) combined a static bias with an external drive to introduce asymmetry for concentrating the populations on one of the sides of the wells. As discussed in Section 6.4, such asymmetry plays a crucial role in observations of dissipative adaptation phenomenon. However, the non-equilibrium population's inversion alone does not prove dissipative adaptations observed in the driven spin-boson model, since the relationship between absorbed work from the external drive and asymmetry of the system has not been established yet. Still regarding Ref. (121), the interpretation of asymmetry remained focused on the effective energy, which depends solely on the system configurations.

Despite the possible occurrence of population's inversion, a non-equilibrium organization exists, since a purely kinetic or thermodynamic effect is still an open question. Although Grifoni and collaborators provided indications of the organization being due to the kinetic effect, our results in Eq.(6.46) suggest the opposite, indicating a thermodynamic effect. Our aim is to examine whether this stationary regime is indeed associated with positive work and if the supply of energy to the system (positive work rate) is truly necessary for the phenomenon of dissipative adaptation to manifest. Regardless of the dynamical results achieved, the question on the thermodynamic aspect remains unanswered.

The literature reports debates on the organization phenomena. On the one hand

is the concept of kinetic asymmetry, as discussed in Ref. (124) and, on the other hand is dissipative adaptation hypothesis put forward by England (Ref. (27)). According to Ref. (124), the importance for cellular organization in biological systems, from the perspective of thermodynamic biochemistry, lies in the asymmetry of transition rates among various configurations of a molecule rather than the work absorbed due to external driving forces, which does not necessarily indicate work being done.

Regarding England's hypothesis (Ref. (27), Sec.4.3), the consideration of the kinetic aspect is crucial. The second term of Eq.(4.5) explicitly depends on that asymmetry and can dominate when a system is kinetically trapped in a high energy arrangement. The relevance of England's equation lies in the asymmetry dynamics and, specifically its relation to trajectories.

An open question that extends beyond the scope of our specific research area still remains and holds significance within the broader domain of biochemistry. It becomes particularly relevant in light of studies such as Ref. (124), which demonstrated competing effects (e.g., kinetic asymmetry versus thermodynamic effect of work absorption and heat dissipation) can play equally important or even more significant roles. Understanding the factors controlling enzyme chemotaxis, analogously to the mechanism by which bacteria move in response to gradients of nutrient molecules, holds substantial utility in elucidating the evolution of complex systems and determining system stability.

The authors explored the complexities of single enzyme chemotaxis, which involves the establishment and sustenance of a non-equilibrium spatial distribution of an enzyme driven by concentration gradients of the substrate and product of the catalyzed reaction. Reaction-diffusion equations revealed the influence of kinetic asymmetry (difference in transition state energies for dissociation/association of substrate and product) and diffusion asymmetry on the determination of the direction of chemotaxis, either positive, or negative. Interestingly, whereas dissipation remains a crucial element of nonequilibrium phenomena, including chemotaxis, those systems do not evolve to extremizing dissipation; rather, they tend to attain greater kinetic stability and accumulate in regions where their effective diffusion coefficient is minimized.

Regarding thermodynamic or kinetic effects on the adaption of systems, the central question revolves around whether the effective energy in driven spin-boson systems is associated with positive work, as proposed by the dissipative adaptation theorem, or whether it is the Kinetic effect that holds greater significance. Although the topic was briefly addressed within the existing literature, ongoing research continues to more deeply delve into the issue. The question remains unanswered within the confines of this thesis; however, we are actively engaged in addressing this and other unresolved inquiries.

This thesis has not addressed the effects of the system's adjustments to the configuration where population inversion occurs affect average work, variance of work, or

average exponential of work. The focus was on the existence of the dissipative adaptation relationship for the driven spin-boson and the way it possibly relates to work and its relevant parameters. The question on which relationship of the work parameter is accurate, especially in scenarios involving quantum aspects, but also incorporates temperature, remains unresolved. The dissipative fluctuation theorem suggests the exponential of work is relevant, whereas the quantum dissipative adaptation theorem (21) proposes the average of W when the temperature is low enough. The answer to this question still requires further investigations.

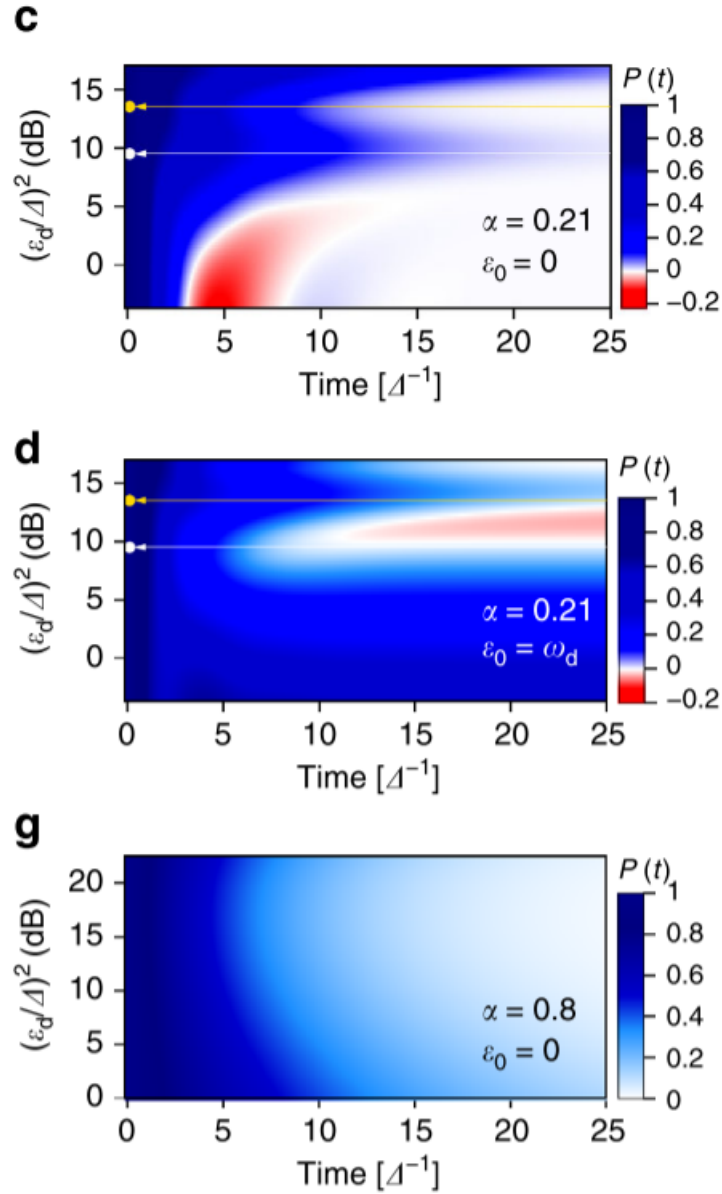


Figure 16 – Reproduction of the colorplot in Fig.3(c, d, g) of Ref. (121). **c, d** Predicted dynamics of $P(t)$ with $P(0) = 1$. For Fig.**c**, $(\epsilon_d/\Delta)^2 \approx 12$, and $\epsilon_0 = 0$, whereas for Fig.**d**, $\epsilon_0 = \omega_d$. The values of the other parameters used in the simulations are: $\Delta/2\pi = 7.23$ GHz, $\alpha = 0.21$, $\omega_p/2\pi = 5.2$ GHz, $\omega_d/2\pi = 9$ GHz, and $T = 175$ mK. The probe is on-resonance with the undriven qubit at the symmetry point. Fig.**g** Time evolution of $P(t)$ calculated at the symmetry point, $\epsilon_0 = 0$. The parameters are: $\Delta/2\pi = 8$ GHz, $\alpha = 0.8$, $\omega_p/2\pi = 4$ GHz, $\omega_d/2\pi = 3$ GHz, and $T = 90$ mK. The selection of ω_p and ω_d exerts a minimal impact on the qualitative characteristics of the driven spectra. $\omega_c/2\pi = 65$ GHz for the three plots.

Source: MAGAZZÙ *et al.* (121).

7 CONCLUSIONS

This doctoral thesis explored classical and quantum dissipative models initially revisiting bilinear and nonlinear models, which involve the behavior of two Brownian particles in a same environment. The discrepancy between those approaches was highlighted. On the one hand, nonlinear system-reservoir couplings predict nonlinear dissipation and an effective interaction potential between a pair of Brownian particles. On the other hand, the standard bilinear model yields free-particle motion for the relative coordinate and lacks mutual interactions between proximal particles.

Our research on the classical dynamics led to a significant finding, i.e., nonlinear dissipation forces were derived from the bilinear model. Towards addressing such reconciliation, a method that introduced a distance-dependent spectral function, establishing a length scale for the Brownian particle dynamics, was developed - this approach served as the foundation for its design. The standard bilinear model revealed incompatible with the method and the nonlinear effective potential did not align with the bilinear model. However, the nonlinear model successfully recovered dissipation rates, which was the goal of this research.

The derived spectral function was modified for describing different scenarios based on diffusion coefficients. As an example, the trigonometric function was transitioned to the Gaussian one for avoiding anomalous diffusion and a phenomenological modified spectral function was adopted to illustrate hydrodynamic correlations between two Brownian particles. Our results help express nonlinear dissipative forces in the dynamics of Brownian particle pairs.

Such a distance-dependent spectral function can be further implemented for more than two particles, which will involve considering the system of interest a bath of harmonic oscillators and deriving the imaginary part of the susceptibility by nonlinear response theory for each pair of particles. Another complementary avenue of research would be to derive three-dimensional equations of motion for two Brownian particles and investigate the correlation forces for determining whether the hydrodynamics extends even further in such systems.

The second part of the thesis focused on the study of TLS in a double well potential, with particular attention to the spin-boson model. The primary objective was to establish a relationship between the transition probability and the work performed by an external drive applied to the system. The study was inspired in the concept of dissipative adaptation proposed by England, who aimed to gain insights into how living organisms evolve in specific environments.

The literature on the spin-boson model within the path integral formalism was summarized and the adoption of such an approach was justified. Moreover, the driven case of the model was investigated. England's hypothesis was introduced in the classical regime and a quantum derivation of a similar relationship was explored. The work functional derivation proposed by Quan (118) derived the results, facilitating the expression linking transition probability and work. However, the fact the driven spin-boson model exhibits characteristics of dissipative adaptation cannot be stated. On the other hand, the organization of the system, particularly the nonequilibrium localization of particles within one side of the well, may occur only with the application of an external driving force, and not necessary may represent the higher energy consumption in that quantum system. Future studies aim to identify whether the driven spin-boson system exhibits dissipative adaptation.

Although the thesis explored dissipative systems in both classical and quantum regimes, specific questions still remain unanswered in both contexts. One of them regards the experimental implementation of the proposed distance-dependent spectral function, which was not discussed, but can be further and potentially explored. Linking techniques such as optical tweezers might extend the approach to experimental settings (125–127).

Optical tweezers pioneered over two decades ago, using focused laser beams to trap and manipulate microscopically small objects. The traps, formed when a laser beam is tightly focused by a microscope objective, can hold small objects in three-dimensional space (51, 52, 128, 129). An analogous experimental setup might involve the study of two colloidal particles suspended in a fluid with a given potential. Colloidal particles, i.e., microscopic solid particles that equilibrate with the suspending fluid due to thermal energy, offer a platform where their positions and motion can be precisely measured by optical methods (130). Such an experimental setup provides a promising avenue for investigations on the dynamics of dissipative systems in a controlled laboratory environment.

In function of the pairwise nature that frequently dictates effective interactions among Brownian particles, our distance-dependent spectral function may find applicability in scenarios involving a more significant number of Brownian particles sharing a same environment, thus enabling characterizing entropy production in nonequilibrium dissipative many-body systems and extending previous investigations conducted with single-quantum Brownian particles (19).

In the context of quantum dissipative adaptation and the driven spin-boson model, an ongoing debate persists within the literature concerning the relative significance of thermodynamics compared to kinetic asymmetry in the evolutionary trajectories of living organisms. The debate remains unresolved, with new elements being continually introduced in studies exploring driven systems.

This doctoral thesis has opened up several avenues for further investigations, since

the connection between dissipative adaptation and quantum correlations poses intriguing questions. Entanglement suppression also questions the relationship between nonequilibrium states and fundamental quantum phenomena. Exploring dissipative self-assembly and adaptation can enhance our comprehension of complex systems (131) and delving into those research domains can unearth fresh perspectives on the dynamics of dissipative systems, potentially paving the path for future breakthroughs and applications across diverse scientific fields.

REFERENCES

- 1 WEISS, U. **Quantum dissipative systems**. Singapore: World Scientific, 2012.
- 2 SCHLOSSHAUER, M. Quantum decoherence. **Physics Reports**, v. 831, p. 1–57, 2019. DOI: 10.1016/j.physrep.2019.10.001.
- 3 UHLENBECK, G. E.; ORNSTEIN, L. S. On the theory of the Brownian motion. **Physical Review**, v. 36, n. 5, p. 823, 1930.
- 4 MORI, H. Transport, collective motion, and Brownian motion. **Progress of Theoretical Physics**, v. 33, n. 3, p. 423–455, 1965.
- 5 GRABERT, H.; TALKNER, P. Quantum Brownian motion. **Physical Review Letters**, v. 50, n. 18, p. 1335, 1983.
- 6 GRABERT, H.; SCHRAMM, P.; INGOLD, G.-L. Quantum Brownian motion: The functional integral approach. **Physics Reports**, v. 168, n. 3, p. 115–207, 1988.
- 7 ZWANZIG, R. **Nonequilibrium statistical mechanics**. Oxford: Oxford University Press, 2001.
- 8 DUARTE, O.; CALDEIRA, A. Effective coupling between two Brownian particles. **Physical Review Letters**, v. 97, n. 25, p. 250601, 2006.
- 9 GELIN, M. F.; EGOROVA, D.; DOMCKE, W. Exact quantum master equation for a molecular aggregate coupled to a harmonic bath. **Physics Review E**, v. 84, p. 041139–1–041139–6, 2011.
- 10 VALENTE, D. Self-replication of a quantum artificial organism driven by single-photon pulses. **Scientific Reports**, v. 11, p. 16433, 2021. DOI: 10.1038/s41598-021-96048-6.
- 11 BRITO, F.; WERLANG, T. A knob for Markovianity. **New Journal of Physics**, v. 17, p. 072001, 2015.
- 12 HENRIET, L. Environment-induced synchronization of two quantum oscillators. **Physics Review A**, v. 100, p. 022119, 2019.
- 13 DUARTE, O.; CALDEIRA, A. Effective quantum dynamics of two Brownian particles. **Physical Review A**, v. 80, n. 3, p. 032110, 2009.
- 14 PAZ, J. P.; RONCAGLIA, A. J. Dynamics of the entanglement between two oscillators in the same environment. **Physical Review Letters**, v. 100, n. 22, p. 220401, 2008.
- 15 ZELL, T.; QUEISSER, F.; KLESSE, R. Distance dependence of entanglement generation via a bosonic heat bath. **Physics Review Letters**, v. 102, p. 160501, 2009.
- 16 VALENTE, D. M.; CALDEIRA, A. O. Thermal equilibrium of two quantum Brownian particles. **Physics Review A**, v. 81, p. 012117, 2010.

- 17 ERMAK, D. L.; MCCAMMON, J. A. Brownian dynamics with hydrodynamic interactions. **The Journal of Chemical Physics**, v. 69, n. 4, p. 1352, 1978.
- 18 PASSOS, M. H. M. *et al.* Experimental investigation of environment-induced entanglement using an all-optical setup. **Physical Review A**, v. 97, p. 022321–1–022321–8, 2018. DOI: 10.1103/PhysRevA.97.022321.
- 19 WEIDERPASS, G.; CALDEIRA, A. von Neumann entropy and entropy production of a damped harmonic oscillator. **Physical Review E**, v. 102, n. 3, p. 032102, 2020.
- 20 LANDI, G. T.; PATERNOSTRO, M. Irreversible entropy production: From classical to quantum. **Reviews of Modern Physics**, APS, v. 93, n. 3, p. 035008, 2021.
- 21 VALENTE, D.; BRITO, F.; WERLANG, T. Quantum dissipative adaptation. **Communications Physics**, v. 4, n. 1, p. 1–8, 2021.
- 22 GOETTEMS, E. I. *et al.* Reconciling nonlinear dissipation with the bilinear model of two Brownian particles. **Physical Review E**, v. 107, n. 1, p. 014107, 2023.
- 23 CALDEIRA, A. O.; LEGGETT, A. J. Quantum tunnelling in a dissipative system. **Annals of Physics**, v. 149, n. 2, p. 374–456, 1983.
- 24 FAGALY, R. Superconducting quantum interference device instruments and applications. **Review of Scientific Instruments**, v. 77, n. 10, p. 101101–1–101101–45, 2006.
- 25 CALDEIRA, A. O. **An introduction to macroscopic quantum phenomena and quantum dissipation**. Cambridge: Cambridge University Press, 2014.
- 26 VERNON, F. L. **The theory of a general quantum system interacting with a linear dissipative system**. 166 p. Thesis (Doctor in Science) — California Institute of Technology, California, 1959. DOI: 10.1016/0003-4916(63)90069-X.
- 27 ENGLAND, J. L. Dissipative adaptation in driven self-assembly. **Nature Nanotechnology**, v. 10, n. 11, p. 919–923, 2015.
- 28 LEGGETT, A. J. *et al.* Dynamics of the dissipative two-state system. **Reviews of Modern Physics**, v. 59, n. 1, p. 1, 1987.
- 29 CUKIER, R.; MORILLO, M. Solvent effects on proton-transfer reactions. **The Journal of Chemical Physics**, v. 91, n. 2, p. 857–863, 1989.
- 30 STOCKBURGER, J. T.; MAK, C. A dynamical theory of electron transfer: Crossover from weak to strong electronic coupling. **The Journal of Chemical Physics**, v. 105, n. 18, p. 8126–8135, 1996.
- 31 THORWART, M. *et al.* Enhanced quantum entanglement in the non-Markovian dynamics of biomolecular excitons. **Chemical Physics Letters**, v. 478, n. 4–6, p. 234–237, 2009.
- 32 HUELGA, S. F.; PLENIO, M. B. Vibrations, quanta and biology. **Contemporary Physics**, v. 54, n. 4, p. 181–207, 2013.

-
- 33 HAN, S.; LAPOINTE, J.; LUKENS, J. Observation of incoherent relaxation by tunneling in a macroscopic two-state system. **Physical Review Letters**, v. 66, n. 6, p. 810, 1991.
- 34 LEPPÄKANGAS, J. *et al.* Quantum simulation of the spin-boson model with a microwave circuit. **Physical Review A**, v. 97, n. 5, p. 052321, 2018.
- 35 CALDEIRA, A. O.; LEGGETT, A. J. Path integral approach to quantum Brownian motion. **Physica A: statistical mechanics and its applications**, v. 121, n. 3, p. 587–616, 1983.
- 36 RAMAZANOGLU, F. M. The approach to thermal equilibrium in the Caldeira-Leggett model. **Journal of Physics A: mathematical and theoretical**, v. 42, n. 26, p. 265303, 2009.
- 37 FERIALDI, L. Dissipation in the Caldeira-Leggett model. **Physical Review A**, v. 95, n. 5, p. 052109, 2017.
- 38 KATO, T.; TANIMURA, Y. Vibrational spectroscopy of a harmonic oscillator system nonlinearly coupled to a heat bath. **The Journal of Chemical Physics**, American Institute of Physics, v. 117, n. 13, p. 6221–6234, 2002.
- 39 KATO, T.; TANIMURA, Y. Two-dimensional raman and infrared vibrational spectroscopy for a harmonic oscillator system nonlinearly coupled with a colored noise bath. **The Journal of Chemical Physics**, American Institute of Physics, v. 120, n. 1, p. 260–271, 2004.
- 40 MENDES, C. F. O. **Dissipação quântica em sistemas abertos finitos**. 2014. 63 p. Dissertação (Mestrado em Física) — Instituto de Física, Universidade Federal do Amazonas, Manaus, 2014.
- 41 GARDINER, C.; ZOLLER, P. **Quantum noise: a handbook of Markovian and non-Markovian quantum stochastic methods with applications to quantum optics**. Springer Science & Business Media, 2004.
- 42 LEMOS, N. A. **Mecânica analítica**. São Paulo: Editora Livraria da Física, 2007.
- 43 ZILL, D. G.; CULLEN, M. R. **Equações diferenciais**. 3.ed. São Paulo: Pearson Education, 2001.
- 44 MUÑOZ, D.; SALOMON, O. **Estudo do acoplamento efetivo entre duas partículas Brownianas quânticas**. 2006. 57 p. Dissertação (Mestrado) — Instituto de Física, Universidade de Campinas, Campinas, 2006. DOI: 10.47749/T/UNICAMP.2006.373577.
- 45 GUINEA, F. Friction and particle-hole pairs. **Physical Review Letters**, v. 53, n. 13, p. 1268, 1984.
- 46 HEDEGÅRD, P.; CALDEIRA, A. Quantum dynamics of a particle in a fermionic environment. **Physica Scripta**, v. 35, n. 5, p. 609, 1987.
- 47 MAGAZZU, L. *et al.* Dissipative dynamics in a quantum bistable system: Crossover from weak to strong damping. **Physical Review E**, v. 92, n. 3, p. 032123, 2015.

- 48 LEGGETT, A. Quantum tunneling in the presence of an arbitrary linear dissipation mechanism. **Physical Review B**, v. 30, n. 3, p. 1208, 1984.
- 49 SCHULZ, M.; STEPANOW, S.; TRIMPER, S. Two harmonically coupled Brownian particles in random media. **Europhysics Letters (EPL)**, v. 54, n. 4, p. 424, 2001.
- 50 MUÑOZ, D.; SALOMON, O. *et al.* **Estudo da dinâmica de partículas Brownianas quânticas**. 2011. 72 p. Tese (Doutorado em Física) — Instituto de Física Gleb Wataghin, Universidade Estadual de Campinas, Campinas, 2011.
- 51 ULANOWSKI, Z. Optical tweezers—principles and applications. **Proceedings of the Royal Microscopical Society**, v. 36, n. 11, p. 6–13, 2001.
- 52 POLIMENO, P. *et al.* Optical tweezers and their applications. **Journal of Quantitative Spectroscopy and Radiative Transfer**, v. 218, p. 131–150, 2018.
- 53 MÜLLER, B. *et al.* Properties of a nonlinear bath: Experiments, theory, and a stochastic prandtl–tomlinson model. **New Journal of Physics**, v. 22, n. 2, p. 023014, 2020.
- 54 HU, B.; PAZ, J. P.; ZHANG, Y. Quantum brownian motion in a general environment. ii. nonlinear coupling and perturbative approach. **Physical Review D**, APS, v. 47, n. 4, p. 1576, 1993.
- 55 CROOKS, G. E. Entropy production fluctuation theorem and the nonequilibrium work relation for free energy differences. **Physical Review E**, v. 60, n. 3, p. 2721, 1999.
- 56 SEIFERT, U. Stochastic thermodynamics, fluctuation theorems and molecular machines. **Reports on Progress in Physics**, v. 75, n. 12, p. 126001, 2012.
- 57 VIALLA, F. *et al.* Unifying the low-temperature photoluminescence spectra of carbon nanotubes: the role of acoustic phonon confinement. **Physical Review Letters**, v. 113, p. 057402, 2014.
- 58 KRUMMHEUER, B.; AXT, V. M.; KUHN, T. Theory of pure dephasing and the resulting absorption line shape in semiconductor quantum dots. **Physical Review B**, v. 65, n. 19, p. 195313, 2002.
- 59 BIAN, X.; KIM, C.; KARNIADAKIS, G. E. 111 years of brownian motion. **Soft Matter**, v. 12, n. 30, p. 6331–6346, 2016.
- 60 DURÃO, L. M.; CALDEIRA, A. O. Statistical entropy of open quantum systems. **Physical Review E**, v. 94, n. 6, p. 062147, 2016.
- 61 DEKKER, H. On the quantization of dissipative systems in the Lagrange-Hamilton formalism. **Zeitschrift für Physik B: condensed matter**, v. 21, n. 3, p. 295–300, 1975.
- 62 INGOLD, G.-L. Path integrals and their application to dissipative quantum systems. *In*: BUCHLEITNER, A.; HORNBERGER, K. (ed.) **Coherent evolution in noisy environments**. Berlin: Springer, 2002. p. 1–53. (Lectures notes in Physics, v. 611).
- 63 FEYNMAN, R. P. Space-time approach to non-relativistic quantum mechanics. **Reviews of Modern Physics**, v. 20, n. 2, p. 367, 1948.

- 64 FEYNMAN, R. P. Mathematical formulation of the quantum theory of electromagnetic interaction. **Physical Review**, v. 80, n. 3, p. 440, 1950.
- 65 FEYNMAN, R. P.; JR, F. V. The theory of a general quantum system interacting with a linear dissipative system. **Annals of Physics**, v. 281, n. 1-2, p. 547–607, 2000.
- 66 SMITH, C. M.; CALDEIRA, A. Generalized Feynman-Vernon approach to dissipative quantum systems. **Physical Review A**, v. 36, n. 7, p. 3509, 1987.
- 67 FEYNMAN, R. P.; HIBBS, A. R.; STYER, D. F. **Quantum mechanics and path integrals**. N. Chelmsford: Courier Corporation, 2010.
- 68 OLIVEIRA, L. **Integral de caminho para transformações canônicas arbitrárias**. 1980. 139 p. Dissertação (Mestrado em Física) — Centro Brasileiro de Pesquisas Físicas, Rio de Janeiro, 1980.
- 69 HÄNGGI, P.; INGOLD, G.-L. Fundamental aspects of quantum brownian motion. **Chaos: an interdisciplinary journal of nonlinear science**, v. 15, n. 2, 2005.
- 70 WEIDERPASS, G. A. **Produção de entropia e fluxo de calor em sistemas quânticos abertos**. 2018. 93 p. Dissertação (Mestrado) — Instituto de Física Gleb Wataghin, Universidade Estadual de Campinas, Campinas, 2018.
- 71 PERUNOV, N.; MARSLAND, R. A.; ENGLAND, J. L. Statistical physics of adaptation. **Physical Review X**, v. 6, n. 2, p. 021036, 2016.
- 72 FEYNMAN, R. P. **Statistical mechanics: a set of lectures**. Boca Raton: CRC Press, 2018.
- 73 GOOLD, J. *et al.* The role of quantum information in thermodynamics—a topical review. **Journal of Physics A: mathematical and theoretical**, v. 49, n. 14, p. 143001, 2016.
- 74 ENGLAND, J. L. Statistical physics of self-replication. **The Journal of Chemical Physics**, v. 139, n. 12, p. 09B623–1, 2013.
- 75 MENENDEZ, S. **The extended second law of thermodynamics suggests a thermodynamic imperative driving the evolution of life systems towards increased complexity**. 2021. Available at: <https://www.biorxiv.org/content/10.1101/2021.09.13.459895v4.full.pdf>. Accessible at: 23 Jan. 2023.
- 76 JANNA, F. C.; MOUKALLED, F.; GÓMEZ, C. A simple derivation of crooks relation. **International Journal of Thermodynamics**, v. 16, n. 3, p. 97–101, 2013.
- 77 BELLAC, M. L.; MORTESSAGNE, F.; BATROUNI, G. G. **Equilibrium and non-equilibrium statistical thermodynamics**. Cambridge: Cambridge University Press, 2004.
- 78 LEBON, G.; JOU, D.; CASAS-VÁZQUEZ, J. **Understanding non-equilibrium thermodynamics**. New York: Springer, 2008.
- 79 GROOT, S. R. D.; MAZUR, P. **Non-equilibrium thermodynamics**. New York: Courier Corporation, 2013.

- 80 MAYR, E. Cause and effect in biology: Kinds of causes, predictability, and teleology are viewed by a practicing biologist. **Science**, v. 134, n. 3489, p. 1501–1506, 1961.
- 81 DARWIN, C. **On the origin of species: or; the preservation of the favoured races in the struggle for life**. New York: Read Books Ltd, 2018.
- 82 KEDIA, H. *et al.* Drive-specific adaptation in disordered mechanical networks of bistable springs. Available at: [http:// arXiv.org](http://arXiv.org). preprint **arXiv:1908.09332**, 2019. Accessible at: 12 Dec.2023.
- 83 KEDIA, H. *et al.* Drive-specific selection in multistable mechanical networks. **The Journal of Chemical Physics**, v. 159, n. 21, 2023.
- 84 TALKNER, P.; LUTZ, E.; HÄNGGI, P. Fluctuation theorems: Work is not an observable. **Physical Review E**, v. 75, n. 5, p. 050102, 2007.
- 85 CAMPISI, M.; HÄNGGI, P.; TALKNER, P. Colloquium: quantum fluctuation relations: foundations and applications. **Reviews of Modern Physics**, v. 83, n. 3, p. 771, 2011.
- 86 SUOMELA, S. *et al.* Moments of work in the two-point measurement protocol for a driven open quantum system. **Physical Review B**, v. 90, n. 9, p. 094304, 2014.
- 87 BINDER, F. *et al.* Thermodynamics in the quantum regime. **Fundamental Theories of Physics**, v. 195, p. 1–2, 2018.
- 88 MAKHLIN, Y.; SCHÖN, G.; SHNIRMAN, A. Quantum-state engineering with josephson-junction devices. **Reviews of Modern Physics**, v. 73, n. 2, p. 357, 2001.
- 89 COHEN-TANNOUJJI, C.; DUPONT-ROC, J.; GRYNBERG, G. **Atom-photon interactions: basic processes and applications**. New York: John Wiley & Sons, 1998.
- 90 HANSON, R. *et al.* Spins in few-electron quantum dots. **Reviews of Modern Physics**, v. 79, n. 4, p. 1217, 2007.
- 91 MORILLO, M.; DENK, C.; CUKIER, R. Control of tunneling reactions with an external field in a four-level system: a general redfield approach. **Chemical Physics**, v. 212, n. 1, p. 157–175, 1996.
- 92 THORWART, M.; GRIFONI, M.; HÄNGGI, P. Tunneling and vibrational relaxation in driven multi-level systems. **Physics Review Letters**, v. 85, n. quant-ph/9912024, p. 860, 2000.
- 93 THORWART, M.; GRIFONI, M.; HÄNGGI, P. Strong coupling theory for driven tunneling and vibrational relaxation. **Physical Review Letters**, v. 85, n. 4, p. 860, 2000. Available at: <https://synthical.com/article/49b773cc-ffde-11ed-90ce-72eb57fa10b3>. Accessible at: 30 Nov. 2023.
- 94 DEKKER, H. Multisite spin hopping analysis of multilevel dissipative quantum tunneling and coherence at finite temperatures: I. general theory. **Physica A: statistical mechanics and its applications**, v. 175, n. 3, p. 485–527, 1991.
- 95 GRIFONI, M.; HÄNGGI, P. Driven quantum tunneling. **Physics Reports**, v. 304, n. 5-6, p. 229–354, 1998.

-
- 96 GARG, A.; ONUCHIC, J. N.; AMBEGAOKAR, V. Effect of friction on electron transfer in biomolecules. **Journal of Chemical Physics**, v. 83, n. 9, p. 4491–4503, 1985.
- 97 MORILLO, M.; CUKIER, R. Control of proton-transfer reactions with external fields. **Journal of Chemical Physics**, v. 98, n. 6, p. 4548–4556, 1993.
- 98 BENDERSKII, V.; GOLDANSKII, V.; MAKAROV, D. E. Quantum dynamics in low-temperature chemistry. **Physics Reports**, v. 233, n. 4/5, p. 195–339, 1993.
- 99 SCHUMM, T. *et al.* Matter-wave interferometry in a double well on an atom chip. **Nature Physics**, v. 1, n. 1, p. 57–62, 2005.
- 100 HALL, B. *et al.* Condensate splitting in an asymmetric double well for atom chip based sensors. **Physical Review Letters**, v. 98, n. 3, p. 030402, 2007.
- 101 FRIEDMAN, J. R. *et al.* Quantum superposition of distinct macroscopic states. **Nature**, v. 406, n. 6791, p. 43–46, 2000.
- 102 CLARKE, J.; WILHELM, F. K. Superconducting quantum bits. **Nature**, v. 453, n. 7198, p. 1031–1042, 2008.
- 103 BALANTEKIN, A.; TAKIGAWA, N. Quantum tunneling in nuclear fusion. **Reviews of Modern Physics**, v. 70, n. 1, p. 77, 1998.
- 104 GOYCHUK, I.; PETROV, E.; MAY, V. Dynamics of the dissipative two-level system driven by external telegraph noise. **Physical Review E**, v. 52, n. 3, p. 2392, 1995.
- 105 HAUSINGER, J.; GRIFONI, M. Dissipative dynamics of a biased qubit coupled to a harmonic oscillator: analytical results beyond the rotating wave approximation. **New Journal of Physics**, v. 10, n. 11, p. 115015, 2008.
- 106 GRIFONI, M. *et al.* Nonlinear response of a periodically driven damped two-state system. **Physical Review E**, v. 48, n. 5, p. 3497, 1993.
- 107 GRIFONI, M. *et al.* Cooperative effects in the nonlinearly driven spin-boson system. **Physical Review E**, v. 52, n. 4, p. 3596, 1995.
- 108 BRAUMÜLLER, J. *et al.* Analog quantum simulation of the rabi model in the ultra-strong coupling regime. **Nature Communications**, v. 8, n. 1, p. 779, 2017.
- 109 LANGFORD, N. K. *et al.* Experimentally simulating the dynamics of quantum light and matter at deep-strong coupling. **Nature Communications**, v. 8, n. 1, p. 1715, 2017.
- 110 ZWOLAK, M. P. **Dynamics and simulation of open quantum systems**. 2008. 177 p. Ph. D. Thesis (Doctor in Philosophy) — California Institute of Technology, California, 2008. DOI: 10.7907/565E-JR05.
- 111 KENNETH, A. R. **Elementary Analysis: the theory of calculus**. Berlin, Springer, 2013.
- 112 NESI, F. *et al.* Spin-boson dynamics beyond conventional perturbation theories. **Physical Review B**, v. 76, n. 15, p. 155323, 2007.

- 113 HENRIET, L. *et al.* Quantum dynamics of the driven and dissipative rabi model. **Physical Review A**, v. 90, n. 2, p. 023820, 2014.
- 114 ORTH, P. P.; IMAMBEKOV, A.; HUR, K. L. Nonperturbative stochastic method for driven spin-boson model. **Physical Review B**, v. 87, n. 1, p. 014305, 2013.
- 115 GÖRLICH, R.; SASSETTI, M.; WEISS, U. Low-temperature properties of biased two-level systems: effects of frequency-dependent damping. **Europhysics Letters**, v. 10, n. 6, p. 507, 1989.
- 116 HARTMANN, L.; GRIFONI, M.; HÄNGGI, P. Dissipative tunneling control by elliptically polarized fields. **Journal of Chemical Physics**, v. 109, n. 7, p. 2635–2643, 1998.
- 117 SPAGNOLO, B.; CAROLLO, A.; VALENTI, D. Enhancing metastability by dissipation and driving in an asymmetric bistable quantum system. **Entropy**, v. 20, n. 4, p. 226, 2018.
- 118 FUNO, K.; QUAN, H. Path integral approach to quantum thermodynamics. **Physical Review Letters**, v. 121, n. 4, p. 040602, 2018.
- 119 QIU, T. *et al.* Path-integral approach to the calculation of the characteristic function of work. **Physical Review E**, v. 101, n. 3, p. 032111, 2020.
- 120 FUNO, K.; QUAN, H. Path integral approach to heat in quantum thermodynamics. **Physical Review E**, v. 98, n. 1, p. 012113, 2018.
- 121 MAGAZZÙ, L. *et al.* Probing the strongly driven spin-boson model in a superconducting quantum circuit. **Nature Communications**, v. 9, n. 1, p. 1403, 2018.
- 122 DAKHNOVSKII, Y.; COALSON, R. D. Manipulating reactant–product distributions in electron transfer reactions with a laser field. **Journal of Chemical Physics**, v. 103, n. 8, p. 2908–2916, 1995.
- 123 GOYCHUK, I.; PETROV, E.; MAY, V. Control of the dynamics of a dissipative two-level system by a strong periodic field. **Chemical Physics Letters**, v. 253, n. 5-6, p. 428–437, 1996.
- 124 MANDAL, N. S.; SEN, A.; ASTUMIAN, R. D. Kinetic asymmetry versus dissipation in the evolution of chemical systems as exemplified by single enzyme chemotaxis. **Journal of the American Chemical Society**, v. 145, n. 10, p. 5730–5738, 2023.
- 125 SUASSUNA, B.; MELO, B.; GUERREIRO, T. Path integrals and nonlinear optical tweezers. **Physical Review A**, v. 103, n. 1, p. 013110, 2021.
- 126 VOLPE, G.; VOLPE, G. Simulation of a Brownian particle in an optical trap. **American Journal of Physics**, v. 81, n. 3, p. 224, 2013.
- 127 KRAMERS, H. A. Brownian motion in a field of force and the diffusion model of chemical reactions. **Physica**, v. 7, n. 4, p. 284, 1940.
- 128 ASHKIN, A. *et al.* Observation of a single-beam gradient force optical trap for dielectric particles. **Optics Letters**, v. 11, n. 5, p. 288–290, 1986.

-
- 129 JONES, P.; MARAGÓ, O.; VOLPE, G. **Optical tweezers**. Cambridge: Cambridge University Press, 2015.
- 130 LU, P. J.; WEITZ, D. A. Colloidal particles: crystals, glasses, and gels. **Annual Review of Condensed Matter Physics**, v. 4, n. 1, p. 217–233, 2013.
- 131 RAGAZZON, G.; PRINS, L. J. Energy consumption in chemical fuel-driven self-assembly. **Nature Nanotechnology**, v. 13, n. 10, p. 882–889, 2018.
- 132 LAGE, E. **Física estatística**. Lisboa: Fundação Calouste Gulbenkian, 1995.
- 133 FURTH, R.; COWPER, A. **Albert Einstein: investigations on the theory of the Brownian movement**. New York: Dover, 1956.
- 134 RISKEN, H. **Fokker-Planck equation**. New York: Springer, 1996.
- 135 GARDINER, C. W. **Handbook of stochastic methods**. 3rd. ed. New York: Springer, 2003.
- 136 SALINAS, S. R. **Introdução à física estatística**. São Paulo: EDUSP, 1997.
- 137 METZLER, R. *et al.* Anomalous diffusion models and their properties: non-stationarity, non-ergodicity, and ageing at the centenary of single particle tracking. **Physical Chemistry Chemical Physics**, v. 16, n. 44, p. 24128–24164, 2014.
- 138 PEKALSKI, A.; SZNAJD-WERON, K. **Anomalous diffusion: from basics to applications**. New York: Springer, 1999.
- 139 METZLER, R.; KLAFTER, J. The random walk’s guide to anomalous diffusion: a fractional dynamics approach. **Physics Reports**, v. 339, n. 1, p. 1–77, 2000.
- 140 OLIVEIRA, F. A. *et al.* Anomalous diffusion: a basic mechanism for the evolution of inhomogeneous systems. **Frontiers in Physics**, v. 7, p. 18, 2019. DOI: 10.3389/fphy.2019.00018.
- 141 KRAPF, D. Mechanisms underlying anomalous diffusion in the plasma membrane. **Current Topics in Membranes**, v. 75, p. 167–207, 2015.
- 142 SABRI, A. *et al.* Elucidating the origin of heterogeneous anomalous diffusion in the cytoplasm of mammalian cells. **Physical Review Letters**, v. 125, n. 5, p. 058101, 2020.
- 143 PIERRO, M. D. *et al.* Anomalous diffusion, spatial coherence, and viscoelasticity from the energy landscape of human chromosomes. **Proceedings of the National Academy of Sciences**, v. 115, n. 30, p. 7753, 2018.
- 144 PLEROU, V. *et al.* Economic fluctuations and anomalous diffusion. **Physical Review E**, v. 62, n. 3, p. R3023, 2000.
- 145 FEYNMAN, R. P.; HIBBS, A. R.; STYER, D. F. **Quantum mechanics and path integrals**. Singapore: Dover Publications, 2005.
- 146 GENARO, M. P. **Termodinâmica quântica de sistemas simples**. 2019. 88 p. Dissertação (Mestrado em Ciências) — Setor de Ciências Exatas, Universidade Federal do Paraná, Curitiba, 2019.

147 VALENTE, D. *et al.* Work on a quantum dipole by a single-photon pulse. **Optics Letters**, v. 43, n. 11, p. 2644–2647, 2018.

APPENDIX

APPENDIX A – TWO-TIME CORRELATION FUNCTIONS AND FLUCTUATION-DISSIPATION THEOREM

This appendix provides a few steps for demonstrating the correlation force derivation by the fluctuation-dissipation theorem.

The following identities can be derived from the condition of thermal equilibrium,

$$\langle \tilde{R}_k(0) \rangle = 0, \quad \langle \dot{R}_k(0) \rangle = 0, \quad (\text{A.1})$$

$$\langle \tilde{R}_k(0) \dot{R}_{k'}(0) \rangle = 0, \quad \langle \dot{R}_k(0) \tilde{R}_{k'}(0) \rangle = 0, \quad (\text{A.2})$$

$$\langle \dot{R}_k(0) \dot{R}_{k'}(0) \rangle = \frac{k_B T}{m_k} \delta_{kk'}, \quad \langle \tilde{R}_k(0) \tilde{R}_{k'}(0) \rangle = \frac{k_B T}{m_k \omega_k^2} \delta_{kk'}, \quad (\text{A.3})$$

where k_B is Boltzmann constant. The formal expressions for the fluctuating forces, as specified in the main text, are given by

$$f_i(t) = - \sum_k C_k^{(i)} \left[\dot{R}_k(0) \frac{\sin \omega_k t}{\omega_k} + \tilde{R}_k(0) \cos \omega_k t \right], \quad (\text{A.4})$$

where the displaced equilibrium positions of the oscillators (due to their couplings with the particles) are $\tilde{R}_k(0) = R_k(0) + (C_k^{(i)} x_i(0) + C_k^{(j)} x_j(0)) / (m_k \omega_k^2)$. $f_q = (f_1 + f_2)/2$ and $f_u = f_1 - f_2$ were also defined and the general form for two-time correlation functions can be obtained by the aforementioned expressions,

$$\langle f_\alpha(t) f_\beta(t') \rangle = 2D_{\alpha\beta}(u) \delta(t - t'), \quad (\text{A.5})$$

where $D_{\alpha\beta}(u)$ is a type of diffusion coefficient that takes on a different form according to the choice of forces dealt with. The continuum limit directly computed them, as in Chap. 2, leading to Eqs.(2.51), (2.53), and (2.52).

For completeness and emphasizing the general form of the fluctuation-dissipation theorem, Eq. (A.5), the original statement of the theorem provided elsewhere is recalled; For a free Brownian particle, Langevin equation states

$$m\dot{v}(t) = -\eta v(t) + f(t), \quad (\text{A.6})$$

where η is a friction coefficient and $f(t)$ is a fluctuating force caused by particle impacts with its surroundings. The fluctuating force satisfies

$$\langle f(t) \rangle = 0, \quad \text{and} \quad \langle f(t) f(t') \rangle = 2D\delta(t - t'), \quad (\text{A.7})$$

where D can be considered a measure of the fluctuating force's strength. The delta function in time indicates there is no correlation between impacts at any distinct time intervals. The solution for the linear, first-order, and inhomogeneous differential equation holds (7)

$$v(t) = e^{-\eta t/m} v(0) + \int_0^t dt' e^{-\eta(t-t')/m} \frac{f(t')}{m}. \quad (\text{A.8})$$

The mean squared velocity can be calculated and analyzed over a long period of time, therefore

$$\langle v^2(\infty) \rangle = \frac{D}{\eta m}. \quad (\text{A.9})$$

The equipartition theorem states $\langle v^2 \rangle_{eq} = k_B T / m$ in thermal equilibrium. Therefore,

$$D = \eta k_B T. \quad (\text{A.10})$$

The fluctuation-dissipation theorem is a correspondence between strength D of random noise, or fluctuating force, and magnitude η of friction, or dissipation rate, explaining why it is known as the fluctuation-dissipation theorem. It expresses the balance between friction and noise required for a thermal equilibrium state at long times.

APPENDIX B – RESPONSE THEORY

This appendix provides a derivation of the response theory for single and two-particles systems, encompassing both linear and nonlinear response theories (22). The dependence of the spectral function on relative distance, defined in Eq.(2.36), is demonstrated.

B.1 Linear response theory of an environment perturbed by one particle

Ref. (25) was revisited towards a more detailed discussion on standard single-particle response theory. The bath's equation of motion for a single Brownian particle with linear coupling is given by

$$m_k \ddot{R}_k + m_k \omega_k^2 R_k - C_k x = 0. \quad (\text{B.1})$$

The Fourier transform of the susceptibility (response function) of $R_k(t)$ to a stimulus $x(t)$ is

$$\tilde{R}_k = -\frac{C_k}{m_k(\omega^2 - \omega_k^2)} \tilde{x}(\omega), \quad (\text{B.2})$$

for each mode with frequency ω . The effective collective coordinates of the environment can be expressed as

$$R_{\text{eff}} = \sum_k C_k \tilde{R}_k(t), \quad (\text{B.3})$$

which corresponds to the expression

$$R_{\text{eff}} = -\sum_k \frac{C_k^2}{m_k(\omega^2 - \omega_k^2)} \tilde{x}(\omega) \quad (\text{B.4})$$

$$= \chi_{\text{env}}(\omega) \tilde{x}(\omega), \quad (\text{B.5})$$

given in Ref. (25), where susceptibility $\chi_{\text{env}}(\omega)$ is defined as

$$\chi_{\text{env}}(\omega) \equiv -\sum_k \frac{C_k^2}{m_k(\omega^2 - \omega_k^2)}. \quad (\text{B.6})$$

The imaginary part of $\chi_{\text{env}}(\omega)$ stems from the usual replacement for causal responses,

$$\omega \pm \omega_k \rightarrow \omega \pm \omega_k + i\epsilon \quad (\text{with } \epsilon \rightarrow 0), \quad (\text{B.7})$$

employing the following identity

$$\frac{1}{\omega \pm \omega_k + i\epsilon} = \mathcal{P} \left(\frac{1}{\omega \pm \omega_k} \right) - i\pi \delta(\omega \pm \omega_k), \quad (\text{B.8})$$

which yields

$$\text{Im}\{\chi_{env}(\omega)\} \equiv \chi''_{env}(\omega) = \frac{\pi}{2} \sum_k \frac{C_k^{(1)2}}{m_k \omega_k} [\delta(\omega - \omega_k) + \delta(\omega + \omega_k)]. \quad (\text{B.9})$$

Since $\omega, \omega_k > 0$, the spectral function can be written as

$$\chi''_{env}(\omega) = J(\omega) = \frac{\pi}{2} \sum_k \frac{C_k^2}{m_k \omega_k} \delta(\omega - \omega_k), \quad (\text{B.10})$$

in agreement with Eq.(2.7, thus concluding our review of the results on the response theory for a single particle. In what follows is the derivation of the results for the two-particle response theory.

B.2 Nonlinear response theory of an environment perturbed by a pair of particles within the nonlinear coupling model

This section addresses the determination of the effective coordinate of environment R_{eff} , analogous to the one outlined in Eq. (B.3), especially in scenarios involving nonlinear couplings between the system and the reservoir.

Let us start with the equations of motion for the bath with nonlinear coupling between particles and bath given by

$$m_k \ddot{R}_{-k} + m_k \omega_k^2 R_{-k} + C_{-k}(x_1) + C_{-k}(x_2) = 0, \quad (\text{B.11})$$

$$m_k \ddot{R}_k + m_k \omega_k^2 R_k + C_k(x_1) + C_k(x_2) = 0, \quad (\text{B.12})$$

which implies Eq.(B.2) and Eq.(B.3) are no longer applied.

Function $C_k(x_i)$ non-linearly combines the Fourier components of a particle's coordinates, denoted as $\tilde{x}_i(\omega)$. From a physical standpoint, if the environment exerts a dissipative force on a pair of particles, i.e., a force that depends non-linearly on the interparticle distance, in response, the particles will perturb the environment in a similar non-linear fashion, thus leading to the non-linear dependence of R_{eff} on the interparticle distance.

Therefore, let us assume

$$R_k(t) = \tilde{R}_k \exp(-i\omega t), \text{ and} \quad (\text{B.13})$$

$$C_k(x_1) + C_k(x_2) \approx [C_k(x_1^0) + C_k(x_2^0)] e^{(-i\omega t)}. \quad (\text{B.14})$$

which can be interpreted as a quasi-static (Born-Oppenheimer) approximation under the condition of the particles' Brownian dynamics varying very slowly compared to the rapid bath dynamics ($\omega \ll \omega_k$). Consequently,

$$x_i^0 \approx x_i = x_i(t), \text{ and} \quad (\text{B.15})$$

$$\exp(-i\omega t) \approx 1. \quad (\text{B.16})$$

Those approximations are analogous to the low-frequency limit commonly assumed in the Ohmic regime.

$$\tilde{R}_{-k}(\omega) \approx -\frac{C_{-k}(x_1) + C_{-k}(x_2)}{m_k(\omega^2 - \omega_k^2)}, \quad (\text{B.17})$$

$$\tilde{R}_k(\omega) \approx -\frac{C_k(x_1) + C_k(x_2)}{m_k(\omega^2 - \omega_k^2)}, \quad (\text{B.18})$$

is then obtained by Fourier transform and the environment's effective (collective) coordinate can be written as

$$R_{\text{eff}} = \sum_k \left(\tilde{R}_k(C_{-k}(x_1) + C_{-k}(x_2)) + \tilde{R}_{-k}(C_k(x_1) + C_k(x_2)) \right), \quad (\text{B.19})$$

which is a linear combination of \tilde{R}_k 's with coefficients now given by $C_{\pm k}(x_i)$.

Replacing \tilde{R}_k and \tilde{R}_{-k} ,

$$R_{\text{eff}} = -2 \sum_k \frac{[(C_{-k}(x_1) + C_{-k}(x_2))(C_k(x_1) + C_k(x_2))]}{m_k(\omega^2 - \omega_k^2)}, \quad (\text{B.20})$$

and also replacing $C_k(x_i) = \kappa_k e^{ikx_i}$ lead to

$$R_{\text{eff}} = -2 \sum_k \frac{\kappa_k \kappa_{-k}}{m_k(\omega^2 - \omega_k^2)} (1 + 2 \cos ku). \quad (\text{B.21})$$

The series representations of $1 + 2 \cos x$ can be used,

$$\begin{aligned} R_{\text{eff}} &= -2 \sum_k \frac{\kappa_k \kappa_{-k}}{m_k(\omega^2 - \omega_k^2)} \left(1 + 2 \sum_{n=0}^{\infty} \frac{(-1)^n (ku)^{2n}}{(2n)!} \right) \\ &= -4 \sum_k \frac{\kappa_k \kappa_{-k}}{m_k(\omega^2 - \omega_k^2)} - 4 \sum_k \frac{\kappa_k \kappa_{-k}}{m_k(\omega^2 - \omega_k^2)} \sum_{n=1}^{\infty} \frac{(-1)^n}{(2n)!} k^{2n} u^{2n-1} u \\ R_{\text{eff}} &= \chi_{\text{env,cte}}(\omega) + \chi_{\text{env,u}}(\omega, u)u, \end{aligned} \quad (\text{B.22})$$

where

$$\chi_{\text{env,u}}(\omega, u) = -4 \sum_k \sum_{n=1}^{\infty} \frac{(-1)^n}{(2n)!} \kappa_k \kappa_{-k} k^{2n} u^{2n-1} \left(\frac{1}{2m_k \omega_k (\omega + \omega_k)} - \frac{1}{2m_k \omega_k (\omega - \omega_k)} \right). \quad (\text{B.23})$$

The imaginary part of $\chi_{\text{env,u}}(\omega)$ using Eq.(B.7) and Eq.(B.8) is given by

$$\text{Im} \chi_{\text{env,u}}(\omega, u) = \chi_{\text{env,u}}''(\omega, u) = 2\pi \sum_k \sum_{n=1}^{\infty} \frac{(-1)^n}{(2n)!} \kappa_k \kappa_{-k} k^{2n} u^{2n-1} \frac{[\delta(\omega - \omega_k) + \delta(\omega + \omega_k)]}{m_k \omega_k}, \quad (\text{B.24})$$

since ω and $\omega_k > 0$, then

$$J_u(\omega) = \chi_{\text{env,u}}''(\omega, u) = 2\pi \sum_k \sum_{n=1}^{\infty} \frac{(-1)^n}{(2n)!} \kappa_k \kappa_{-k} k^{2n} u^{2n-1} \frac{\delta(\omega - \omega_k)}{m_k \omega_k}, \quad (\text{B.25})$$

$$= \frac{\pi}{2} \sum_k \frac{h_{nl}(k, u)}{m_k \omega_k} \delta(\omega - \omega_k), \quad (\text{B.26})$$

with

$$h_{nl}(k, u) = 4 \sum_{n=1}^{\infty} \frac{(-1)^n}{(2n)!} \kappa_k \kappa_{-k} k^{2n} u^{2n-1}. \quad (\text{B.27})$$

Next, the derivation provided here is extended towards elucidating the physical meaning of our nonlinear susceptibility, as introduced in Eq.(2.36).

B.3 Nonlinear response theory of an environment perturbed by a pair of particles within the bilinear coupling model (modified bilinear model)

Drawing an analogy with the effective (collective) bath coordinate, as defined in Eq.(B.20), a tangible physical interpretation to our nonlinear susceptibility can be attributed, as expressed in Eq.(2.36).

The equations of motion for two Brownian particles with bilinear coupling model are given by

$$m\ddot{x}_i + \sum_k C_k^{(i)} R_k + \frac{C_k^{(i)}}{m_k \omega_k^2} (C_k^{(1)} x_1 + C_k^{(2)} x_2) = 0, \quad (\text{B.28})$$

$$\sum_k m_k \ddot{R}_k + m_k \omega_k^2 R_k + C_k^{(1)} x_1 + C_k^{(2)} x_2 = 0. \quad (\text{B.29})$$

For each physical system that represents the reservoir there is a certain noise characteristic of this reservoir whose Fourier transform provides a characteristic spectral function.

Utilizing Fourier transform within the equations of motion for the bath directly led to

$$\tilde{R}_k(\omega) = -\frac{(C_k^{(1)} x_1(\omega) + C_k^{(2)} x_2(\omega))}{m_k(\omega^2 - \omega_k^2)},$$

This was achieved by employing center of mass and relative coordinates

$$\tilde{R}_k(q, u) = -\frac{(\bar{c}q + \Delta c \frac{u}{2})}{m_k(\omega^2 - \omega_k^2)}, \quad (\text{B.30})$$

with

$$\bar{c} = C_k^{(1)} + C_k^{(2)}, \quad (\text{B.31})$$

$$\Delta c = C_k^{(1)} - C_k^{(2)}. \quad (\text{B.32})$$

Instead of assuming nonlinearity originates solely from the nonlinear couplings $C_k(x_i)$, as described in Eq.(B.20), the notion the collective coordinate inherently comprises a nonlinear amalgamation of bath modes is considered. Consequently, the collective coordinate of the environment can be expressed as

$$R_{\text{eff}} \equiv \sum_k \left(C_k^{(1)} F_k^{(1)}[\tilde{R}_k(q, u)] + C_k^{(2)} F_k^{(2)}[\tilde{R}_k(q, u)] \right), \quad (\text{B.33})$$

where functions $F_k^{(i)}[\bullet]$ must be appropriately chosen so as to reproduce the phenomenological behavior of the system of interest. Without loss of generality, $F_k^{(i)}[\bullet]$ can be expanded in a power series as

$$F_k^{(1)} = \sum_{n=0}^{\infty} F_{k,n}^{(1)} \frac{[\tilde{R}_k(q, u)]^n}{n!}, \text{ and} \quad (\text{B.34})$$

$$F_k^{(2)} = \sum_{m=0}^{\infty} F_{k,m}^{(2)} \frac{[\tilde{R}_k(q, u)]^m}{m!}. \quad (\text{B.35})$$

Assuming renormalizing $F_{k,n}^{(1)}$ and $F_{k,m}^{(2)}$ results in

$$F_{k,n}^{(1)} = f_{k,n}^{(1)} (m_k (\omega^2 - \omega_k^2))^{n-1}, \text{ and} \quad (\text{B.36})$$

$$F_{k,m}^{(2)} = f_{k,m}^{(2)} (m_k (\omega^2 - \omega_k^2))^{m-1}. \quad (\text{B.37})$$

Therefore,

$$R_{\text{eff}} = \sum_k C_k^{(1)} \left(\sum_{n=0}^{\infty} F_{k,n}^{(1)} \frac{[\tilde{R}_k(q, u)]^n}{n!} \right) + \sum_k C_k^{(2)} \left(\sum_{m=0}^{\infty} F_{k,m}^{(2)} \frac{[\tilde{R}_k(q, u)]^m}{m!} \right) \quad (\text{B.38})$$

$$= \sum_k C_k^{(1)} \left(\sum_{n=0}^{\infty} f_{k,n}^{(1)} (m_k (\omega^2 - \omega_k^2))^{n-1} \frac{[\tilde{R}_k(\omega)]^n}{n!} \right) \\ + \sum_k C_k^{(2)} \left(\sum_{m=0}^{\infty} f_{k,m}^{(2)} (m_k (\omega^2 - \omega_k^2))^{m-1} \frac{[\tilde{R}_k(\omega)]^m}{m!} \right)$$

$$R_{\text{eff}} = - \sum_k \frac{1}{m_k (\omega^2 - \omega_k^2)} \left(C_k^{(1)} \sum_{n=0}^{\infty} \frac{(-1)^{n-1}}{n!} f_{k,n}^{(1)} \left[\bar{c}q + \Delta c \frac{u}{2} \right]^n \right. \\ \left. + \sum_k C_k^{(2)} \sum_{m=0}^{\infty} \frac{(-1)^{m-1}}{m!} f_{k,m}^{(2)} \left[\bar{c}q + \Delta c \frac{u}{2} \right]^m \right). \quad (\text{B.39})$$

The formula of binomial expansion $(a + b)^n = \sum_{p=0}^n \binom{n}{p} a^{n-p} b^p$ leads to

$$R_{\text{eff}} = - \sum_k \frac{1}{m_k (\omega^2 - \omega_k^2)} \left[C_k^{(1)} \sum_{n=0}^{\infty} \frac{(-1)^{n-1}}{n!} f_{k,n}^{(1)} \sum_{p=0}^n (\bar{c}q)^{n-p} (\Delta c \frac{u}{2})^p \binom{n}{p} \right. \quad (\text{B.40})$$

$$\left. + \sum_k C_k^{(2)} \sum_{m=0}^{\infty} \frac{(-1)^{m-1}}{m!} f_{k,m}^{(2)} \sum_{p'=0}^m (\bar{c}q)^{m-p'} (\Delta c \frac{u}{2})^{p'} \binom{m}{p'} \right]$$

$$= - \sum_k \frac{1}{m_k (\omega^2 - \omega_k^2)} \sum_{n'=0}^{\infty} \frac{(-1)^{n'-1}}{n'!} (C_k^{(1)} f_{k,n'}^{(1)} + C_k^{(2)} f_{k,n'}^{(2)}) \sum_{m'=0}^{n'} \binom{n'}{m'} (\bar{c}q)^{n'-m'} \left(\Delta c \frac{u}{2} \right)^{m'}$$

$$= - \sum_k \frac{1}{m_k (\omega^2 - \omega_k^2)} \sum_{n'=0}^{\infty} \frac{(-1)^{n'-1}}{n'!} (C_k^{(1)} f_{k,n'}^{(1)} + C_k^{(2)} f_{k,n'}^{(2)}) \sum_{m'=0}^{n'} \binom{n'}{m'} \bar{c}^{n'-m'} \left(\frac{\Delta c}{2} \right)^{m'} q^{n'-m'} u^{m'}$$

$$R_{\text{eff}} = \sum_{n'=0}^{\infty} \alpha_{n'm'} q^{n'-m'} u^{m'},$$

where, explicitly,

$$\alpha_{n'm'} \equiv - \sum_k \frac{(-1)^{n'-1}}{m_k (\omega^2 - \omega_k^2) n'!} (C_k^{(1)} f_{k,n'}^{(1)} + C_k^{(2)} f_{k,n'}^{(2)}) \sum_{m'=0}^{n'} \binom{n'}{m'} \bar{c}^{n'-m'} \left(\frac{\Delta c}{2} \right)^{m'}. \quad (\text{B.41})$$

q -dependent and u -dependent systems can be distinguished,

$$R_{\text{eff}} = \sum_{n'=0}^{\infty} \frac{\alpha_{n'm'}}{2} q^{n'-m'-1} u^{m'} q + \sum_{n'=0}^{\infty} \frac{\alpha_{n'm'}}{2} q^{n'-m'} u^{m'-1} u. \quad (\text{B.42})$$

Therefore,

$$R_{\text{eff}} = \chi_{\text{env},q}(\omega, q, u)q + \chi_{\text{env},q,u}(\omega, u)u, \quad (\text{B.43})$$

where

$$\chi_{\text{env},q}(\omega, q, u) = - \sum_{k,n'} \frac{(-1)^{n'-1}}{2m_k(\omega^2 - \omega_k^2)n!} \left(C_k^{(1)} f_{k,n'}^{(1)} + C_k^{(2)} f_{k,n'}^{(2)} \right) \sum_{m'=0}^{n'} \binom{n'}{m'} \bar{c}^{n'-m'} \left(\frac{\Delta c}{2} \right)^{m'} q^{n'-m'-1} u^{m'}, \quad (\text{B.44})$$

$$\chi_{\text{env},u}(\omega, q, u) = - \sum_{k,n'} \frac{(-1)^{n'-1}}{2m_k(\omega^2 - \omega_k^2)n!} \left(C_k^{(1)} f_{k,n'}^{(1)} + C_k^{(2)} f_{k,n'}^{(2)} \right) \sum_{m'=0}^{n'} \binom{n'}{m'} \bar{c}^{n'-m'} \left(\frac{\Delta c}{2} \right)^{m'} q^{n'-m'} u^{m'-1}. \quad (\text{B.45})$$

The imaginary part of susceptibilities stems from Eq.(B.7) and Eq.(B.8) and provides

$$\text{Im}\{\chi_{\text{env},q}(\omega, q, u)\} \equiv \chi''_{\text{env},q}(\omega, q, u) = \frac{\pi}{2} \sum_k \frac{h'(k, q, u)}{m_k \omega_k} (\delta(\omega - \omega_k) + \delta(\omega + \omega_k)), \quad (\text{B.46})$$

$$\text{Im}\{\chi_{\text{env},u}(\omega, q, u)\} \equiv \chi''_{\text{env},u}(\omega, q, u) = \frac{\pi}{2} \sum_k \frac{h''(k, q, u)}{m_k \omega_k} (\delta(\omega - \omega_k) + \delta(\omega + \omega_k)), \quad (\text{B.47})$$

where

$$h'(k, q, u) \equiv \sum_{n'} \frac{(-1)^{n'-1}}{2n!} \left(C_k^{(1)} f_{k,n'}^{(1)} + C_k^{(2)} f_{k,n'}^{(2)} \right) \sum_{m'=0}^{n'} \binom{n'}{m'} \bar{c}^{n'-m'} \left(\frac{\Delta c}{2} \right)^{m'} q^{n'-m'-1} u^{m'}, \quad (\text{B.48})$$

and

$$h''(k, q, u) = \sum_{n'} \frac{(-1)^{n'-1}}{2n!} \left(C_k^{(1)} f_{k,n'}^{(1)} + C_k^{(2)} f_{k,n'}^{(2)} \right) \sum_{m'=0}^{n'} \binom{n'}{m'} \bar{c}^{n'-m'} \left(\frac{\Delta c}{2} \right)^{m'} q^{n'-m'} u^{m'-1} \quad (\text{B.49})$$

was defined. Since ω and $\omega_k > 0$, only $\delta(\omega - \omega_k)$ remains in the above equation. $h'(k, q, u) = h''(k, q, u)$ might be assumed, resulting in $q = u$. Additionally, $h'(k, q, u) = h''(k, q, u) = h(k, u)$ is selected as Eq.(2.37), leading to $\text{Im} \chi_k^{(ij)}(\omega) = \chi''_{\text{env}}(\omega, q, u)$.

$$h(k, u) = \sum_{n'} \frac{(-1)^{n'-1}}{2n!} \left(C_k^{(1)} f_{k,n'}^{(1)} + C_k^{(2)} f_{k,n'}^{(2)} \right) \sum_{m'=0}^{n'} \binom{n'}{m'} \bar{c}^{n'-m'} \left(\frac{\Delta c}{2} \right)^{m'} u^{n'-1}. \quad (\text{B.50})$$

The above equations illustrate the derivation of our distance-dependent susceptibility, stemming from the application of a nonlinear response theory to a bath of oscillators influenced by a pair of Brownian particles. If either the standard nonlinear coupling model, or our bilinear model with a modified spectral function is considered, the bath of oscillators exhibits a nonlinear reaction when subjected to the disturbance induced by the pair of Brownian particles.

APPENDIX C – DIFFUSION COEFFICIENT

Some characteristics from the statistical analysis of the fluctuating forces, such as diffusion coefficient, should be expanded, since some features are explored in Sec. 2.3.2.

Some fundamental concepts must also be investigated. A diffusion process can be described as spread of the particles due to some difference in concentration, e.g., in particles. The transport process enables the evolution of non-equilibrium systems towards equilibrium (132), which can be determined through the diffusion equation in terms of probability density function $\rho(x, t)$. Fick's law* and continuity equation† govern diffusion equation

$$\frac{\partial \rho(x, t)}{\partial t} = \tilde{D} \frac{\partial^2}{\partial x^2} \rho(x, t), \quad (\text{C.1})$$

where \tilde{D} is diffusion constant, which governs the diffusion process in a non-uniform colloidal solution.

On the one hand, in 1905, Einstein derived diffusion coefficient (133), leading to an explicit form connected to macroscopic characteristics, from which

$$\tilde{D} = \frac{k_B T}{\gamma}, \quad (\text{C.2})$$

where $\gamma = 6\pi n r$ is the inverse of the dissipation rate, with viscosity of fluid n and Brownian particle radius r .

However, according to our description, the diffusion coefficient is the constant appearing in the fluctuation of Langevin forces. Assuming the limit of one dimension in Eq.(C.2) leads to our diffusion coefficient given by

$$D = \eta k_B T, \quad (\text{C.3})$$

where η is our dissipation rate, for close enough particles, the dissipation rate increases with the distance because the effective area of the two Brownian particles also increases due to the collisions with the fluid particles.

As an example (7, 134, 135), a one-dimensional free colloidal particle can be analyzed, resembling Eq.(1.1) in case of vanishing potential, $V(q) = 0$,

$$M\dot{v} + \gamma v = f(t).$$

Replacing velocity by the position derivative and multiplying it with the position result in

$$Mx \frac{d\dot{x}}{dt} + \gamma x \frac{dx}{dt} = x f(t).$$

* Linear relationship between $\rho(x, t)$ and the current density of particles j .

† Conservation of number of particles.

Using $x \frac{d\dot{x}}{dt} = \frac{d(x\dot{x})}{dt} - \dot{x}^2$ and taking the average over a large number of different particles, the following mean squared displacement is derived:

$$M \frac{d\langle x\dot{x} \rangle}{dt} - M \langle \dot{x}^2 \rangle + \gamma \langle x\dot{x} \rangle = \langle xf(t) \rangle.$$

Applying equipartition theorem $\frac{1}{2}M \langle \dot{x}^2 \rangle = \frac{k_B T}{2M}$ and considering position and random force are uncorrelated, $\langle xf(t) \rangle = \langle x \rangle \langle f(t) \rangle = 0$, by integration, the equation can be solved

$$\langle x\dot{x} \rangle = \frac{k_B T}{\gamma} + C e^{-\gamma t/M},$$

where C is an arbitrary constant. Using $\langle x\dot{x} \rangle = \frac{1}{2} \frac{d\langle x^2 \rangle}{dt}$ and the initial condition of $x(0) = 0$, the result for the mean squared displacement is recovered as

$$\langle x^2(t) \rangle = \frac{2k_B T}{\gamma} \left(t - \frac{M}{\gamma} (1 - e^{-\gamma t/M}) \right). \quad (\text{C.4})$$

For $t \gg \frac{M}{\gamma}$, then

$$\langle x^2 \rangle = 2 \frac{k_B T}{\gamma} t = 2\tilde{D}t, \quad (\text{C.5})$$

which reads the relation between the diffusion coefficient and the mean squared displacement.

Up to this point, the discussion involved what is commonly known as normal diffusion, which refers to the linear mean squared displacement behavior over time. The normal diffusion assumes (136)

- (i) the particles are independent,
- (ii) consecutive displacements are uncorrelated,
- (iii) the displacement's distribution has finite variance.

In contrast, anomalous diffusion (137), from which at least one of the above assumptions is not valid, can also be explored. A nonlinear growth for mean squared displacement in time can be identified as (134, 135, 138–140)

$$\langle \Delta x^2 \rangle \simeq D_\alpha t^\alpha \begin{cases} \alpha < 1, & \text{sub-diffusion process,} \\ \alpha > 1, & \text{super-diffusion process,} \\ \alpha = 1, & \text{Brownian process.} \end{cases} \quad (\text{C.6})$$

D_α is the anomalous diffusion of dimension $[length]^2/[time]^\alpha$. The behavior of anomalous diffusion can be observed in both Biology (141–143) and Economics (144) contexts.

APPENDIX D – PATH INTEGRAL FORMALISM

The focus here is on the evaluation of Kernel, which appears in the path integral formalism (25). As addressed in the scope of this thesis, in classical mechanics, the path taken by a particle extremizes the action, given by the integral of the Lagrangian of the system

$$S = \int_{t_a}^{t_b} L(\dot{x}, x, t) dt,$$

with t_a, t_b as initial and final times. The path also satisfies the equation of motion

$$\frac{d}{dt} \left(\frac{\partial L}{\partial \dot{x}} \right) - \frac{\partial L}{\partial x} = 0.$$

On the other hand, in quantum mechanics, the probability of transitioning from an initial point to a final one is proportional to the square of the amplitude (see Sec. 3.2) - this amplitude is the sum of the contributions from each path

$$K(b, a) = \sum_{\text{all paths}} \phi[x(t)],$$

where ϕ has a phase proportional to action $\phi[x(t)] = C e^{iS[x(t)]/\hbar}$, with constant C .

Utilizing an analog of the Riemann integral to define the summation across all paths, choosing a subset of all paths, and dividing the time into steps of width ϵ result in a set of values t_i spaced in an interval ϵ between t_a and t_b values of time. For each time t_i , a point x_i can be selected and, then, the sum is calculate performing a multiple integral over all values of x_i from i between 1 and $N - 1$, where

$$\begin{aligned} N_\epsilon &= t_b - t_a, \\ \epsilon &= t_{i+1} - t_i, \\ t_0 &= t_a, t_N = t_b, \\ x_0 &= x_a, x_N = x_b. \end{aligned}$$

The resulting equation is

$$K(b, a) \sim \int \dots \int \int \phi[x(t)] dx_1 dx_2 \dots dx_{N-1}.$$

Reducing the value of ϵ leads to a more representative sample of all paths between points a and b . Since such a limit does not exist, a normalization factor must be defined, which, for a specific Lagrangian, has a simple form. Specific factor A enables taking the limit and writing

$$K(b, a) = \lim_{\epsilon \rightarrow 0} \frac{1}{A} \int \dots \int \int e^{(i/\hbar)S[b,a]} \frac{dx_1}{A} \frac{dx_2}{A} \dots \frac{dx_{N-1}}{A}.$$

The sum over all paths can be rewritten as

$$K(b, a) = \int_a^b \mathcal{D}x(t) e^{(i/\hbar)S[b,a]},$$

which is called a path integral.

APPENDIX E – DERIVATION OF ACTION BY PATH INTEGRAL FORMALISM

Examples of actions that can be derived from the path integral formalism in classical systems are explored in this appendix and the expressions for the kernels of free and driven harmonic oscillators are derived with some details.

E.1 Free harmonic oscillator

The Lagrangian of the harmonic oscillator is given by

$$L = \frac{m}{2}(\dot{x}^2 - \omega^2 x^2), \quad (\text{E.1})$$

assuming $t_b - t_a = T$ only for this exercise. From Euler Lagrange equation

$$\frac{d}{dt} \left(\frac{\partial L}{\partial \dot{x}} \right) - \frac{\partial L}{\partial x} = 0 \implies \ddot{x} + \omega^2 x = 0, \quad (\text{E.2})$$

the solution for such differential equation is

$$x(t) = A \cos(\omega t) + B \sin(\omega t), \quad (\text{E.3})$$

where $t = t' - t_a$, implying the use of the difference as a parameter instead of t' (time from the real axis)*, leading to conditions

$$x(0) = A \cos(\omega 0) + B \sin(\omega 0) = A = x_a, \quad (\text{E.4})$$

$$x(T) = A \sin(\omega T) + B \cos(\omega T) = x_b \implies B = \frac{x_b - x_a \cos(\omega T)}{\sin \omega T}, \quad (\text{E.5})$$

thus,

$$x(t) = x_a \cos \omega t + \frac{x_b - x_a \cos \omega T}{\sin \omega T} \sin \omega t. \quad (\text{E.6})$$

Taking the first derivative

$$\dot{x}(t) = -x_a \omega \sin(\omega t) + \left(\frac{x_b - x_a \cos(\omega T)}{\sin(\omega T)} \right) \omega \cos(\omega t), \quad (\text{E.7})$$

squaring it

$$\dot{x}^2(t) = \omega^2(x_a^2 \sin^2(\omega t) + B^2 \cos^2(\omega t) - 2x_a B \sin(\omega t) \cos(\omega t)), \quad (\text{E.8})$$

and observing

$$\omega^2 x^2(t) = \omega^2(x_a^2 \cos^2(\omega t) + B^2 \sin^2(\omega t) + 2x_a B \sin(\omega t) \cos(\omega t)). \quad (\text{E.9})$$

* If t' provides a solution, then any time shifting should also work for the real interval.

Substituting the above expression into the action equation leads to

$$S = \frac{m\omega^2}{2} \int_0^T \left[x_a(\sin^2 \omega t - \cos^2 \omega t) + B^2(\cos^2 \omega t - \sin^2 \omega t) - 4x_a B \sin \omega t \cos \omega t \right] dt. \quad (\text{E.10})$$

Taking relation $\sin^2 \omega t - \cos^2 \omega t = -\cos 2\omega t$ and $\sin \omega t \cos \omega t = (\sin 2\omega t)/2$ and observing

$$\int_0^T \cos(2\omega t) dt = \frac{\sin \omega T \cos \omega T}{\omega}, \quad (\text{E.11})$$

$$\int_0^T \sin(2\omega t) dt = \frac{\sin^2 \omega T}{\omega}, \quad (\text{E.12})$$

the action is

$$\begin{aligned} S &= \frac{m\omega}{2} \left[-x_a^2 \sin \omega T \cos \omega T + B^2 \sin \omega T \cos \omega T - 2x_a B \sin \omega T \right] \\ &= \frac{m\omega}{2} \left[-x_a^2 \sin \omega T \cos \omega T + \frac{x_b^2 - 2x_a x_b \cos \omega T + x_a^2 \cos^2 \omega T}{\sin^2 \omega T} \sin \omega T \cos \omega T \right. \\ &\quad \left. - \frac{x_a x_b - x_a^2 \cos \omega T}{\sin \omega T} (2 \sin^2 \omega T) \right] \\ &= \frac{m\omega}{2 \sin \omega T} \left[-x_a^2 \sin^2 \omega T \cos \omega T + x_b^2 \cos \omega T - 2x_a x_b \cos^2 \omega T + x_a^2 \cos^3 \omega T - 2x_a x_b \sin^2 \omega T \right. \\ &\quad \left. + 2x_a^2 \sin^2 \omega T \cos \omega T \right] \\ &= \frac{m\omega}{2 \sin \omega T} \left[x_a^2 (\cos^3 \omega T + \sin^2 \omega T \cos \omega T) + x_b^2 \cos \omega T - 2x_a x_b \right] \\ S &= \frac{m\omega}{2 \sin \omega T} \left[(x_a^2 + x_b^2) \cos(\omega T) - 2x_a x_b \right]. \quad (\text{E.13}) \end{aligned}$$

Now, the factor must be calculated for the path integral

$$K(b, a) = \exp \left[\frac{i}{\hbar} S_{cl} \right] \int_0^0 \mathcal{F}(t_a, t_b) \mathcal{D}y(t), \quad (\text{E.14})$$

where S_{cl} represents the action evaluated along the classical path and the prefactor for an arbitrary quadratic Lagrangian is given by

$$\mathcal{F}(t_a, t_b) = \int_0^0 \exp \left\{ \left[\frac{i}{\hbar} \int_{t_a}^{t_b} a(t) \dot{y}^2 + b(t) y \dot{y} + c(t) y^2 dt \right] \right\} \mathcal{D}y. \quad (\text{E.15})$$

Towards determining its shape for a free harmonic oscillator, $a(t) = m/2$, $c(t) = m\omega^2/2$ and $b(t) = d(t) = e(t) = f(t) = 0$ is obtained in the generic quadratic Lagrangian

$$L = a(t) \dot{x}^2 + b(t) \dot{x} x + c(t) x^2 + d(t) \dot{x} + e(t) x + f(t), \quad (\text{E.16})$$

where

$$\mathcal{F}(t_a, t_b) = \exp\left\{\frac{i}{\hbar} \int_{t_a}^{t_b} a(t) \dot{y}^2 + b(t) y \dot{y} + c(t) y^2 dt\right\}. \quad (\text{E.17})$$

Therefore, the prefactor becomes

$$\mathcal{F}(t_a, t_b) = \int_0^0 \exp\left[\int_{t_a}^{t_b} \frac{1}{2} m \dot{y}^2 - \frac{1}{2} m \omega^2 y^2 dt\right] \mathcal{D}y. \quad (\text{E.18})$$

Still with the conventional derivation method outlined by Feynman (145), Fourier series is employed to the equation. Since $y(t)$ goes from 0 at $t = 0$ to 0 at $t = t_b - t_a$, then

$$y(t) = \sum_{n=1}^{\infty} a_n \sin \frac{n\pi t}{T}. \quad (\text{E.19})$$

Applying the transformation to each term within the action integral,

$$\frac{m}{2} \int_0^T \dot{y}^2 dt = \frac{m}{2} \sum_{n=1}^{\infty} \sum_{m=1}^{\infty} \frac{n\pi}{T} \frac{m\pi}{T} a_n a_m \int_0^T \cos \frac{n\pi t}{T} \cos \frac{m\pi t}{T} dt = \frac{m}{2} \frac{T}{2} \sum_{n=1}^{\infty} \left(\frac{n\pi}{T}\right)^2 a_n^2, \quad (\text{E.20})$$

where the potential energy term is

$$\frac{m\omega^2}{2} \int_0^T y^2 dt = \frac{m\omega^2}{2} \sum_{n=1}^{\infty} \sum_{m=1}^{\infty} a_n a_m \int_0^T \sin \frac{n\pi t}{T} \sin \frac{m\pi t}{T} dt = \frac{m\omega^2}{2} \frac{T}{2} \sum_{n=1}^{\infty} a_n^2. \quad (\text{E.21})$$

Since time T is divided into discrete steps of length ϵ , coefficients a_n must be finite and the path integral becomes

$$\mathcal{F}(T) = J \frac{1}{A} \int_{-\infty}^{\infty} \cdots \int_{-\infty}^{\infty} \exp\left\{\frac{im}{2\hbar} \frac{T}{2} \sum_{n=1}^N \left[\left(\frac{n\pi}{T}\right)^2 - \omega^2\right] a_n^2\right\} \frac{da_1}{A} \cdots \frac{da_N}{A}, \quad (\text{E.22})$$

where Jacobian factor, J , is not explicitly calculated. Since it does not depend on ω , a trick must be adopted. From the previous equation,

$$\int_{-\infty}^{\infty} \exp\left\{\frac{im}{2\hbar} \frac{T}{2} \left(\frac{n^2\pi^2}{T^2} - \omega^2\right) a_n^2\right\} \frac{da_n}{A} = \left(\frac{2}{\epsilon T}\right)^{1/2} \left(\frac{n^2\pi^2}{T^2} - \omega^2\right)^{-1/2}, \quad (\text{E.23})$$

where $A = (2\pi i \epsilon \hbar / m)^{1/2}$ and $i^{-1/2} e^{-i\pi/4} = 1$ were used. Substituting the result leads to

$$\mathcal{F}(T) = J \left(\frac{m}{2\pi i \hbar \epsilon}\right) \prod_{n=1}^N \left(\frac{2}{\epsilon T}\right)^{N/2} \left(\frac{n^2\pi^2}{T^2} - \omega^2\right)^{-N/2}. \quad (\text{E.24})$$

Next, the terms within the given expression are separated

$$\mathcal{F}(T) = C \prod_{n=1}^N \left(1 - \frac{\omega^2 T^2}{n^2 \pi^2}\right)^{N/2}, \quad (\text{E.25})$$

where C contains all terms that do not depend on ω . Although the limit in the expression of $\mathcal{F}(T)$ has been omitted, when it is taken for $N \rightarrow \infty$ and $\epsilon \rightarrow 0$ in the above product term, then

$$\lim_{N \rightarrow \infty} \prod_{n=1}^N \left(1 - \frac{\omega^2 T^2}{n^2 \pi^2}\right)^{N/2} = \left(\frac{\sin \omega T}{\omega T}\right)^{-1/2}. \quad (\text{E.26})$$

As previously demonstrated, if $\omega = 0$, the term should equate to 1 and $\mathcal{F}(T)$ would resemble that of the free particle, which is

$$\mathcal{F}(T) = \left(\frac{m}{2\pi i \hbar T}\right)^{1/2}. \quad (\text{E.27})$$

For comparison purposes, for the harmonic oscillator,

$$\mathcal{F}(T) = \left(\frac{m\omega}{2\pi i \hbar \sin \omega T}\right)^{1/2}. \quad (\text{E.28})$$

Therefore, the propagator for a free harmonic oscillator is given by

$$K(x_b, T; x_a, 0) = \left(\frac{m\omega}{2\pi i \hbar \sin \omega T}\right)^{1/2} \exp \left\{ \frac{i}{\hbar} \frac{m\omega}{2 \sin \omega T} \left[(x_a^2 + x_b^2) \cos(\omega T) - 2x_a x_b \right] \right\} \quad (\text{E.29})$$

where $T = t_b - t_a$, as addressed elsewhere.

E.2 Driven harmonic oscillator

The Lagrangian for the driven harmonic oscillator is given by

$$L = \frac{1}{2} m \dot{x}^2 - \frac{1}{2} m \omega^2 x^2 + f(t)x, \quad (\text{E.30})$$

where $f(t)$ represents the external force acting on a particle of mass m . The equation of motion is

$$\ddot{x} + \omega^2 x = \frac{f(t)}{m}, \quad (\text{E.31})$$

whose solution is given by $x = x_h + x_p$, where x_h is the homogeneous solution and x_p is the particular one. The homogeneous solution stems from

$$\ddot{x} + \omega^2 x = 0, \quad (\text{E.32})$$

which gives

$$x_h = A \cos \omega t + B \sin \omega t \quad (\text{E.33})$$

where A and B are arbitrary constants.

The other solution can be solved by Green's function method, in which

$$\frac{d^2G(t, t')}{dt^2} + \omega^2G(t, t') = \delta(t - t'), \quad (\text{E.34})$$

where $G(t, t')$ is Green's function and $t' \in (t' - \varepsilon, t' + \varepsilon)$. Next, the equation over the given interval is integrated

$$\int_{t'-\varepsilon}^{t'+\varepsilon} \frac{d^2G(t, t')}{dt^2} dt' + \omega \int_{t'-\varepsilon}^{t'+\varepsilon} G(t, t') dt' = \int_{t'-\varepsilon}^{t'+\varepsilon} \delta(t - t') dt' \quad (\text{E.35})$$

and analyzed term by term. For instance, by definition, Dirac's $\int_{t'-\varepsilon}^{t'+\varepsilon} \delta(t - t') dt' = 1$. ω is a continuous function in the entire interval of t . Since $G(t, t')$ is continuous at $t = t'$ by construction, then $\int_{t'-\varepsilon}^{t'+\varepsilon} G(t, t') dt' = 0$ in the limit of $\varepsilon \rightarrow 0$. Therefore,

$$\lim_{\varepsilon \rightarrow 0} \left[\frac{dG(t, t' + \varepsilon)}{dt'} - \frac{dG(t, t' - \varepsilon)}{dt'} \right] = 1, \quad (\text{E.36})$$

which reveals the derivative of Green's function experiences a discontinuity of magnitude 1 at t' . By generality, $x_h(t) = Ax_1(t) + Bx_2(t)$; therefore, the general form of Green's function is written as

$$G(t, t') = ax_1(t) + bx_2(t), \quad t - t' > 0, \quad (\text{E.37})$$

$$G(t, t') = cx_1(t) + dx_2(t), \quad t - t' < 0. \quad (\text{E.38})$$

The relation of continuity of G and discontinuity of derivative of G at t' yields

$$ax_1(t') + bx_2(t') = cx_1(t') + dx_2(t'), \quad (\text{E.39})$$

$$a\dot{x}_1(t') + b\dot{x}_2(t') = c\dot{x}_1(t') + d\dot{x}_2(t') + 1. \quad (\text{E.40})$$

It is adjusted accordingly by

$$(a - c)x_1(t') + (b - d)x_2(t') = 0, \quad (\text{E.41})$$

$$(a - c)\dot{x}_1(t') + (b - d)\dot{x}_2(t') = 1. \quad (\text{E.42})$$

Solving $a - c$ by Kramers' method yields

$$(a - c) = \frac{\begin{vmatrix} 0 & x_2(t') \\ 1 & \dot{x}_2(t') \end{vmatrix}}{\begin{vmatrix} x_1(t') & x_2(t') \\ \dot{x}_1(t') & \dot{x}_2(t') \end{vmatrix}} = -\frac{x_2(t')}{W(t')}, \quad (\text{E.43})$$

where $W(t') = x_1(t')\dot{x}_2(t') - \dot{x}_1(t')x_2(t')$ is the Wronskian. Similarly

$$(b - d) = \frac{x_1(t')}{W(t')}. \quad (\text{E.44})$$

Those results are substituted in $G(t, t')$ leaving out c and d to be determined by boundary conditions

$$G(t, t') = cx_1(t) + dx_2(t) - \frac{x_1(t)x_2(t') - x_2(t)x_1(t')}{W(t')}, \quad t - t' > 0 \quad (\text{E.45})$$

$$G(t, t') = cx_1(t) + dx_2(t), \quad t - t' < 0. \quad (\text{E.46})$$

Green's function can be explicitly demonstrated by homogeneous solution

$$G(t, t') = cA \cos \omega t + dB \sin \omega t - \frac{AB[(\cos \omega t)(\sin \omega t') - (\sin \omega t)(\cos \omega t')]}{AB\omega[(\cos \omega t')(\cos \omega t') - (-\sin \omega t')(\sin \omega t)]}, \quad t - t' > 0 \quad (\text{E.47})$$

$$G(t, t') = cA \cos \omega t + dB \sin \omega t, \quad t - t' < 0. \quad (\text{E.48})$$

Renaming the constants, $C = cA$ and $D = dB$, and using some trigonometry relation such as $\sin(a - b) = \sin a \cos b - \sin b \cos a$, lead to

$$G(t, t') = C \cos \omega t + D \sin \omega t - \frac{1}{\omega} \sin \omega(t - t'), \quad t - t' > 0, \quad (\text{E.49})$$

$$G(t, t') = C \cos \omega t + D \sin \omega t, \quad t - t' < 0. \quad (\text{E.50})$$

Since our interest is in the action, a two-point boundary condition is required and also satisfies the inhomogeneous boundary condition mathematically. Besides the absence of velocity information provided, there is a subtle aspect wherein $x_a = x(t_a)$ and $x_b = x(t_b)$ are designated as initial and final conditions, thereby encapsulating the entire concept of a trajectory.

The two-point boundary condition is given by

$$G(t_a, t') = G(t_b, t') = 0, \quad (\text{E.51})$$

from which

$$G(t_b, t') = C \cos \omega t_b + D \sin \omega t_b - \frac{1}{\omega} \sin \omega(t_b - t') = 0, \quad t_b - t' > 0, \quad (\text{E.52})$$

$$G(t_a, t') = C \cos \omega t_a + D \sin \omega t_a = 0, \quad t_a - t' < 0. \quad (\text{E.53})$$

Therefore, C and D can be determined substituting the below equation[†]

$$C = -D \frac{\sin \omega t_a}{\cos \omega t_a}, \quad (\text{E.54})$$

into

$$C \cos \omega t_b + D \sin \omega t_b - \frac{1}{\omega} \sin \omega(t_b - t') = 0, \quad (\text{E.55})$$

[†] However, $\omega t_a \neq (2n + 1)\pi/2$ with $n = 0, 1, 2, \dots$ were assumed.

results in

$$D = -\frac{1}{\omega} \frac{\sin \omega(t_b - t') \cos \omega t_a}{\sin \omega(t_b - t_a)} \implies C = \frac{1}{\omega} \frac{\sin \omega(t_b - t') \sin \omega t_a}{\sin \omega(t_b - t_a)}. \quad (\text{E.56})$$

The solution for C and D leads to the final form for Green's function

$$G(t, t') = \frac{1}{\omega} \frac{\sin \omega(t_b - t')}{\sin \omega(t_b - t_a)} \sin \omega(t_a - t) + \frac{1}{\omega} \sin \omega(t - t'), \quad t - t' > 0, \quad (\text{E.57})$$

$$G(t, t') = \frac{1}{\omega} \frac{\sin \omega(t_b - t')}{\sin \omega(t_b - t_a)} \sin \omega(t_a - t), \quad t - t' < 0. \quad (\text{E.58})$$

Another situation, in which $\omega(t_b - t_a) \neq 2n\pi$ with $n = 0, 1, 2, \dots$, is considered. In this case, the solution of the equation of motion is represented by equation

$$x(t) = A \cos \omega t + B \sin \omega t + \int_{t_a}^{t_b} G(t, t') \frac{f(t')}{m} dt'. \quad (\text{E.59})$$

Utilizing the different forms of $G(t, t')$ over the (t_a, t_b) interval, the equation above can be expressed as

$$x(t) = A \cos \omega t + B \sin \omega t + \int_{t_a}^t G(t, t') \frac{f(t')}{m} dt' + \int_t^{t_b} G(t, t') \frac{f(t')}{m} dt'. \quad (\text{E.60})$$

The third term on the left side of the equation is given at $t - t' > 0^\ddagger$

$$\int_{t_a}^t G(t, t') \frac{f(t')}{m} dt' = \frac{1}{m\omega} \int_{t_a}^t \left[\frac{\sin \omega(t_b - t')}{\sin \omega(t_b - t_a)} \sin \omega(t_a - t) + \sin \omega(t - t') \right] f(t') dt'. \quad (\text{E.61})$$

The fourth term on the left side of the equation is given at interval $t - t' < 0$

$$\int_t^{t_b} G(t, t') \frac{f(t')}{m} dt' = \frac{1}{m\omega} \left[\int_t^{t_b} \frac{\sin \omega(t_b - t')}{\sin \omega(t_b - t_a)} \sin \omega(t_a - t) \right] f(t') dt' \quad (\text{E.62})$$

leading to the generic solution for the driven harmonic oscillator dynamics

$$x(t) = A \cos \omega t + B \sin \omega t + \frac{1}{m\omega} \frac{\sin \omega(t_a - t)}{\sin \omega(t_b - t_a)} \int_{t_a}^{t_b} \sin \omega(t_b - t') f(t') dt' + \int_{t_a}^t \frac{\sin \omega(t - t')}{m\omega} f(t') dt'. \quad (\text{E.63})$$

Using boundary condition $x(t_a) = x_a$, $x(t_b) = x_b$ yields

$$x_a = A \cos \omega t_a + B \sin \omega t_a, \quad (\text{E.64})$$

$$x_b = A \cos \omega t_b + B \sin \omega t_b. \quad (\text{E.65})$$

Applying Kramer's method to solve for A and B

$$A = \frac{\begin{vmatrix} x_a & \sin \omega t_a \\ x_b & \sin \omega t_b \end{vmatrix}}{\begin{vmatrix} \cos \omega t_a & \sin \omega t_a \\ \cos \omega t_b & \sin \omega t_b \end{vmatrix}} = \frac{x_a \sin \omega t_b - x_b \sin \omega t_a}{\sin \omega(t_b - t_a)}, \quad (\text{E.66})$$

[‡] Since t' must be in interval $[t_a, t]$, the integration makes sense.

$$B = \frac{\begin{vmatrix} \cos \omega t_a & x_a \\ \cos \omega t_b & x_b \end{vmatrix}}{\begin{vmatrix} \cos \omega t_a & \sin \omega t_a \\ \cos \omega t_b & \sin \omega t_b \end{vmatrix}} = \frac{x_b \cos \omega t_a - x_a \cos \omega t_b}{\sin \omega(t_b - t_a)}. \quad (\text{E.67})$$

After some arrangements and using $\sin(a - b) = \sin(a) \cos(b) - \sin(b) \cos(a)$,

$$x(t) = \frac{1}{\sin \omega(t_b - t_a)} [x_a \sin \omega(t_b - t) + x_b \sin \omega(t - t_a)] + \frac{1}{m\omega} \left[\int_{t_a}^t \sin \omega(t - t') f(t') dt' + \frac{\sin \omega(t_a - t)}{\sin \omega(t_b - t_a)} \int_{t_a}^{t_b} \sin \omega(t_b - t') f(t') dt' \right] \quad (\text{E.68})$$

is found. Next, x is differentiated with respect to t and squared

$$\dot{x}(t) = \frac{\omega}{\sin \omega(t_b - t_a)} [-x_a \cos \omega(t_b - t) + x_b \cos \omega(t - t_a)] + \frac{1}{m} \left[\int_{t_a}^t \cos \omega(t - t') f(t') dt' - \left(\frac{\cos \omega(t_a - t)}{\sin \omega(t_b - t_a)} \int_{t_a}^{t_b} \sin \omega(t_b - t') f(t') dt' \right) \right]. \quad (\text{E.69})$$

The action yields

$$S = \int_{t_a}^{t_b} \left(\frac{1}{2} m \dot{x}^2 - \frac{1}{2} m \omega^2 x^2 + f(t)x \right) dt, \quad (\text{E.70})$$

and using

$$\int_{t_a}^{t_b} \frac{1}{2} m \dot{x} dt = \frac{m}{2} \left(x \dot{x} \Big|_{t_a}^{t_b} - \int_{t_a}^{t_b} x \ddot{x} dt \right). \quad (\text{E.71})$$

Therefore,

$$\begin{aligned} S &= \frac{m}{2} x \dot{x} \Big|_{t_a}^{t_b} - \int_{t_a}^{t_b} \frac{m}{2} x \ddot{x} + \frac{m}{2} \omega^2 x^2 dt + \int_{t_a}^{t_b} f(t)x dt = \frac{m}{2} \left(x(t_b) \dot{x}(t_b) - x(t_a) \dot{x}(t_a) \right) + \frac{1}{2} \int_{t_a}^{t_b} f(t)x(t) dt \\ &= \frac{m}{2} \left\{ \frac{\omega}{\sin \omega(t_b - t_a)} \left[-x_b x_a + x_b^2 \cos \omega(t_b - t_a) \right] + \frac{x_b}{m} \int_{t_a}^{t_b} \cos \omega(t_b - t') f(t') dt' \right. \\ &\quad \left. - \frac{x_b \cos \omega(t_a - t_b)}{m \sin \omega(t_b - t_a)} \int_{t_a}^{t_b} \sin \omega(t_b - t') f(t') dt' - \frac{\omega}{\sin \omega(t_b - t_a)} \left[-x_a^2 \cos \omega(t_b - t_a) + x_a x_b \right] \right. \\ &\quad \left. + \frac{x_a}{m} \left[\frac{1}{\sin \omega(t_b - t_b)} \int_{t_a}^{t_b} \sin \omega(t_b - t') f(t') dt' \right] \right\} \\ &\quad + \frac{1}{2 \sin \omega(t_b - t_a)} \left[x_a \int_{t_a}^{t_b} \sin \omega(t_b - t) f(t) dt + x_b \int_{t_a}^{t_b} \sin \omega(t - t_a) f(t) dt \right] \\ &\quad + \frac{1}{2m\omega} \left[\int_{t_a}^{t_b} \int_{t_a}^t \sin \omega(t - t') f(t') f(t) dt' dt + \int_{t_a}^{t_b} \frac{\sin \omega(t_a - t)}{\sin \omega(t_b - t_a)} f(t) dt \int_{t_a}^{t_b} \sin \omega(t_b - t') f(t') dt' \right] \\ S &= \frac{m}{2} \left\{ \frac{\omega}{\sin \omega(t_b - t_a)} [(x_b^2 + x_a^2) \cos \omega(t_b - t_a) - 2x_b x_a] \right\} \\ &\quad + \frac{x_b}{2 \sin \omega(t_b - t_a)} \left[\int_{t_a}^{t_b} \cos \omega(t_a - t_b) \sin \omega(t_b - t') f(t') dt' + \int_{t_a}^{t_b} \cos \omega(t_b - t') f(t') \sin \omega(t_b - t_a) dt' \right. \\ &\quad \left. + \int_{t_a}^{t_b} \sin \omega(t - t_a) f(t) dt \right] + \frac{x_a}{\sin \omega(t_b - t_a)} \int_{t_a}^{t_b} \sin \omega(t_b - t) f(t) dt \\ &\quad + \frac{1}{2m\omega} \left[\int_{t_a}^{t_b} \int_{t_a}^t \sin \omega(t - t') f(t') f(t) dt' dt + \int_{t_a}^{t_b} \frac{\sin \omega(t_a - t)}{\sin \omega(t_b - t_a)} f(t) dt \int_{t_a}^{t_b} \sin \omega(t_b - t') f(t') dt' \right]. \end{aligned}$$

After the last equal sign, the functions are simplified inside square brackets

$$\left[\cos \omega(t_a - t_b) \sin \omega(t_b - t) + \cos \omega(t_b - t) \sin \omega(t_b - t_a) + \sin \omega(t - t_a) \right] = 2 \sin \omega(t - t_a).$$

After some more simplifications, the action can be rewritten as

$$S = \frac{m\omega}{2 \sin \omega(t_b - t_a)} \left\{ (x_b^2 + x_a^2) \cos \omega(t_b - t_a) - 2x_b x_a + \frac{2x_b}{m\omega} \int_{t_a}^{t_b} \sin \omega(t - t_a) f(t) dt \right. \\ \left. + \frac{2x_a}{m\omega} \int_{t_a}^{t_b} \sin \omega(t_b - t) f(t) dt - \frac{2}{m^2 \omega^2} \int_{t_a}^{t_b} \int_{t_a}^t \sin \omega(t_b - t) \sin \omega(t' - t_a) f(t) f(t') dt' dt \right\}. \quad (\text{E.72})$$

As depicted in Eq. (E.28), the identical expression for the influence function is found. Employing Eq. (E.14) leads to

$$K(x_b, t_b; x_a, t_a) = \left(\frac{m\omega}{2\pi i \hbar \sin \omega T} \right)^{1/2} \exp \left\{ \frac{i}{\hbar} \frac{m\omega}{2 \sin \omega(t_b - t_a)} \left\{ (x_b^2 + x_a^2) \cos \omega(t_b - t_a) \right. \right. \\ \left. \left. - 2x_b x_a + \frac{2x_b}{m\omega} \int_{t_a}^{t_b} \sin \omega(t - t_a) f(t) dt + \frac{2x_a}{m\omega} \int_{t_a}^{t_b} \sin \omega(t_b - t) f(t) dt \right. \right. \\ \left. \left. - \frac{2}{m^2 \omega^2} \int_{t_a}^{t_b} \int_{t_a}^t \sin \omega(t_b - t) \sin \omega(t' - t_a) f(t) f(t') dt' dt \right\} \right\}. \quad (\text{E.73})$$

APPENDIX F – INFLUENCE FUNCTIONAL

This appendix addresses the derivation of the influence functional expression. The term regarding the dissipative dynamics is the influence functional given by

$$\begin{aligned}
\mathcal{F}[x, y] &= \int d\mathbf{R}d\mathbf{R}'d\mathbf{Q}'\rho_R(\mathbf{R}', \mathbf{Q}', 0) \int_{\mathbf{R}'}^{\mathbf{R}} \int_{\mathbf{Q}'}^{\mathbf{Q}} \mathcal{D}\mathbf{R}\mathcal{D}\mathbf{Q} \exp\left\{\frac{i}{\hbar} [S_{SR}[x, \mathbf{R}] - S_{SR}[y, \mathbf{Q}]]\right\} \\
&= \prod_{k=1}^N \int dR_k dR'_k dQ'_k \rho_B(R'_k, Q'_k, 0) \int_{R'_k, Q'_k}^{R_k, Q_k} \mathcal{D}R_k(t') \mathcal{D}Q_k(t') \\
&\quad \times \exp\left\{\frac{i}{\hbar} [S_{SR}[x(t'), R_k(t')] - S_{SR}[y(t'), Q_k(t')]]\right\},
\end{aligned} \tag{F.1}$$

which is separable and can be expressed as the product of N influence functionals, of which each corresponds to a particle interacting with the bath.

The path integrals of Eq.(F.1) can be evaluated, for the action of the system-reservoir is known. Furthermore, since the classical Lagrangian embodies a harmonic oscillator and the global system under study is linear, only the evaluation of the action S_{SR} along classical paths R_k of each oscillator in the thermal bath is required.

The Lagrangian is given by

$$\begin{aligned}
L &= L_S + L_R + L_I \\
&= \frac{m\dot{x}^2}{2} - V(x) + \sum_k \frac{m_k \dot{R}_k^2}{2} - \sum_k \frac{m_k \omega_k^2}{2} \left(R_k - \frac{C_k x}{m_k \omega_k^2} \right)^2.
\end{aligned} \tag{F.2}$$

Those classical paths are the solution of equation of motion Eq. F.3

$$\begin{aligned}
\frac{d}{dt} \left(\frac{dL_{SR}}{d\dot{R}_k} \right) - \frac{dL_{SR}}{dR_k} &= 0, \\
\ddot{R}_k + \omega_k^2 R_k &= \frac{C_k x}{m_k}.
\end{aligned} \tag{F.3}$$

The path integrals in Eq.(F.1) correspond to the kernel for a driven harmonic oscillator, except for term $\frac{(C_k x)^2}{2m_k \omega_k^2}$. Such a contribution can be factored out of the path integral because it contains no term that depends on the classical paths of the bath oscillators. The solution of Eq.(F.3) can be split into a homogeneous solution and a particular one $R_k = R_k^h + R_k^p$. The homogeneous solution stems from

$$\ddot{R}_k + \omega_k^2 R_k = 0, \tag{F.4}$$

which gives

$$R_k^h = A \cos(\omega t) + B \sin(\omega t), \tag{F.5}$$

where A and B are arbitrary constants.

The other solution can be solved by Green's function method, in which

$$\frac{d^2 G(t, t')}{dt^2} + \omega_k^2 G(t, t') = \delta(t - t'), \quad (\text{F.6})$$

where $G(t, t')$ is Green's function and $t' \in (t' - \varepsilon, t' + \varepsilon)$, so that the equation can be integrated around such an interval

$$\int_{t'-\varepsilon}^{t'+\varepsilon} \frac{d^2 G(t, t')}{dt'^2} dt' + \omega_k \int_{t'-\varepsilon}^{t'+\varepsilon} G(t, t') dt' = \int_{t'-\varepsilon}^{t'+\varepsilon} \delta(t - t') dt'. \quad (\text{F.7})$$

The equation is analyzed term by term. For instance, by definition, Dirac's delta provides $\int_{t'-\varepsilon}^{t'+\varepsilon} \delta(t - t') dt' = 1 - \omega_k$ is a continuous function in the entire interval of t . Since $G(t, t')$ is continuous at $t = t'$ by construction, then $\int_{t'-\varepsilon}^{t'+\varepsilon} G(t, t') dt' = 0$ in the limit of $\varepsilon \rightarrow 0$. Therefore

$$\lim_{\varepsilon \rightarrow 0} \left[\frac{dG(t, t' + \varepsilon)}{dt'} - \frac{dG(t, t' - \varepsilon)}{dt'} \right] = 1. \quad (\text{F.8})$$

The above equations reveal the derivative of Green's function experiences a discontinuity of magnitude 1 at t' . By generality, $R_k^h(t) = AR_k^{(1)}(t) + BR_k^{(2)}(t)$ and the general form of Green's function can be written as

$$G(t, t') = aR_k^{(1)}(t) + bR_k^{(2)}(t), \quad t - t' > 0, \quad (\text{F.9})$$

$$G(t, t') = cR_k^{(1)}(t) + dR_k^{(2)}(t), \quad t - t' < 0. \quad (\text{F.10})$$

The relation of continuity of G and discontinuity of derivative of G at t' yields

$$aR_k^{(1)}(t') + R_k^{(2)}(t') = cR_k^{(1)}(t') + dR_k^{(2)}(t') \quad (\text{F.11})$$

$$a\dot{R}_k^{(1)}(t') + b\dot{R}_k^{(2)}(t') = c\dot{R}_k^{(1)}(t') + d\dot{R}_k^{(2)}(t') + 1, \quad (\text{F.12})$$

It is adjusted accordingly by

$$(a - c)R_k^{(1)}(t') + (b - d)R_k^{(2)}(t') = 0 \quad (\text{F.13})$$

$$(a - c)\dot{R}_k^{(1)}(t') + (b - d)\dot{R}_k^{(2)}(t') = 1. \quad (\text{F.14})$$

Solving $a - c$ by Kramers' method yields

$$(a - c) = \frac{\begin{vmatrix} 0 & R_k^{(2)}(t') \\ 1 & \dot{R}_k^{(2)}(t') \end{vmatrix}}{\begin{vmatrix} R_k^{(1)}(t') & R_k^{(2)}(t') \\ \dot{R}_k^{(1)}(t') & \dot{R}_k^{(2)}(t') \end{vmatrix}} = -\frac{R_k^{(2)}(t')}{W(t')}, \quad (\text{F.15})$$

where $W(t') = R_k^{(1)}(t')\dot{R}_k^{(2)}(t') - \dot{R}_k^{(1)}(t')R_k^{(2)}(t')$ is the Wronskian. Similarly,

$$(b - d) = \frac{R_k^{(1)}(t')}{W(t')}. \quad (\text{F.16})$$

Those results are substituted in $G(t, t')$ leaving out c and d to be determined by boundary conditions

$$G(t, t') = cR_k^{(1)}(t) - R_k^{(1)}(t)\frac{R_k^{(2)}(t')}{W(t')} + dR_k^{(2)}(t) + R_k^{(2)}(t)\frac{R_k^{(1)}(t')}{W(t')}, \quad t - t' > 0, \quad (\text{F.17})$$

$$G(t, t') = cR_k^{(1)}(t) + dR_k^{(2)}(t) - \frac{R_k^{(1)}(t)R_k^{(2)}(t') - R_k^{(2)}(t)R_k^{(1)}(t')}{W(t')}, \quad t - t' > 0, \quad (\text{F.18})$$

$$G(t, t') = cR_k^{(1)}(t) + dR_k^{(2)}(t), \quad t - t' < 0. \quad (\text{F.19})$$

Green's function can be explicitly demonstrated by homogeneous solution

$$G(t, t') = cA \cos \omega_k t + dB \sin \omega_k t - \frac{AB[(\cos \omega_k t)(\sin \omega_k t') - (\sin \omega_k t)(\cos \omega_k t')]}{AB\omega_k[(\cos \omega_k t')(\cos \omega_k t) - (-\sin \omega_k t')(\sin \omega_k t)]}, \quad t - t' > 0,$$

$$G(t, t') = cA \cos \omega_k t + dB \sin \omega_k t, \quad t - t' < 0.$$

Renaming the constants, $C = cA$ and $D = dB$, and using some trigonometry relation such as $\sin(a - b) = \sin(a) \cos(b) - \sin(b) \cos(a)$, lead to

$$G(t, t') = C \cos \omega_k t + D \sin \omega_k t - \frac{1}{\omega_k} \sin \omega_k(t - t'), \quad t - t' > 0, \quad (\text{F.20})$$

$$G(t, t') = C \cos \omega_k t + D \sin \omega_k t, \quad t - t' < 0. \quad (\text{F.21})$$

Again, since our interest is in the action, a two-point boundary condition is required. Besides the absence of velocity information provided, there is a subtle aspect wherein $R'_k = R_k(t_a = 0)$ and $R_k = R_k(t_b = t)$ are designated as initial and final conditions, thereby encapsulating the entire concept of a trajectory. The two-point boundary condition is given by

$$G(t_a, t') = G(t_b, t') = 0, \quad (\text{F.22})$$

from which

$$G(t_b, t') = C \cos \omega_k t + D \sin \omega_k t - \frac{1}{\omega_k} \sin \omega_k(t - t') = 0, \quad t - t' > 0,$$

$$G(t_a, t') = C = 0, \quad t - t' < 0,$$

$C = 0 \implies D = \frac{1}{\omega_k} \frac{\sin \omega_k(t - t')}{\sin \omega_k t}$. The solutions provide the final form for Green's function

$$G(t, t') = 0, \quad t - t' > 0, \quad (\text{F.23})$$

$$G(t, t') = -\frac{\sin \omega_k(t - t')}{\omega_k}, \quad t - t' < 0. \quad (\text{F.24})$$

Therefore, the solution to the equation of motion is

$$R_k(t) = A \cos \omega_k t + B \sin \omega_k t + \frac{C_k}{m_k} \int_0^t G(t, t') x(t') dt'. \quad (\text{F.25})$$

The different forms of $G(t, t')$ along $(0, t)$ enable writing the solution for the driven harmonic oscillator dynamics

$$R_k(t) = A \cos \omega_k t + B \sin \omega_k t + \frac{C_k}{m_k \omega_k} \int_0^t \sin \omega_k(t - t') x(t') dt', \quad (\text{F.26})$$

and employing boundary conditions

$$R_k(0) = R'_k = A, \quad (\text{F.27})$$

$$R_k(t) = R_k = A \cos \omega_k t + B \sin \omega_k t \quad (\text{F.28})$$

then $B = \frac{R_k - R'_k \cos \omega_k t}{\sin \omega_k t}$. After some arrangements,

$$R_k(t) = \frac{1}{\sin \omega_k t} \left[R'_k \sin \omega(t - t') + R_k \sin \omega_k(t') \right] \quad (\text{F.29})$$

$$+ \frac{C_k}{m_k \omega_k} \left[\int_0^t \sin \omega_k(t - t') x(t') dt' - \int_0^t \sin \omega_k(t - t'') x(t'') dt'' \right] \quad (\text{F.30})$$

is found.

R_k must be differentiated with respect to t and squared,

$$\dot{R}_k(t) = \frac{\omega_k}{\sin \omega_k t} \left[-R'_k \cos \omega_k(t - t') + R_k \cos \omega_k t' \right] \quad (\text{F.31})$$

$$+ \frac{C_k}{m_k} \left[\int_0^{t'} \cos \omega_k(t' - t'') x(t'') dt'' + \left(\frac{\cos \omega_k t'}{\sin \omega_k t} \int_0^t \sin \omega_k(t - t') x(t') dt' \right) \right]. \quad (\text{F.32})$$

Let us focus on the action

$$S_{cl}^{(k)} = \int_0^t \left(\frac{m_k}{2} \dot{R}_k^2 - \frac{m_k \omega_k^2}{2} R_k^2 + C_k x(t') \right) dt', \quad (\text{F.33})$$

which is rewritten as

$$S_{cl}^{(k)} = \frac{m_k \omega_k}{2 \sin \omega_k t} \left[(R_k^2 + R_k'^2) \cos \omega_k t - 2 R_k R_k' \right] + \frac{R_k C_k}{\sin \omega_k t} \int_0^t \sin \omega_k t' x(t') dt' \quad (\text{F.34})$$

$$+ \frac{R_k' C_k}{\sin \omega_k t} \int_0^t \sin \omega_k(t - t') x(t') dt' - \frac{C_k^2}{m_k \omega_k \sin \omega_k t} \int_0^t \int_0^{t'} \sin \omega_k(t - t') \sin \omega_k t'' x(t') x(t'') dt' dt''. \quad (\text{F.35})$$

Moreover, for a Gaussian integral, the kernel is provided by

$$K(b, a) = e^{\frac{i}{\hbar} S_{cl}} \int_0^0 F(t_a, t_b) \mathcal{D}y(t), \quad (\text{F.36})$$

where S_{cl} represents the action evaluated along the classical path and the prefactor for an arbitrary quadratic Lagrangian is given by

$$F(t_a, t_b) = \int_0^0 \exp \left\{ \frac{i}{\hbar} \int_{t_a}^{t_b} a(t) \dot{y}^2 + b(t) y \dot{y} + c(t) y^2 dt \right\} \mathcal{D}y. \quad (\text{F.37})$$

Towards determining its shape for a free harmonic oscillator, $a(t) = m_k/2$, $c(t) = m_k\omega_k^2/2$ and $b(t) = d(t) = e(t) = f(t) = 0$ is defined in the above equation and our prefactor becomes

$$F(t_a, t_b) = \int_0^0 \exp \left[\int_{t_a}^{t_b} \frac{1}{2} m_k \dot{y}^2 - \frac{1}{2} m_k \omega_k^2 y^2 dt \right] \mathcal{D}y \quad (\text{F.38})$$

by Fourier series. Since $y(t)$ goes from 0 at $t = 0$ to 0 at $t = t_b - t_a$ and recalling $t_a = 0$, $t_b = t$, it can be written as

$$y(t) = \sum_{n=1}^{\infty} a_n \sin \left(\frac{n\pi t}{\tau} \right). \quad (\text{F.39})$$

Time τ is divided into discrete steps of length ϵ and coefficients a_n are assumed to be finite. Performing a transformation on each term of the action integral, the prefactor is

$$F(0, t) = \sqrt{\frac{m_k \omega_k}{2\pi i \hbar \sin \omega_k t}}. \quad (\text{F.40})$$

The result is the integrals below

$$\int_{R'_k}^{R_k} \mathcal{D}R_k(t') \exp \left\{ \frac{i}{\hbar} S_{SR}[x(t'), R_k(t')] \right\} = K_{SR}^{(k)} = \sqrt{\frac{m_k \omega_k}{2\pi i \hbar \sin \omega_k t}} \exp \left\{ \frac{i}{\hbar} S_{cl}^{(k)}[x, R_k] \right\}$$

$$\int_{Q'_k}^{Q_k} \mathcal{D}Q_k(t') \exp \left\{ -\frac{i}{\hbar} S_{SR}[y(t'), Q_k(t')] \right\} = K_{SR}^{*(k)} = \sqrt{-\frac{m_k \omega_k}{2\pi i \hbar \sin \omega_k t}} \exp \left\{ -\frac{i}{\hbar} S_{cl}^{(k)}[y, Q_k] \right\}.$$

Using the above expressions and the expression for the initial bath density operator and after performing integrations over R'_k , R_k , Q'_k the influence functional reads

$$\mathcal{F}_k[x, y] = \exp \left\{ -\frac{iC_k^2}{\hbar} (x' + y') \int_0^t dt' \frac{\cos(\omega_k t')}{2m_k \omega_k^2} [x(t') - y(t')] \right\} \quad (\text{F.41})$$

$$\times \exp \left\{ -\frac{iC_k^2}{\hbar} \int_0^t \int_0^{t'} dt' dt'' \frac{\cos \omega_k (t' - t'')}{2m_k \omega_k^2} [\dot{x}(t'') + \dot{y}(t'')] [x(t') - y(t')] \right\} \quad (\text{F.42})$$

$$\times \exp \left\{ -\frac{C_k^2}{2\hbar m_k \omega_k^2} \int_0^t \int_0^{t'} dt' dt'' \coth \left(\frac{\hbar \beta \omega_k}{2} \right) \cos \omega_k (t' - t'') [x(t') - y(t')] [x(t'') - y(t'')] \right\}. \quad (\text{F.43})$$

The above expression describes the influence of k -th oscillator in the thermal bath on the i -th oscillator in the system of interest.

APPENDIX G – INITIAL ENVIRONMENT DENSITY OPERATOR

This appendix addresses the derivation of the density operator for the environment at initial time. The expression for Kernel for a free harmonic oscillator was derived in the previous appendices as

$$K(x_b, t_b; x_a, t_a) = \left(\frac{m\omega}{2\pi i \hbar \sin \omega t} \right)^{1/2} \exp \left\{ \frac{i}{\hbar} \frac{m\omega}{2 \sin \omega(t_b - t_a)} \left[(x_b^2 + x_a^2) \cos \omega(t_b - t_a) - 2x_b x_a \right] \right\}. \quad (\text{G.1})$$

Assuming the initial state of the environment is Gibbs state

$$\rho_G^R = \frac{e^{-H_R/k_B T}}{Z}, \quad (\text{G.2})$$

the imaginary time must be applied for deriving the correct kernel, hence, the expression for the initial density operator for environment.

In the above equation, by substituting imaginary time $\beta = it/\hbar$ (Wick's rotation), $U(t) \rightarrow Z_{\rho_G}$, where Z represents the partition function. Consequently, the driven term becomes null. Evaluating the expression yields

$$i \sin(\omega t) = i \sin \left(\frac{\omega \beta \hbar}{i} \right) = i \left[\frac{e^{i(\frac{\omega \beta \hbar}{i})} - e^{-i(\frac{\omega \beta \hbar}{i})}}{2i} \right] = \frac{e^{\omega \beta \hbar} - e^{-\omega \beta \hbar}}{2} = \sinh(\omega \beta \hbar), \quad (\text{G.3})$$

$$\cos(\omega t) = \cos \left(\frac{\omega \beta \hbar}{i} \right) = \frac{e^{i(\frac{\omega \beta \hbar}{i})} + e^{-i(\frac{\omega \beta \hbar}{i})}}{2} = \frac{e^{\omega \beta \hbar} + e^{-\omega \beta \hbar}}{2} = \cosh(\omega \beta \hbar), \quad (\text{G.4})$$

where $\beta = \frac{1}{k_B T}$ and substituting it into the expression for the kernel results in

$$K(x_b, t_b; x_a, t_a) = \left(\frac{m\omega}{2\pi \hbar \sinh(\omega \beta \hbar)} \right)^{1/2} \exp \left\{ -\frac{m\omega}{2\hbar \sinh(\omega \beta \hbar)} \left[(x_b^2 + x_a^2) \cosh(\omega \beta \hbar) - 2x_b x_a \right] \right\}. \quad (\text{G.5})$$

Assuming $\text{Tr } \rho = 1$, the initial density operator can be written in the environment coordinates as

$$\begin{aligned} \rho_R^G(R', Q') &= \sum_j \rho_R^{(j)}(R', Q', 0) \\ &= \sum_j \frac{m_j \omega_j}{2\pi \hbar \sinh(\frac{\hbar \omega_j}{k_B T})} \exp \left\{ -\frac{m_j \omega_j}{2\hbar \sinh(\frac{\hbar \omega_j}{k_B T})} \left[(R_j'^2 + Q_j'^2) \cosh \left(\frac{\hbar \omega_j}{k_B T} \right) - 2R_j' Q_j' \right] \right\}. \end{aligned} \quad (\text{G.6})$$

APPENDIX H – QUANTUM WORK OF A SINGLE PHOTON

The derivation presented here is based on Refs.(21, 146, 147).

Let us consider a global state of the atom-field system as

$$|\xi(t)\rangle = \psi(t) |e, 0\rangle + \sum_{\omega} \phi_{\omega}(t) a_{\omega}^{\dagger} |g, 0\rangle, \quad (\text{H.1})$$

where $|e, 0\rangle = |e\rangle \otimes |0\rangle$ is the tensorial product between excited and vacuum states and $|g, 0\rangle = |g\rangle \otimes |0\rangle$ is the tensorial product between ground and vacuum states. $\psi(t) |e, 0\rangle$ is associated with the excited state of a two-level system, whereas $\sum_{\omega} \phi_{\omega}(t) a_{\omega}^{\dagger} |g, 0\rangle$ is associated with the ground state and the presence of the photon. $\phi(t)$ is the probability amplitude to find the system in the excited state $|e\rangle$. $\phi_{\omega}(t)$ is the probability amplitude of occupation of each mode*.

$|0\rangle = \prod_{\omega} |0_{\omega}\rangle$ is the vacuum state of the field in each mode of frequency ω with creation operator a_{ω}^{\dagger} . Then,

$$\sum_{\omega} a_{\omega}^{\dagger} a_{\omega} |1\rangle \equiv \sum_{\omega} a_{\omega}^{\dagger} a_{\omega} \sum_{\omega'} \phi_{\omega'}(t) a_{\omega'}^{\dagger} |0\rangle = 1 |1\rangle, \quad (\text{H.2})$$

which implies superposition $\sum_{\omega} \phi_{\omega}(t) a_{\omega}^{\dagger} |0\rangle \equiv |1\rangle$, i.e., this electromagnetic pulse contains a single excitation.

From Eq.(H.1), the average dipole of an atom driven by a single-photon pulse is zero, i.e.,

$$\langle \hat{d}(t) \rangle = \langle \xi(t) | \hat{d} | \xi(t) \rangle = 0, \quad (\text{H.3})$$

where $\hat{d} = d_{eg}(|e\rangle \langle g| + |g\rangle \langle e|)$ is the dipole operator and d_{eg} is the transition dipole moment.

The combination of quantum thermodynamics and open quantum systems techniques characterized the work performed by the electromagnetic field on the electric dipole in Refs.(21, 146, 147).

The aforementioned relation implies the field does not perform work on the dipole, recalling the electromagnetic theory predicts the classical field depends on time $E(t)$ and performs work in a classical dipole momentum with rate

$$\dot{W}_{cl} = E(t) \dot{d}(t) \quad (\text{H.4})$$

where dots indicate time derivative. The quantum description of the electrical field is then

$$\dot{W}_{quant} = E(t) \langle \partial_t \hat{d}(t) \rangle, \quad (\text{H.5})$$

* which is initially normalized $\sum_{\omega} |\phi_{\omega}(0)|^2 = 1$.

since $\langle \partial_t \hat{d}(t) \rangle = 0$, then $\dot{W} = 0$. The following definition of work is adopted for circumventing that issue and obtaining a correct description of the dynamics:

$$\langle \Delta W \rangle \equiv \int_{t_0}^{t_f} dt \text{Tr} \{ \rho(t) \dot{H}(t) \}, \quad (\text{H.6})$$

which, combined with the quantum open system out-of-equilibrium approach, can fully describe the dynamics using a full quantum model.

The total Hamiltonian is given by

$$H = \hbar\omega_0 \sigma_+ \sigma_- + \sum_{\omega} \hbar\omega a_{\omega}^{\dagger} - i\hbar g \sum_{\omega} (a_{\omega} \sigma_+ - a_{\omega}^{\dagger} \sigma_-), \quad (\text{H.7})$$

where $\sigma_+ = \sigma_-^{\dagger} = |e\rangle \langle g|$ and $\omega_S(t)$ is the time-dependent frequency induced by the incident field. The reduced two-level system state is $\rho_S(t) = \text{Tr}_{field} [|\xi(t)\rangle \langle \xi(t)|]$ and the evolution follows Schrodinger's equation, which suggested the use of master equation

$$\partial_t \rho_S(t) = -\frac{i}{\hbar} [H_S(t), \rho_S(t)] + \mathcal{L}_t[\rho_S(t)]. \quad (\text{H.8})$$

The description provides the effective Hamiltonian of the system, given by

$$H_S(t) = \hbar\omega_S(t) \sigma_+ \sigma_-, \quad (\text{H.9})$$

emphasizing the non-unitary component of the master equation, then

$$\mathcal{L}_t[\rho_S(t)] = \Gamma(t) \left(\sigma_- \rho_S(t) \sigma_+ - \frac{1}{2} \{ \sigma_+ \sigma_-, \rho_S(t) \} \right) \quad (\text{H.10})$$

where $\{.,.\}$ is the anticommutator. $\Gamma(t)$ is the time-dependent tunneling rate induced by the pulse and $\mathcal{L}_t[\rho_S(t)]$ is the Lindblad form.

Inserting the two above expressions in the master equation, the solution of $H_S(t)$ when $\omega_S(t) = -Im[\partial_t \psi(t)/\psi(t)]$ and $\Gamma(t) = -2Re[\partial_t \psi(t)/\psi(t)]$ is recovered. The expression for the quantum work done by a single photon pulse is written as

$$W \equiv \int_{t_0}^{t_f} \text{Tr} \{ \rho_S(t) \partial_t H_S(t) \} dt = \hbar \int_{t_0}^{t_f} |\psi(t)|^2 (\partial_t \omega_S(t)) dt, \quad (\text{H.11})$$

and the heat involved in the process is

$$Q \equiv \int_{t_0}^{t_f} \text{Tr} \{ \partial_t \rho_S(t) H_S(t) \} dt = \hbar \int_{t_0}^{t_f} (\partial_t |\phi(t)|^2) \omega_S(t) dt. \quad (\text{H.12})$$

Work originates in the temporal dependence of $\omega_S(t)$ and heat depends on a change in the excitation probability of the two-level system $|\psi(t)|^2$.

Unlike Ref.(147), Ref.(21) uses a definition of work compatible with the Heisenberg representation. Where the definition of work in the Heisenberg picture and in the rotating-wave approximation can be written as

$$\langle W_{abs} \rangle_a = \int_0^{\infty} \langle (\partial(t)) E_{in}(t) \rangle dt, \quad (\text{H.13})$$

where $E_{in}(t)$ represents the driving field.

APPENDIX I – DERIVATION OF FUNCTIONAL OF WORK

The derivation presented here is based on Ref.(118–120).

The characteristic function of work is written as

$$\chi_W(\nu) = \text{Tr}[U_S e^{-i\nu H_S(\lambda_0)} \rho_S(0) U_S^\dagger e^{i\nu H_S(\lambda_\tau)}], \quad (\text{I.1})$$

where $U(\tau) = \mathcal{T}[\exp(-i\hbar \int_0^\tau dt H(\lambda_\tau))]$ is the time evolution operator, $[0, \tau]$ is the time interval for controlled parameter λ_τ ,

$$H_S = p^2/2m + V(\lambda_\tau, x), \quad (\text{I.2})$$

is the Hamiltonian, and $\rho_S(0)$ is the initial state of the system.

The following steps are taken for deriving the path integral expression as per the reference:

$$\langle x_f | U_S e^{-i\nu H_S(\lambda_0)} | x_i \rangle = \int \mathcal{D}x e^{(i/\hbar)S_1^\nu[x]}, \quad (\text{I.3})$$

$$\langle y_i | U_S^\dagger e^{i\nu H_S(\lambda_\tau)} | y_f \rangle = \int \mathcal{D}y e^{(-i/\hbar)S_2^\nu[y]}. \quad (\text{I.4})$$

Inserting the relation above into Eq.(I.1) and using identity $\int dx |x\rangle \langle x| = 1$ lead to

$$\begin{aligned} \chi_W(\nu) &= \int dx_i dx'_i dx_f dx'_f \delta(x_f - x'_f) |x_f\rangle U_S e^{-i\nu H_S(\lambda_0)} \langle x_i | x_i \rangle \rho_S(0) \langle x'_i | x'_i \rangle U_S e^{i\nu H_S(\lambda_\tau)} \langle x'_f | \\ &= \int dx_i dx'_i dx_f dx'_f \delta(x_f - x'_f) \mathcal{D}x \mathcal{D}x' e^{(i/\hbar)(S_1^\tau[x] - S_2^\tau[x'])} \rho(x_i, x'_i), \end{aligned} \quad (\text{I.5})$$

where $|x_i\rangle \rho_S(0) \langle x'_i| = \rho(x_i, x'_i)$ is the density operator in the coordinate representation and the actions are defined as

$$\begin{aligned} S_1^\tau[x] &= S_1[x, \tau] = \int_0^{\hbar\nu} dt \mathcal{L}[\lambda_0, x(t)] + \int_{\hbar\nu}^{\tau+\hbar\nu} dt \mathcal{L}[\lambda_{t-\hbar\nu}, x(t)], \\ S_2^\tau[x] &= S_2[x', \tau] = \int_0^\tau ds \mathcal{L}[\lambda_s, x'(s)] + \int_\tau^{\tau+\hbar\nu} ds \mathcal{L}[\lambda_\tau, x'(s)]. \end{aligned} \quad (\text{I.6})$$

This definition of action is inherently related to the definition that path integral requires for the propagator. The derivation of a characteristic function that depends explicitly on the work requires the observation of the following identity:

$$\frac{i}{\hbar} S_1^\tau[x] = \frac{i}{\hbar} S_2^\tau[x] + i\nu W_\nu[x]. \quad (\text{I.7})$$

Its validity can be verified by initially observing

$$\frac{i}{\hbar} S_1^\tau[x, 0] = \frac{i}{\hbar} S_2^\tau[x, 0] + i\nu W_\nu[x, 0], \quad (\text{I.8})$$

which leads to

$$i\nu W_\nu[x, 0] = \frac{i}{\hbar} \left[\int_0^{\hbar\nu} dt \mathcal{L}[\lambda_0, x(t)] - \int_0^{\hbar\nu} ds \mathcal{L}[\lambda_0, x(s)] \right] = 0, \quad (\text{I.9})$$

since the system does not perform any work at time $t = 0$. On the other hand, if the action derivative in time is taken, then

$$\begin{aligned} \frac{d}{du} S_1^\tau[x, u] &= \mathcal{L}[\lambda_u, x(u + \hbar\nu)], \\ \frac{d}{du} S_2^\tau[x, u] &= \mathcal{L}[\lambda_u, x(u + \hbar\nu)] + \int_u^{u+\hbar\nu} \dot{\lambda}_u \frac{\delta}{\delta \lambda_u} \mathcal{L}[\lambda_u, x(s)] ds \end{aligned} \quad (\text{I.10})$$

then

$$\frac{d}{du} S_2^\tau[x, u] = \frac{d}{du} S_1^\tau[x, u] + \int_u^{u+\hbar\nu} \dot{\lambda}_u \frac{\delta}{\delta \lambda_u} \mathcal{L}[\lambda_u, x(s)] ds. \quad (\text{I.11})$$

Taking integral form 0 to τ again results in

$$\begin{aligned} S_2^\tau[x, \tau] - S_2^\tau[x, 0] &= S_1^\tau[x, \tau] - S_1^\tau[x, 0] + \int_0^\tau \int_u^{u+\hbar\nu} \dot{\lambda}_u \frac{\delta}{\delta \lambda_u} \mathcal{L}[\lambda_u, x(s)] ds du, \\ S_1^\tau[x, \tau] - S_2^\tau[x, \tau] &= S_1^\tau[x, 0] - S_2^\tau[x, 0] - \int_0^\tau \int_u^{u+\hbar\nu} \dot{\lambda}_u \frac{\delta}{\delta \lambda_u} \mathcal{L}[\lambda_u, x(s)] ds du, \\ S_1[x, \tau] - S_2[x, \tau] &= - \int_0^\tau \int_u^{u+\hbar\nu} \dot{\lambda}_u \frac{\delta}{\delta \lambda_u} \mathcal{L}[\lambda_u, x(s)] ds du, \end{aligned} \quad (\text{I.12})$$

If $u = t$ is setting and performing substitution $s \rightarrow s + t$ on the right-hand side term above, the work functional is defined as

$$W_\nu[x, \tau] = \frac{1}{\hbar\nu} \int_0^\tau \int_0^{\hbar\nu} ds dt \dot{\lambda}_t \frac{\delta}{\delta \lambda_t} \mathcal{L}[\lambda_t, x(s + t)]. \quad (\text{I.13})$$